

A&A manuscript no.
(will be inserted by hand later)

Your thesaurus codes are:
11.01.2 - 11.17.3 - 13.25.3

ASTRONOMY
AND
ASTROPHYSICS
7.2.2000

Radio and X-ray Bright AGN: The ROSAT - FIRST Correlation

W. Brinkmann¹, S. A. Laurent-Muehleisen^{2,3,4}, W. Voges¹, J. Siebert¹, R. H. Becker³, M. S. Brotherton², R. L. White⁵, and M. D. Gregg³

¹ Max-Planck-Institut für extraterrestrische Physik, Giessenbachstrasse, D-85740 Garching, FRG

² Institute for Geophysics and Planetary Physics, Lawrence Livermore National Laboratory, Livermore, CA 94450, USA

³ Physics Dept., University of California, Davis, CA 95616, USA

⁴ Visiting Astronomer, Kitt Peak National Observatory, National Optical Astronomy Observatory, USA

⁵ Space Telescope Science Institute, 3700 San Martin Drive, Baltimore, MD 21218, USA

J, K, N,

Received / accepted ..

Abstract. We present the results of a correlation of the ROSAT All-Sky Survey with the April 1997 release of the VLA 20cm FIRST catalogue. We focus our analysis on the 843 X-ray sources which have unique radio counterparts. The majority of these objects (84%) have optical counterparts on the POSS 1 plates. Approximately 30% have been previously classified and we obtain new spectroscopic classifications for 85 sources by comparison with the ongoing FIRST Bright Quasar Survey and 106 additional sources from our own new spectroscopic data. Approximately 51% of the sources are presently classified, and the majority of the unclassified objects are optically faint. The newly classified sources are generally radio weak, exhibiting properties intermediate with previous samples of radio- and X-ray-selected AGN. This also holds for the subsample of 71 BLLacs which includes many intermediate objects. The 146 quasars show no evidence for a bimodal distribution in their radio-loudness parameter, indicating that the supposed division between radio-quiet and radio-loud AGN may not be real. The X-ray and radio luminosities are correlated over two decades in radio luminosity, spanning the radio-loud and radio-quiet regimes, with radio-quiet quasars showing a linear correlation between the two luminosities. Many of the sources show peculiar or unusual properties which call for more detailed follow-up observations. We also give the X-ray and radio data for the 518 X-ray sources for which more than one radio object is found. Because of the difficulties inherent in identifying optical counterparts to these complex sources, we do not consider these data in the current analysis¹.

Key words: Galaxies: active – quasars; X-rays: general – Radio sources: general.

1. Introduction

Active Galactic Nuclei (AGN) exhibit a wide variety of observable properties resulting in a complex classification scheme. Current unification schemes attribute many of the observational differences to different viewing angles of the sources' anisotropic emission (e.g., Antonucci 1993, Orr & Browne 1982, Barthel 1989, Urry & Padovani 1995). Large, unbiased samples of AGN are powerful tools for understanding the different physical conditions in the cores of these objects and to test unification schemes. All classes of AGN appear in X-ray surveys. Samples based on the ROSAT All-Sky Survey (RASS), the first soft X-ray survey of the whole sky using an imaging X-ray telescope (Trümper 1983), are well suited for investigating the unification of various AGN classes. There are more than 80.000 RASS sources, of which some 60% are expected to be AGN (Voges et al. 1999), ensuring a statistically useful number of objects belonging to the various AGN subclasses. Unfortunately, the large majority of the ROSAT sources remain to be optically identified.

One of the largest obstacles to identifying RASS sources is that the positional accuracy is limited to $\approx 30''$, making identification of optical counterparts problematic. Correlation with large-scale radio surveys can alleviate this problem, but at the expense of preferentially selecting radio-loud AGN; however, deep radio surveys are capable of detecting radio-quiet AGN, since 'radio-quiet' does not necessarily mean radio-silent. Formally, the radio-loudness is given by the parameter, R , where $R = f_5 \text{ GHz} / f_{2500\text{\AA}}$

Send offprint requests to: W. Brinkmann, e-mail: wpb@mpg.de

¹ The tables are available in electronic form at the CDS via anonymous ftp from 130.79.128.5

fell purely by chance in the 1 arcmin field, most “multiply matched” ROSAT sources had three counterparts. Closer examination of the radio maps showed these sources often had a complex morphology, where identification of a radio core component is highly problematic. A physical picture for these associations might be a distant X-ray emitting cluster of galaxies where the radio sources are individual galaxies in the cluster. A first support for this scenario is coming from ROSAT HRI observations of the source RX J1234.6+2350 (Gliozzi et al. 1999). Because of the considerable uncertainty in identifying an optical counterpart, we have chosen to exclude these objects from much of the detailed analysis which follows, although we give the relevant radio and X-ray data in Table 2. McMahon et al. (2000) discuss in some detail the distribution of optical counterparts for double (and triple) FIRST sources.

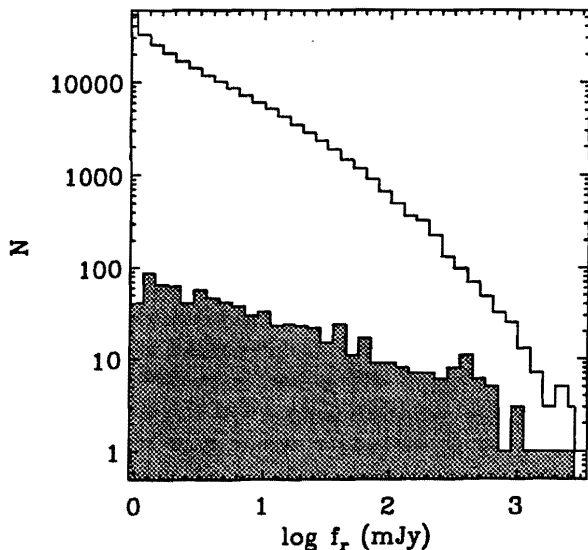


Fig. 3. Distribution of peak radio fluxes for all FIRST sources (open histogram) compared to the ROSAT - FIRST matches (shaded area).

The distribution of the angular separation of the one-to-one or “single” FIRST/RASS matches is well represented by a Gaussian with $\sigma \sim 10''$ for angular separations up to $\approx 30''$. From simple geometric arguments, using the catalogue sizes and areas covered in both wave bands, we estimate the number of chance coincidences to be about 35, i.e., $\sim 2\%$ up to angular separations of $30''$. The increasing slope in the “one-to-one” matches beyond $30-40''$ is a direct indicator for the increasing number of chance coincidences at larger extraction radii (Fig. 2).

The number of X-ray - radio correlations found in a certain radio flux interval is subject to a strong selection effect caused by the limiting sensitivity of the X-ray survey. In Fig. 3 we show the total number of FIRST sources

as function of the measured peak flux as an open histogram; the corresponding number of radio-X-ray matches is given as a shaded histogram. The detection probability rises from about 0.25% at the lowest radio flux levels to a few percent of the sources with a flux of ~ 500 mJy. These numbers are considerably smaller than found for previous correlations where less sensitive radio surveys were used and thus reflect the influence of the RASS flux limit on the source detection.

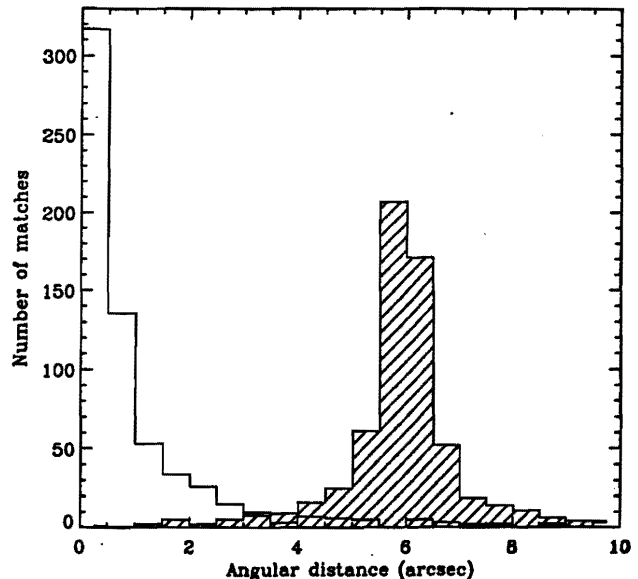


Fig. 4. Number of matches as function of angular distances between single radio sources and APM counterparts. Each bin is $0.5''$. The open histogram represents the actual data; for the hatched histogram the radio positions were shifted by $+6''$ in declination.

For all singly matched FIRST sources, optical counterparts were determined from Automatic Plate Measuring (APM) scans of the O and E POSS plates (McMahon 1991). Following White et al. (2000, W00), we have used the FIRST survey positions to correct the APM positions on a plate-by-plate basis. The increased accuracy of the optical positions yields a far more successful match rate (McMahon et al. 2000) since it excludes many spurious matches and eliminates few true matches. Past experience has shown that the agreement between radio and optical positions depends on the optical morphology of the counterpart where the offsets for galaxies tend to be larger than for stellar counterparts. Therefore, we associate the radio source with an optical counterpart if the angular distance between the two objects is $\delta_{ro} \leq 1.5''$ for a starlike counterpart and $\delta_{ro} \leq 2''$ for a resolved optical counterpart. In addition, we have relaxed these radio-optical position offset criteria for heavily resolved optical objects (optical sizes $>10''$). The criterion we use for these objects is that

the radio/optical position difference be less than 25% of the total optical extent. This ensures that objects such as NGC 6173 which are significantly optically extended, are not considered unidentified.

A rigorous analysis of the reliability and completeness of the current sample is desirable; however, an analysis relying on the positional coincidence of the objects in the different wavelength bands only, for example with a Likelihood Ratio analysis as done for flux-limited radio - optical surveys (Windhorst et al. 1984), seems to be insufficient for a quantitative assessment as we are dealing with a 'pre-selected' sample (via the radio - X-ray correlations). The X-ray selection is spatially and spectrally inhomogeneous and depends in a not well understood way on the classes of the sources. To assess the reliability of the radio and optical matching, we estimated the number of chance coincidences by shifting the radio positions by $+6''$ in declination and counted the number of cases where the nearest optical candidate was found inside a given angular distance.

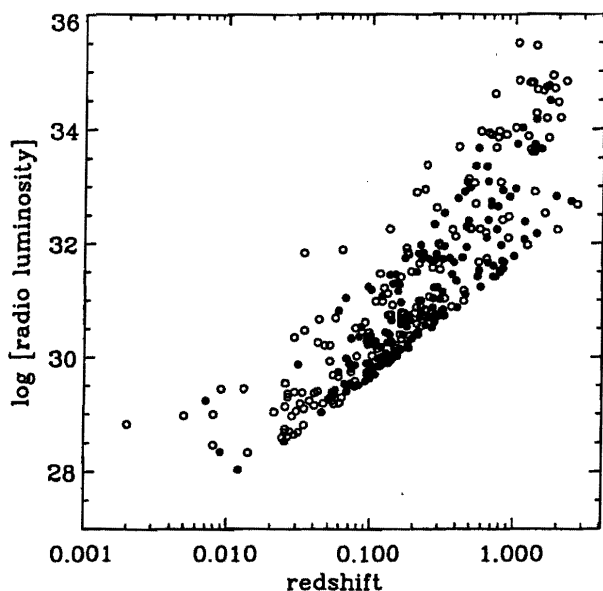


Fig. 5. 1.4 GHz radio luminosity as function of redshift for the spectroscopically classified sources. Open circles are previously known objects, solid dots the newly classified objects.

In Fig. 4 we plot the distribution of the angular distances between the radio sources and the proposed optical counterparts (open histogram). This distribution peaks at separations $\lesssim 1''$. The probability of finding an unrelated point-like optical object within a given radius is indicated by the hatched histogram which shows the match rate when the radio positions were shifted by $6''$. This distribution peaks at the offset position of $6''$, but we can use the wings of this distribution to estimate the false match

rate. Specifically, at a matching radius of $\leq 2''$ only $\sim 1\%$ of the optical - radio matches (~ 7 sources) are likely chance coincidences.

Finally, there is another direct argument for the correctness of the association of the X-ray, radio and optical sources for the majority of the objects of the sample: while the rate of optical - radio source coincidences is rather low (approximately 15% of the FIRST point sources have an optical counterpart at angular distances less than $2''$; McMahon et al. 2000), 706 of the 843 singly matched RASS/FIRST sources (84%) have a counterpart on the POSS plates.

Raw APM photometric magnitudes are accurate to ~ 0.5 mag, but zero point uncertainties, saturation effects, and systematic errors for bright extended objects (galaxies) which vary from plate to plate make the effective uncertainty higher. However, the O-E colors can be used for a rough characterization of the objects (McMahon, 1991) and are reliable in the range $-1 \leq O - E \leq 3$; outside this range non linearity effects start to dominate.

The APM magnitudes overestimate the brightness of optical sources by ~ 0.3 mag (e.g. W00). To improve the photometric accuracy and uniformity of the sample, the APM magnitudes are being recalibrated plate-by-plate (McMahon et al. 2000) using magnitudes from the Minnesota Automated Plate Scanner POSS-I catalogue (APS⁴, Pennington et al. 1993). In addition, although this is a high Galactic latitude sample, some sources lie in areas of high reddening. We therefore used these recalibrated magnitudes, and list an approximate $A(E)$ extinction correction (which has not been applied to the tabulated magnitudes) for each candidate object. Although the zero-point corrections can be quite large (>0.5 mag), the extinction corrections are usually quite small (the median values are $A(E) = 0.058$ and $A(O) = 0.094$, see also W00) but even these corrections can become significant at the high and low RA edges of the survey reaching up to 0.3 mag in the E bandpass (see Fig. 3 in W00). The recalibration of the APM magnitudes is currently available only for the northern RASS/FIRST sample (see Sect. 2).

Using the NASA/IPAC Extragalactic Data Base (NED), recent FIRST-related optical identification programs, and our own followup spectroscopic observations (see below), we have determined spectroscopic classifications for a total of 454 objects. The majority of unclassified objects are found at the lower end of the radio flux scale (see next section), where large scale surveys with high sensitivity have recently become available, further indicating that previous attempts for an optical identification of radio sources have been biased towards the brightest radio sources. We also see changes in the typical source popula-

⁴ The APS databases are supported by the National Science Foundation, the National Aeronautics and Space Administration, and the University of Minnesota, and are available at <http://aps.umn.edu>.

tion: at low radio fluxes the fraction of galaxies and AGN compared to the number of quasars is higher than at high radio fluxes. X-ray detection biases and selection effects in the optical identification of the sources also influence the sample composition.

2.1. New Spectroscopic Observations

We obtained low dispersion optical spectra of 108 objects in the RASS-FIRST catalogue over the course of 13 observing runs from 1996 through April 1998 using the Lick 120" Shane reflector plus Kast double spectrograph and the Kitt Peak National Observatory's 2.1-m telescope with the GoldCam spectrograph and F3KC Ford CCD. While most of our observations were of previously unknown bright ($O < 18.5$ mag) objects, some previously known and fainter unclassified objects were also observed as time and observing conditions allowed. Spectra were taken through a 2" slit, resulting in a resolution of 6 Å for the Lick spectra and 4 Å for the Kitt Peak spectra. Wavelength coverage generally extends from 3700Å to 7500Å. At Lick, the slit was always rotated to the parallactic angle. This was not done at Kitt Peak since it adds significant overhead to the observing, but an effort was made to observe objects as they crossed the meridian.

The goal of these observations was to be able to spectroscopically classify these radio- and X-ray-emitting objects as belonging to one of several broadly defined classes - Galactic stars, galaxies, starbursts, BL Lac objects, and broad or narrow-lined AGN. We therefore required spectra with sufficiently high S/N ratios to unambiguously detect features characteristic of these different classes. Simulated spectra consisting of various line widths and strengths plus a Poisson noise contribution show that a broad emission line of $W_\lambda \approx 5$ Å can be detected at a $\sim 4\sigma$ confidence level in a ~ 10 Å resolution spectrum when the $S/N \approx 30$.

Reduction proceeded in the standard manner using IRAF V2.11. Wavelength calibration was carried out using comparison lamps generally taken at the beginning of the night. Comparison of our measured redshifts with published values for previously observed sources shows our values are accurate to ± 0.002 for $z < 1.0$ and ± 0.005 for $z > 1.0$. The latter limit is more uncertain because the high-redshift objects generally exhibit only broad emission lines. Figure 6 shows example spectra corresponding to each of the major spectroscopic classifications (see below). Source name and redshift are given at the top of each panel.

2.2. Data

In Table 1 we present the relevant data for all 843 unique RASS-FIRST matches. We present only a sample page of the table here; a full copy of the table is available from the CDS via anonymous ftp to cdsarc.u-strasbg.fr.

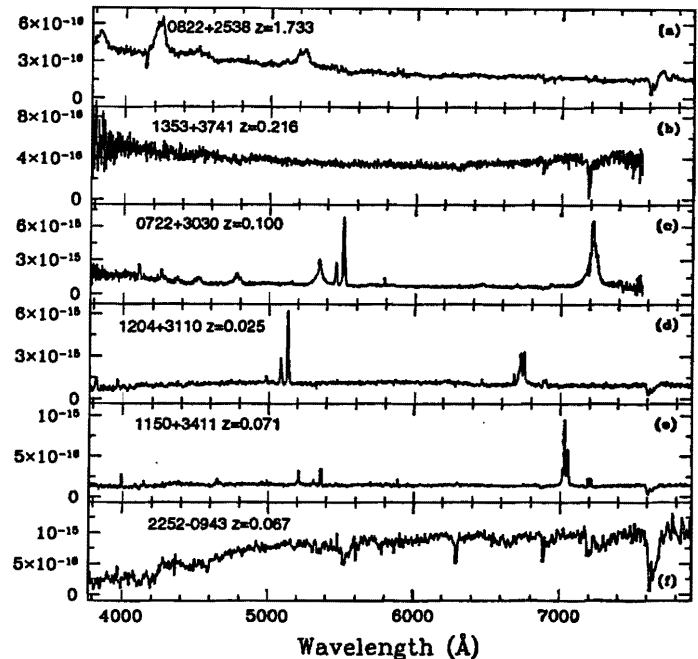


Fig. 6. Sample new spectra for the RASS-FIRST correlation. One object from each major class is shown. From top, (a) Quasar, (b) BL Lac, (c) Broad-line AGN (d) Narrow-line AGN, (e) Starburst, (f) Galaxy.

Column 1 gives the ROSAT All-Sky Survey identification of the X-ray source, followed by the J2000 position of the FIRST source, which is assumed to be the radio counterpart. Column 3 lists the distance in arcsec between the radio and the X-ray source followed by a common name obtained from NED, truncated to the first 14 characters.

The next two entries give the type of the object and the reference for its classification: "QSO" is any object with broad (> 1000 km s^{-1}) lines and $M_B < -22.5$; "A" are narrow line objects (< 1000 km s^{-1}) with $[OIII]/H\beta > 2.0$ and/or $[NII]/H\alpha > 0.6$. "BA" are objects with broad (> 1000 km s^{-1}) lines and $M_B > -22.5$; "H" are starbursts with $[OIII]/H\beta < 2.0$ and/or $[NII]/H\alpha < 0.6$; "G" denote galaxies, objects with no emission lines and Ca II break contrasts $> 30\%$ (but see the definition of BL Lacs given below) and "B" are BL Lacs as defined in Laurent-Muehleisen et al. (1998). "S" are stars and "Cl" are possible clusters (based on the proximity of a known cluster). It should be noted that the galaxy / cluster designation is based on either visual inspection of the optical environment of the source or NED classification of a cluster. For these sources, the multiwavelength fluxes should be treated with caution as the radio and optical emission might be from a galaxy in a cluster whereas the X-ray flux may be dominated by emission from extended cluster gas. Objects denoted by 'rad' are spectroscopically unclassified radio sources, which were part of the RGB survey (B95). For previously known objects, the data found in NED were

used to avoid confusion. For this reason, some objects are designated as “Sy”, “Irs”, “Vis”, “UvE”, etc. In the following analyses, objects with these classifications were either grouped with one of the standard classifications (e.g., quasar) or were excluded if it proved impossible to determine a standard classification. A small number of objects are most likely associated with bright Galactic stars (from Simbad: ‘Smb’) although an optical identification is not always unambiguous so care should be taken with these tentative associations. Objects classified with spectra taken as part of this program are designated “New” in the tables, objects referenced as “id” have been spectroscopically classified and will be discussed in Becker et al. (2000). There also exist several cases where the given identification is ambiguous and/or where there are more than one candidate for the X-ray object at small distances. References for classifications include NED, Simbad, this paper, and the FIRST spectroscopic followup papers W00, Becker et al. (2000), and Gregg et al. (1996).

Following the redshift in column 5, we give the FIRST 1.4 GHz peak flux (in mJy) in column 6. The X-ray flux in the 0.1 - 2.4 keV energy range with its statistical error in units of 10^{-12} erg cm^{-2} s^{-1} (for details see below) is given in column 7, followed by the power-law photon index of the X-ray source deduced under the assumption of Galactic absorption. If no values are given the quality of the data does not allow the determination of a meaningful spectral index. In the following four columns, the E- and O-magnitudes of the optical counterpart are given as well as a value for the classification of the optical object: 1 for ‘non-stellar’, -1 for ‘star-like’, 0 for ‘noise-like’, 2 for ‘possible blend’. We give the extinction correction in column 13 (see Sect. 2) and the the angular distance between radio and optical position (in seconds of arc) in the last column.

Table 2 contains similar information (sans data about optical counterparts; see Sect. 2) for the 518 RASS fields with multiple FIRST counterparts. The first line contains the X-ray flux, classification/redshift (if known) and the following lines contain the X-ray–radio angular separation, position (J2000) and peak radio flux (mJy).

Table 1 shows that about 63% of the $\gtrsim 1400$ classified sources are ‘star-like’, 25% are ‘non-stellar’, and 12% are blends on the O plates. Very few objects are ‘noise-like’. These ratios are slightly different on the E-plates with more objects classified as ‘non-stellar’ and ‘blend’ instead of ‘star-like’. Both classifications are, therefore, given in the table.

We obtained the X-ray fluxes from the measured count rates by assuming an average photon index of $\Gamma = 2.2$ for the underlying X-ray spectrum and Galactic absorption (Dickey & Lockman 1990, Stark et al. 1992; for details see Brinkmann et al. 1994). The stated errors reflect the errors in the counting statistics of the survey sources and do not incorporate deviations from the assumed power-law slope, additional absorption, or systematic errors depending on

the form of the local X-ray background or on details of the detection algorithm. A reasonable estimate of the total error of the X-ray flux is therefore of the order of $\lesssim 25\%$.

The quoted photon indices were estimated using the two hardness ratios given by the RASS II processing (Voges et al. 1999) and applying the method described in Brinkmann et al. (1994), for fixed Galactic absorption. The errors of the power-law indices were estimated from the errors of the hardness ratios (Schartel 1995).

3. The radio to X-ray properties of the objects

The sample of 843 “singly matched” objects contains 241 objects with existing spectroscopic classifications while classifications for an additional 217 sources were obtained through follow-up observations of the FIRST survey or specifically as part of this program. The remaining 385 sources remain spectroscopically unclassified. A more detailed break down into the various classes is given in Table 3.

Table 3. Source contents of the sample

type of object	previous ID	new identifications
quasars	73	73
broad line AGN / Sy	37	42
narrow line AGN	14	14
galaxies	85	14
clusters	8	
BL Lacs	23	48
others		23
total	241	217

According to the classification scheme given above, most of the new identifications listed as ‘others’ are starburst galaxies.

In Fig. 5 we plot the 1.4 GHz radio luminosity of all spectroscopically classified sources as function of redshift. The open circles denote previously known objects, the full dots the newly classified sources from the sample. Many of the objects are close to the lower radio luminosity limit as can be seen from a comparison with Fig. 1 and many of the new identifications cluster around a redshift of ~ 0.15 . Further, there is a substantial number of ‘known’ objects close to the luminosity limit which are not present in Fig. 1. These are previously known objects for which radio counterparts had not previously been identified.

3.1. Flux distributions

In Fig. 7 we show the distribution of the objects as function of their fluxes in the different wavelength bands; (top: peak 1.4 GHz flux density (in mJy); middle: soft X-ray

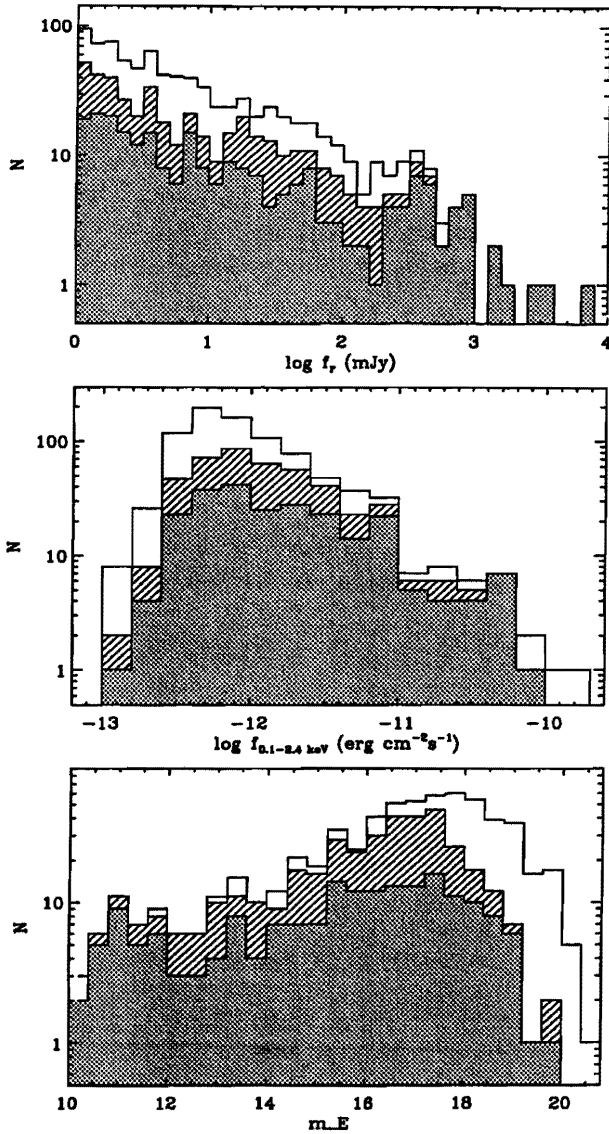


Fig. 7. Distribution of RASS/FIRST sources as function of their fluxes in different wavelength bands. From top to bottom: number of objects per radio flux density, soft 0.1 - 2.4 keV X-ray flux and optical magnitude. The open histograms denote the total sample, the grey-shaded areas indicate previously optically classified objects; the hatched areas represent the newly classified objects.

flux; bottom: optical magnitude m_E , obtained from from the POSS plates).

The top line represents all objects in the sample, the grey shaded areas are the previously known objects, and the hatched regions represent the newly classified objects. The sharp decline in the number of objects at low radio and X-ray fluxes is a direct consequence of the sensitivity limit of the RASS and the corresponding $\log(N) - \log(S)$ distribution (Fig.2 of B95) which shows that the X-ray sensitivity is insufficient to detect radio sources at all flux

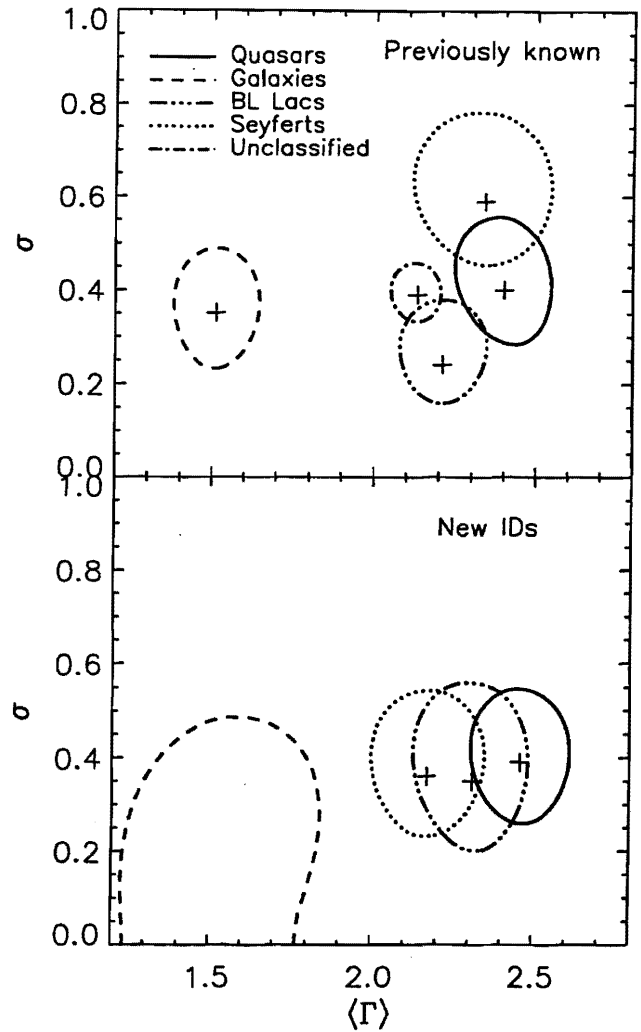


Fig. 8. Best-fit mean spectral index from 0.1 - 2.4 keV and Gaussian standard deviation for power-law fits to different classes of objects assuming Galactic absorption. Contours correspond to 90% confidence levels. Upper panel: previously known objects; lower panel: newly classified sources.

densities at the same rate. Clearly visible are the identification biases with respect to the observed fluxes. This effect is particularly strong for the radio fluxes as most of the sources with fluxes above a few hundred mJy have been identified previously. In the optical band, more than half of the unclassified objects are fainter than 18th magnitude. The figure thus directly reflects previous biases towards identification of stronger sources and demonstrates the importance of sensitive large scale sky surveys for the study and characterization of multi-wavelength class properties of sources.

3.2. X-ray properties

Because the average Survey exposure on a source is rather low (~ 400 s), formal spectral fits can be attempted for only the strongest sources. Fortunately, the low background of the PSPC detector allows an approximate determination of the X-ray spectral parameters from a relatively small number of photons. Spectral fits were therefore obtained for the majority of sources using the hardness ratio method. This method uses the hardness ratios provided by the SASS processing, and maps them onto power law slopes, assuming either free or Galactic absorption (for details of the method see B95). This allows an approximate spectral determination for objects with count rates as low as 0.03 cts/s or even less if the exposure is correspondingly higher. If Galactic absorption is assumed, this leaves only one free parameter in the procedure which is then equivalent to a least squares fit of the underlying power-law slope.

3.2.1. Spectral properties

The results of a maximum-likelihood analysis for the distribution of power-law slopes assuming Galactic N_H for the previously known and the newly classified sources are given in Table 4 (for details of the analysis see Maccacaro et al. 1988, Worrall & Wilkes 1990). The 90% confidence contours for the various classes as a function of spectral index and intrinsic dispersion are shown in Fig. 8.

A significant intrinsic dispersion is an indicator for either the inhomogeneity of the sample; i.e., it consists of different subclasses with different spectral properties grouped together into one larger class (for example for the 'Low Luminosity AGN' group which contains Seyferts and Broad and Narrow line Radio galaxies), or that the individual sources show an intrinsically large dispersion of their spectral properties, perhaps showing intrinsic absorbers, Compton scatterers or other components. Due to the limited photon statistics for most of the sources, we cannot apply more complex spectral models to the data.

The photon indices of the previously known and newly classified sources appear the same to within the 1σ uncertainties. The average index of the unclassified objects indicates that these sources are mostly a mixture of quasars and BL Lacs. The Seyfert class includes all Seyfert subclassifications in NED and, for the newly classified sources, all broad and narrow-line objects, as given in Table 1. This nonspecific classification of all types into one group likely leads to the large dispersion of their spectral index distributions.

In contrast to previous studies of ROSAT - radio correlations (Brinkmann et al. 1994, B95), the galaxy class is characterized by flat spectral indices. This is likely caused by a number of galaxies being members of an X-ray emitting cluster. While the BL Lac objects have a spectral index distribution very similar to those of the RASS-Green

Bank (RGB) sample (see Laurent-Muehleisen et al. 1998, Brinkmann et al. 1997b), the quasar distribution is shifted to steeper slopes and shows a larger dispersion. It appears that, due to the low detection limit of the radio fluxes, we see a smooth transition of the quasar population between radio-loud objects with flat spectral indices (Brinkmann et al. 1997a, B97) and radio-quiet objects with on average considerably steeper spectra (Yuan et al. 1998). The narrow 90% confidence contour (the small error of ± 0.07) for the unclassified sources must be primarily related to the large number of objects.

3.3. The $\alpha_{ro} - \alpha_{ox}$ diagram

Flux ratios combining data from the radio to the X-ray have been extensively used for classification of extragalactic objects (e.g., Tananbaum et al. 1979, Stocke et al. 1991). Based on two-point spectral indices, the radio-to-optical $\alpha_{ro} = \log(S_{\nu_{rad}}/S_{\nu_{opt}})/\log(\nu_{opt}/\nu_{rad})$ and optical-to-X-ray $\alpha_{ox} = -\log(S_{\nu_x}/S_{\nu_{opt}})/\log(\nu_x/\nu_{opt})$, it has been shown that different classes of objects typically populate different regions of the $\alpha_{ro} - \alpha_{ox}$ diagram.

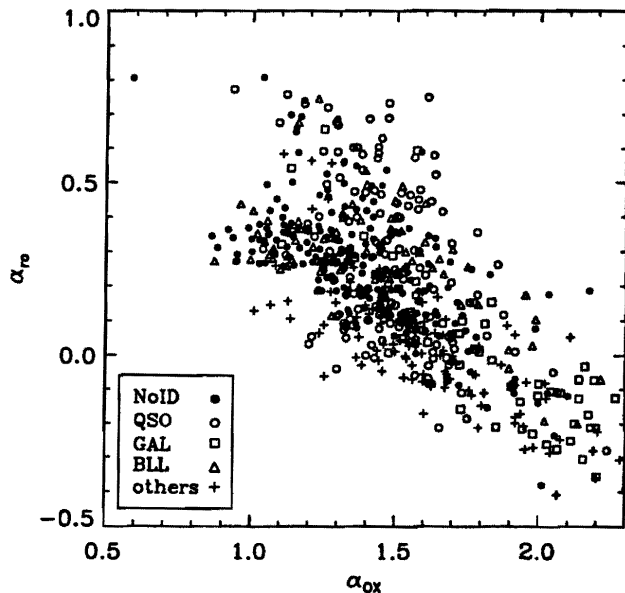


Fig. 9. Broad band energy distribution of all sources. Spectroscopically unclassified objects are marked as bullets, others (plus signs) are all objects in the sample not belonging to one of the indicated classes.

For the construction of the $\alpha_{ro} - \alpha_{ox}$ diagram, the 1.4 GHz VLA flux densities were converted to 5 GHz flux densities by assuming a power law $S_{\nu} \sim \nu^{-\alpha}$, with slope $\alpha_r = 0.5$. For the monochromatic optical fluxes at 2500 Å we took the E-magnitudes from the POSS plates and an optical power-law slope $\alpha_o = 0.5$. The monochromatic X-

Table 4.

Object class	Previously known			Newly classified		
	N	$\bar{\Gamma} \pm 1\sigma$	σ^{intr}	N	$\bar{\Gamma} \pm 1\sigma$	σ^{intr}
Quasars	58	2.40±0.15	0.40±0.16	57	2.46±0.15	0.39±0.16
Galaxies	62	1.51±0.14	0.35±0.14	8	1.50±0.34	0.0±0.49
Low Lum. AGN	42	2.34±0.22	0.59±0.19	39	2.17±0.18	0.36±0.18
BL Lacs	22	2.21±0.14	0.24±0.14	36	2.31±0.18	0.35±0.21
Unclassified	250	2.13±0.08	0.39±0.07			

ray fluxes at 2 keV were computed from the (0.1 - 2.4 keV) fluxes assuming a power law with an average photon index of $\langle \Gamma \rangle = 2.2$. The adoption of this mean value allows us to avoid the large scatter of the spectral indices introduced by the limited photon statistics, although in some cases it may result in an incorrect flux determination if the actual spectral index of a source truly differs from the mean value.

In contrast to similar diagrams (B95, Brinkmann et al. 1994), the fluxes are not K-corrected as the types and the redshifts of many of the objects remain unknown. The shift in phase space expected from the K-corrections for, e.g., an object at $z = 1$ with the above typical quasar power-law slopes is, however, rather small: $\Delta\alpha_{ox} \leq 0.1$, while the value of α_{ro} does not change for the assumed spectral indices.

The majority of known objects are found along the diagonal swath from high- α_{ro} and low- α_{ox} to low- α_{ro} and high- α_{ox} , the region generally occupied by radio-loud quasars and blazars, and, at large α_{ox} values, by bright galaxies with low X-ray and radio emission. Many of the unclassified objects are found in the region of classical X-ray selected BL Lacs, i.e., at $0.0 \leq \alpha_{ro} \leq 0.5$ and $\alpha_{ox} \leq 1.6$, although a large fraction of them have $\alpha_{ox} > 1.4$ indicating a more intermediate nature. In contrast to the RGB sample, the upper left of the diagram remains empty, i.e., there are no objects with unusually low optical fluxes but with strong radio- and X-ray emission (so-called "Optically Quiet Quasars", see Kollgaard et al. 1995).

Most of the classified objects are found in the region of phase space typical for their class; few sources appear to be misplaced, possibly due to questionable classification, incorrect association of the radio/optical/X-ray sources, or spectral properties largely different from the average values for a particular subclass.

3.4. Flux ratios

Because we lack redshifts for many sources, we cannot employ luminosity correlations to study the bulk emission properties of the sample. Instead, flux ratios pro-

vide distance-independent measures of emission characteristics, neglecting K-corrections. In Fig. 10 we show from top to bottom the flux ratios f_x/f_r versus f_{opt}/f_r for quasars, BL Lacs, galaxies, and the spectroscopically unclassified objects, respectively. The open symbols represent objects which have been classified previously, although not necessarily identified with a radio counterpart. For comparison with previous papers, we have used the monochromatic X-ray fluxes at 2 keV, optical fluxes at 2500 Å, and radio fluxes at 5 GHz.

While many of the previously known quasars occupy the phase space of classical radio-loud objects (see Fig. 16 of B97), most of the newly classified quasars are found in the 'radio-intermediate' transition region between radio-loud and radio-quiet quasars (see W00). A similar situation holds for the BL Lac objects where the newly classified sources reside primarily in an intermediate region between the HBL (High energy peaked BL Lacs) and LBL (Low energy peaked, Giommi & Padovani 1994) classes. These Intermediate BL Lacs have been found previously in the RGB survey (Laurent-Muehleisen et al. 1999), as well as in the DXRBS (Deep X-ray Radio Blazar Survey; Perlman et al. 1996) and REX (Radio Emitting X-ray; Caccianiga et al. 1999) surveys. A large number of unclassified objects inhabit the same region of phase space as the intermediate BL Lacs and thus it is expected that many of these objects are BL Lac objects or extreme flat-spectrum quasars.

Most of the galaxies were previously known. Three objects with extreme flux ratios at the left at low f_o/f_r ratios might be misidentifications: a classification for one (RXS J1504.5+2854) is based on a low signal-to-noise spectrum while the other two (RXS J1317.3+3925 and RXS J1625.5+2705) have X-ray luminosities of $> 5 \times 10^{45}$ erg s⁻¹ and $> 5 \times 10^{45}$ erg s⁻¹, respectively, far in excess of that expected from a galaxy. These "optically passive X-ray galaxies" have been seen in a number of other surveys including the RGB (Laurent-Muehleisen et al. 1998), the Einstein Two-Sigma catalog (Moran et al. 1996) and some deep ROSAT PSPC fields (Griffiths et al. 1995). These sources are good candidates for new clusters, since that could easily account for the large X-ray luminosity

associated with these optically unremarkable sources, although other explanations including hidden AGN or early type galaxies with an extraordinarily hot ISM are also possible.

4. Specific classes

The FIRST radio survey is a factor of ~ 3 more sensitive than other large-scale radio surveys, deep enough to see transitional populations, such as quasars intermediate between typically 'radio-loud' to 'radio-quiet' objects.

4.1. Quasars

Quasars, the largest individual group of objects in our sample, are traditionally divided into a radio-quiet and a radio-loud class, with apparently markedly different properties (Kellerman et al. 1989, B97, Yuan et al. 1998).

Figure 11 shows the radio-loudness distribution of all quasars. The top line represents all quasars, while the hatched region denotes newly classified quasars. Classical radio-loud quasars typically have $3 \lesssim \log R \lesssim 4$ (see Fig. 16 of B97). The histogram shows that most RASS-FIRST quasars have $\log R$ values near the radio-quiet - radio-loud transition and there is no evidence for a radio-loud / radio-quiet bimodality. These results are consistent with those of the FIRST Bright Quasar Survey (FBQS; W00) which showed that the distribution of R for a large sample FIRST-selected quasars falls steadily from $\log R \approx 0.5$ to $\log R \approx 3$ and that when the insensitivity of the FIRST survey to quasars with $\log R \leq 0.5$ is taken into account, the distribution of R should rise smoothly down to $\log R = -0.5$ (see Fig. 15 in W00). Previously known quasars exhibited a bimodal distribution in R . W00 conclude that the FBQS result is not due to selection effects arising in the FIRST survey, but rather the sensitivity of the FIRST survey to sources with intermediate values of R . Our data show there are a large number of 'previously known' (X-ray bright) quasars at $\log R \lesssim 0.5$, i.e., in the intermediate regime between radio-loud and radio-quiet. With a few exceptions, these objects have very low 1.4 GHz fluxes (1 - 3 mJy) and previously were not associated with any known radio source.

4.1.1. Spectral variations

The average X-ray power-law slopes of the RASS/FIRST quasars are steeper than those of radio-loud quasars, but flatter than those of radio-quiet quasars (Sect. 3.2.1). Previously, it was thought that the X-ray photon index correlates with radio-loudness R (Williams et al. 1992), however, in B97 it was argued that radio-loudness, core dominance, and radio spectral slope are, in the framework of unification schemes, similar indicators for the orientation of the source and thus the principal origin of the correlations between the X-ray spectra and the radio properties of the quasars remains unknown. A further complication

is introduced by redshift-dependent effects, caused by different redshift distributions of the samples.

The present study's quasars constitute a low-redshift sample: 107 of the 146 total objects are at $z \leq 1.0$ and only four are at $z > 2$ (one of them is the $z=4.71$ object RXS J1430.4+4204). A regression analysis, disregarding six quasars without redshift information and the extreme $z=4.71$ object, shows that the slopes follow a redshift dependence like $\Gamma = (2.586 \pm 0.179) - (0.230 \pm 0.199) \times z$. The errors are at 95% confidence and the 'no regression' hypothesis is rejected at the 97.4% confidence level. These values are very similar to the results found for radio-quiet quasars ($\Gamma = 2.63 - 0.20 \times z$, Yuan et al. 1998), however with larger errors due to the smaller sample size. Classical radio-loud quasars show a smaller value for $\Gamma_{z=0}$ (~ 2.28 ; B97).

If radio-loud quasars are physically different objects from radio-quiet quasars, the photon index should not depend on the orientation. A correlation between X-ray slope and radio-loudness, where the values of R cover the transition between radio-loud and radio-quiet objects, might indicate an intrinsic physical transition between these two classes. Indeed, as suggested from Fig. 12 there exists a correlation between these quantities: $\Gamma = (2.58 \pm 0.145) - (0.132 \pm 0.082) \times \log R$ and the 'no-regression' hypothesis can be rejected with 99.79% confidence, although the scatter of the photon indices as well as the errors of the individual slopes are rather large. A correlation between Γ and R might be introduced by redshift effects: Γ varies with redshift due to the intrinsic curvature of the spectrum and the radio-loudness correlates with z ($\log R = (0.457 \pm 0.3659) + (1.077 \pm 0.407) \times z$, at 99.9% confidence). This is, at least partly, a result of the flux-limits of the radio selection such that at larger redshifts only the radio-loudest objects are detected. To assess quantitatively the extent of a spurious correlation introduced by distance effects, the partial linear correlation coefficient $R_{\Gamma, \log R; z}$ (e.g. Hald 1962, Kembhavi et al. 1986) can be used. We determined the partial correlation coefficients $R_{\Gamma, \log R; z}$ with the effect of redshift eliminated and found that the no-regression hypothesis is rejected at the 17.8% confidence level only, which means that the $\Gamma - \log R$ correlation could be just a redshift dependent selection effect.

Finally, we performed a regression analysis for both the extreme ends of the $\Gamma - \log R$ - distribution, checking the radio-quiet and the radio-loud sample separately. For the objects with $\log R \leq 1$ we obtain $\Gamma = (2.63 \pm 0.148) - (0.129 \pm 0.268) \times \log R$ with the 'no-regression' hypothesis rejected at the 64.9% confidence level only. For the radio-loud quasars ($\log R > 1$) we get $\Gamma = (2.25 \pm 0.432) - (0.006 \pm 0.176) \times \log R$ at a 5.1% confidence level. Both the low confidence levels as well as the large errors indicate that we are seeing the two different slopes of the radio-quiet and radio-loud quasar population, with nearly the

same average values as found for the two classes previously (B97, Yuan et al. 1998).

4.1.2. Luminosity correlations

A knowledge of the exact form of the luminosity correlations $L_x \sim L_o^{\beta_o}$ and $L_x \sim L_r^{\beta_r}$ is required to relate the quasar statistics (e.g., evolution, luminosity function) in the different wave-bands and to understand the quasars' broad-band emission. Early studies usually found values for the slopes of $\beta_i \neq 1$, but follow-up programs produced results which differed markedly and also seemed to depend not only on the quasar selection criteria but also on the exact correlation method (see the discussion by Padovani 1992, Franceschini et al. 1994, and La Franca et al. 1995). B97 and Yuan et al. (1998) showed convincingly, by using orthogonal direction regression (ODR) analysis, that $\beta_o \sim 1$ and that the value obtained for β_r depends on the core dominance of the radio emission. For highly beamed sources, the X-ray luminosity correlated linearly with the core radio flux but in general both the core flux as well as the total radio flux contribute to the correlation. Further, using a generalized ODR analysis which takes into account measurement errors as well as allowing for intrinsic variances (Fasano & Vio 1988, (FV88)), the correlation yielded non-zero intrinsic variances in all cases, i.e., the data scatter (intrinsically) around the regression line.

Figure 13 presents the correlation between the monochromatic (in $\text{erg s}^{-1} \text{Hz}^{-1}$) X-ray and radio luminosities, where radio-loud objects ($\log R > 1$) are indicated by open symbols, and radio-quiet quasars ($\log R \leq 1$) by filled symbols. Applying the FV88 ODR analysis, and assuming a typical error for the radio flux of 5% and for the X-ray flux of 30% (B95), the radio-loud subgroup shows a correlation of the form $l_x = (11.22 \pm 1.63) + (0.483 \pm 0.049) \times l_r$, with an intrinsic variance $\sigma_{rl} = 0.180 \pm 0.028$. For the radio-quiet objects, this correlation is $l_x = (-4.57 \pm 2.55) + (1.012 \pm 0.083) \times l_r$, with an intrinsic variance of $\sigma_{rq} = 0.245 \pm 0.05$. The slope for the radio-loud objects is very similar to that found in B97 for the correlation between the X-ray and total radio luminosity. This, as well as the large value of the intrinsic variance, indicates an inhomogeneous population of resolved and unresolved radio sources. The slope of $\beta_{rq} \sim 1$ is a strong indicator that in radio-quiet quasars the radio emission is a direct tracer of the nuclear activity, as in radio-loud quasars with high core dominance. This is consistent with the results of a VLA study of nearby low-redshift radio-quiet quasars where Kukula et al. (1998) find that the radio emission originates in a compact nuclear source, directly associated with the central engine of the quasar and that radio-quiet quasars generally have steep spectral indices ($\alpha_r \sim 0.7$).

The most radio- and X-ray luminous object is the $z=4.715$ quasar B3 1428+422, a known radio-loud ROSAT source (B95) only recently classified as a quasar (Hook &

McMahon 1998). It appears that at a given radio luminosity, radio-quiet quasars have a larger X-ray luminosity, however, at a given radio luminosity, a radio-quiet quasar is optically brighter than a radio-loud quasar. And indeed, the $l_x - l_o$ correlation (Fig.14) indicates that the X-ray luminosity scales similarly with optical luminosity for both types of quasars ($l_x = (-16.56 \pm 2.83) + (1.419 \pm 0.092) \times l_o$), with the well-known tendency that radio-loud quasars are X-ray brighter at a given optical luminosity (B97).

Table 5. Average Monochromatic Quasar luminosities (in $\text{erg s}^{-1} \text{Hz}^{-1}$)

type	L_{rad}	L_{opt}	L_x
radio-quiet	$2.41 \cdot 10^{31}$	$8.11 \cdot 10^{30}$	$1.40 \cdot 10^{28}$
radio-loud	$1.23 \cdot 10^{34}$	$1.43 \cdot 10^{31}$	$3.92 \cdot 10^{28}$

This raises the question which of the three energy bands provides the most direct measure of a quasar's activity. Table 5 lists the average monochromatic luminosities (in $\text{erg s}^{-1} \text{Hz}^{-1}$) of the two quasar populations (radio-loud vs. radio-quiet). The optical luminosities differ by a factor of order unity, and the X-ray luminosities of radio-loud quasars are higher by a factor of ~ 3 (and depend further on the the radio properties of the objects, B97). The radio-luminosities are differ greatly and seem to be the main separator of the two classes. Selection effects and the small sample sizes do not allow more quantitative conclusions.

The two classes of quasars populate distinct regions in the $\log(l_x) - \log(l_o) - \log(l_r)$ phase space - the dividing plane is $\log(l_o/l_r) = 1$ for all $\log(l_x)$. Any two-dimensional plot is thus only a projection of this distribution. Apart from the above mentioned different averages, the radio-loud quasars show a more 'compact' distribution, while the radio-quiet objects have a larger dispersion.

The relatively large intrinsic dispersion of $\sigma = 0.35 \pm 0.06$ obtained from the FV88 ODR regression analysis for the $\log(l_x) - \log(l_o)$ correlation is directly visible in Fig. 14 and is mainly caused by low-luminosity radio-quiet objects. Most of the 'optical outliers' at low X-ray luminosities in the figure are newly classified quasars. While it is possible there is a systematic overestimation of the source's optical brightnesses by as much as 0.3 mag (see W00), this alone cannot account for the large offsets. Other possible causes are incorrect K-corrections due to unusual spectral slopes, strong variability of the X-ray emission, or genuine luminosity differences. Previous ROSAT studies of quasars (B97, Yuan et al. 1998) also found a small fraction of objects which seem to deviate significantly from the usual trend.

4.2. Galaxies

The second largest group of objects in the RASS-FIRST correlation are the 99 galaxies. We lack complete information for all of these, and therefore limit our discussion to the 59 galaxies for which all fluxes and redshifts are available and believed to be reliable.

Figure 15 shows the X-ray versus radio luminosity. Galaxies extend to lower luminosities from the quasar population (Fig. 14), with a general trend of lower X-ray luminosities at similar optical luminosities, although with some overlap. The most luminous X-ray galaxy is RGB J1514+366. The radio position coincides with the $z=2.723$ protogalaxy cB58 which would result in an extreme X-ray luminosity from the source of $L_{0.1-2.4 \text{ keV}} \sim 10^{46} \text{ erg s}^{-1}$. It appears likely that the dominant part of the X-ray emission is either from the positionally coincident cluster of galaxies MS 1512.4+3647 or, as proposed by Hamana et al. (1997), the X-ray flux from cB58 is amplified by gravitational lensing from the foreground cluster.

Two other galaxies with unusually high radio and X-ray luminosities are RXS J1625.5+2705 (87GB 1623+2712) and RXS J1317.3+3925 (B3 1315+396). Both are at high redshift indicating the galaxy classification could be in error. Classifications for both these sources come from NED, and we have no independent measurement of these objects' optical spectra. RXS J1625.5+2705 is classified by Stocke et al. (1991) as an 'AGN' and B3 1315+396 seems to be a genuine quasar (Vigotti et al. 1990). Even after eliminating these three objects from consideration, the galaxy $l_x - l_{opt}$ as well as the $l_{opt} - l_r$ relations do not indicate any correlation. All galaxies (with the exception of the above three suspicious cases) are found at redshifts below $z = 0.3$. While the $l_x - z$ as well as the $l_r - z$ plots display cutoffs due to the flux limits of the corresponding surveys, the optical luminosities are unaffected by redshift related selection effects.

4.3. BL Lacs

A total of 71 objects are classified as BL Lacs or as possible BL Lacs. Redshift information is available for 41 of these, including 12 previously known BL Lacs. The newly discovered objects have generally lower X-ray and radio luminosities than the previously known sources. As suggested in Fig. 9, the flux ratios indicate that the 'previously known' BL Lacs populate the traditional 'X-ray selected' BL Lac region while the new objects belong to the 'radio-selected BL Lac' branch and extend into the region of phase space traditionally occupied by galaxies.

This transitional nature is demonstrated in Fig. 16 where we show the distribution of the radio - to -X-ray spectral index, α_{rx} , of various well known BL Lac samples, including the 'radio selected' 1 Jy BL Lacs (RBLs) and the 'X-ray selected' EMSS BL Lacs (XBLs). The dashed line represents the classical division between X-ray and

radio-selected BL Lacs (Padovani & Giommi 1996). The FIRST-RASS BL Lacs (thick line) are mainly 'intermediate' objects like those of the RGB sample (Siebert et al. 1999, Laurent-Muehleisen et al. 1999) clearly demonstrating that at least part of the previously claimed bimodality of the BL Lac population must be attributed to selection effects. The soft X-ray spectral indices are found in the same range as the 'classical' BL Lacs (Fig. 8 and Fig. 2 of Brinkmann et al. 1996). The luminosities of the current sample extend to lower values both in $\log(l_x)$ and $\log(l_r)$ than the XBL population in Fig. 3a of Brinkmann et al. (1996), while the optical luminosity is on average higher than the optical luminosities of previously known the XBLs (Fig. 3b of Brinkmann et al. 1996).

4.4. AGN

The remaining large subclass contains 117 AGN, categorized as 'broad emission line AGN' ('BA' in table 1: 48 objects), 'narrow emission line AGN' ('A': 21 objects), and 28 previously classified Seyfert galaxies of various types, as found from NED. We also group the 20 starburst galaxies ('H' in the tables) into the present discussion.

The lowest X-ray luminosities ($l_x < 10^{24} \text{ erg s}^{-1} \text{ Hz}^{-1}$) are exhibited by the narrow-line objects RXS J0316.0-0226, RXS J0919.0+2616, RXS J1204.7+3110, and RXS J1258.6+2736. These sources are classified in NED as galaxies, with various peculiarities which would justify a more detailed study. In addition, the Seyfert 1 galaxy RXS J 1220.1+2916 has an X-ray luminosity below the lower plot boundary. The only other broad-line AGN with such a low X-ray luminosity in Figs. 17 or 18 is RXS J1140.2+2441 which is also classified as a 'galaxy' in NED. However, all these objects show emission-line properties which indicate AGN-activity, but their low luminosity undoubtedly signals a very weak nucleus.

Another aberrant group of objects are some extremely X-ray and radio luminous Broad-lined AGN, like RXS J0035.9-0912, RXS J0746.0+2226, and RXS J2228.9-0753, all at rather high redshifts $z > 0.6$. From their deduced absolute optical magnitudes they are borderline objects, still belonging to the AGN class, but with X-ray and radio luminosities like low luminosity radio-loud quasars.

There are clear correlations between the X-ray and the radio luminosities for all classes. Interestingly the starbursts ("H") are narrowly confined in $l_x - l_r$ phase space by about an order of magnitude in both luminosities while the other groups exhibit a much larger dispersion. The X-ray luminosity shows no dependence on optical luminosity for any of the classes (Fig. 18). The narrow emission line sources and the Seyferts span the entire optical luminosity range between $29 \lesssim \log(l_{opt}) \lesssim 32$ whereas the broad-line objects and the starbursts are considerably optically fainter and exhibit a narrow distribution of optical luminosities $29 \lesssim \log(l_{opt}) \lesssim 30$, where the luminosities are

given in $\text{erg s}^{-1} \text{Hz}^{-1}$. However, the narrow-line objects have the on average lowest X-ray luminosities.

4.5. Unclassified sources

Nearly half of the objects in the sample are presently spectroscopically unclassified. The obvious reason for this can be seen immediately in Fig. 19, where we plot the E-magnitude versus the logarithm of the 1.4 GHz flux for all objects. Open circles are classified sources, solid circles are unclassified. Most of the unclassified objects are at faint optical magnitudes, directly indicating a selection bias. Some unclassified objects are rather bright: in most cases they are confused regions requiring a detailed identification effort or the positions are close to bright stars, complicating spectroscopic observations.

Interestingly, the flux ratios (Fig. 10) show that most of the unclassified objects belong to the region of phase space typically populated by BL Lacs. These objects' average X-ray spectral indices are also similar to those exhibited by BL Lacs. The large dispersion, however, indicates a mixture of object classifications. Finally, a certain number of the formally 'classified' objects must strictly be regarded as 'unclassified', for example, galaxies that might be members of clusters or objects classified as 'galaxies' purely by their appearance on optical plates, without spectroscopic confirmation.

5. Conclusions

We have presented the broad band properties of a sample of 843 radio emitting X-ray sources, obtained from a correlation of the FIRST 1.4 GHz survey and ROSAT All-Sky Survey. About half of the sources remain to be spectroscopically classified. The other half have been classified previously, many as part of independent followup FIRST programs or with data obtained specifically for this project.

The largest class of objects are quasars. Due to the low limiting radio flux of $\sim 1 \text{ mJy}$ of the FIRST survey, the radio-loudnesses of the sources ranges from classical radio-loud to radio-quiet objects. No bimodality is found in the distribution of R , indicating that the previously observed sharp boundary between radio-loud and -quiet objects is related to the higher flux limits of previous radio surveys.

The X-ray luminosity correlates with both the optical and the radio luminosities. Interestingly, the radio-quiet subclass exhibits a good linear correlation between $\log(l_x)$ and $\log(l_r)$, even though the radio-emission of these objects is typically a factor of 500 weaker than it is in radio-loud quasars. This indicates a common origin of the emission from the compact cores of the quasars. This direct correlation is found in 'classical' radio-loud quasars only for objects with very high core dominances (B97). It therefore seems plausible that these intermediate, radio-emitting (but radio-quiet) quasars are objects

where we see the radio emission only because of a favorable orientation of the jets to the line of sight and a corresponding Doppler boosting. 'Classical' radio-quiet quasars might also have radio-emission connected with their X-ray emission, but their unfavorable orientation makes their radio fluxes undetectable (see also Falcke et al. 1995). A clarification of these questions might come from the measurement of the radio spectral slopes of these objects as classical radio-loud core-dominant quasars usually are flat spectrum objects while radio-quiet quasars generally have steep spectral indices (Kukula et al. 1998).

The 71 BL Lacs (23 previously known and 48 newly classified) are mostly 'intermediate' between the HBL and LBL subclasses, again indicating that the previously claimed bimodality was an artifact of the considerably higher flux limits characteristic of earlier surveys. Interestingly, in terms of their luminosities, the newly classified objects constitute a low-luminosity extension (in both radio and X-ray) to the XBL class (see Fig. 3a of Brinkmann et al. 1996).

The galaxies and low-luminosity AGN constitute rather inhomogeneous samples. In a limited number of cases, the identifications appear questionable or, at least, insufficiently detailed. Some of the galaxies may reside in X-ray luminous clusters, artificially enhancing their reported X-ray luminosities, while others appear to legitimately produce X-ray luminosities that border on that of quasars. Broad emission line AGN show the highest radio luminosities and have, like Seyferts, the highest X-ray luminosities; narrow emission line AGN are most prominent at optical luminosities.

More than 400 objects remain unclassified. As these typically populate the regions of fainter optical fluxes, spectroscopy represents a cumbersome task. Their broad-band properties indicate that many of them are BL Lacs.

The ROSAT - FIRST sample indicates that there is a smooth transition from radio-quiet to radio-loud AGN of various types. These new objects, many at the faintest fluxes measured so far for their individual classes, often have properties deviating from the bulk properties of their class, indicating the transition to the other, less luminous types of objects.

Acknowledgements. The ROSAT project is supported by the Bundesministerium für Bildung, Wissenschaft, Forschung und Technologie (BMBF) and the Max-Planck-Gesellschaft. We thank our colleagues from the ROSAT group for their support. The success of the FIRST survey is in large measure due to the generous support of a number of organizations. In particular, we acknowledge support from the NRAO, the NSF (grants AST-98-02791 and AST-98-02732), The NASA ADP program (NAG5-8391), the Institute of Geophysics and Planetary Physics (operated under the auspices of the U.S. Department of Energy by Lawrence Livermore National Laboratory under contract No. W-7405-Eng-48), the Space Telescope Science Institute, NATO, the National Geographic Society (grant NGS No. 5393-094), Columbia University, and Sun Microsystems. This research has made use of the SIMBAD database

operated at CDS, Strasbourg, France and the NASA/IPAC Extragalactic Data Base (NED) which is operated by the Jet Propulsion Laboratory, California Institute of Technology, under contract with the National Aeronautics and Space Administration.

References

- Antonucci R.R.J., 1993, ARA&A 31, 473
 Avni Y., Tananbaum H., 1986, ApJ 305, 83
 Barthel P.D., 1989, ApJ 336, 319
 Becker R.H., White R.L., Helfand D.J., 1995, ApJ 450, 559
 Becker R.H., White R.L., Price T., et al., 2000, submitted to ApJ
 Brinkmann W., Siebert J., Boller Th., 1994, A&A 281, 355
 Brinkmann W., Siebert J., Reich W., et al., 1995, A&AS 109, 147 (B95)
 Brinkmann W., Siebert J., Kollgaard R.I., Thomas H.-C., 1996, A&A 313, 356
 Brinkmann W., Yuan W., Siebert J., 1997a, A&A 319, 413 (B97)
 Brinkmann W., Siebert J., Feigelson E.D., et al., 1997b, A&A 323, 739
 Caccianiga A., Maccacaro R., Wolter A., et al. 1999, ApJ 513, 51
 Condon J.J., Broderick J.J., Seielstad G.A., 1989, AJ 97, 1064
 Dickey J.M., Lockman F.J., 1990, ARA&A 28, 215
 Falcke H., Malkan M.A., Biermann P.L., 1995, A&A 298, 375
 Fasano G., Vio R., 1988, Newsletter of the Working Group for "Modern Astronomical Methodology", 7, 2 (FV88)
 Franceschini A., La Franca F., Cristiani S., Mirones J.M., 1994, MNRAS 269, 683
 Giommi P., Padovani P., 1994, MNRAS 268, L51
 Gliozzi M., Brinkmann W., Laurent-Muehleisen S.A., Takalo L.O., Sillanpää, A., 1999, A&A 352, 437
 Gregg M. D., Becker R. H., White R. L., et al., 1996, AJ 112, 407
 Griffiths R. E., Georgantopoulos I., Boyle B. J., et al., 1995, MNRAS, 275, 77
 Hamana T., Hattori M., Ebeling H., et al., 1997, ApJ 484, 574
 Hald A., 1962, Statistical Theory with Engineering Applications, John Wiley, New York
 Hook I.M., McMahon R.G., 1998, MNRAS 294, L7
 Kellermann K. I., Sramek R. A., Schmidt M., et al., 1989, AJ 98, 1195
 Kembhavi A., Feigelson E.D., Singh K.P., 1986, MNRAS 220, 51
 Kollgaard R. I., Feigelson E. D., Laurent-Muehleisen S. A. et al., 1995, ApJ 449, 61
 Kühr H., Nauber U., Pauliny-Toth I.I.K., Witzel A., 1979, MPIfR preprint No. 55
 Kühr H., Witzel A., Pauliny-Toth I.I.K., Nauber U., 1981a, A&AS 45, 367
 Kukula M.J., Dunlop J.S., Hughes D.H., Rawlings S., 1998, MNRAS 297, 366
 La Franca F., Franceschini A., Cristiani S., Vio R., 1995, A&A 299, 19
 Laurent-Muehleisen S.A., Kollgaard R.I., Ryan P.J., et al., 1997, A&AS 122, 235
 Laurent-Muehleisen S.A., Kollgaard R.I., Ciardullo, R.B., et al., 1998, ApJS 118, 127
 Laurent-Muehleisen S.A., Kollgaard R.I., Feigelson E.D., Brinkmann W., Siebert J., 1999, ApJ 525, 127
 Maccacaro T., Gioia I. M., Wolter A., Zamorani G., Stocke J., 1988, ApJ 326, 680
 McMahon R.G., 1991, in: The Space Distribution of Quasars, Ed. D. Crampton, ASP Conference Series, Vol 21, p. 129
 McMahon, R. G., White, R. L., Helfand, D. J. & Becker, R. H., 2000, ApJS, submitted
 Moran E. C., Helfand D. J., Becker R. H., et al., 1996, ApJ 461, 127
 Orr M.J.L., Browne I.W.A., 1982, MNRAS 200, 1067
 Padovani P., 1992, A&A 256, 399
 Padovani P., Giommi P., 1996, MNRAS 279, 526
 Pennington R.L., Humphreys R.M., Odewahn S.C., Zumach W., Thurmes P.M., 1993, PASP 105, 521
 Periman E. S., Stocke J. T., Wang Q. D., et al. 1996, ApJ 456, 451
 Schärtel N., 1995, PhD thesis, University of München
 Siebert J., Brinkmann W., Laurent-Muehleisen S.A., 1999, in: The BL Lac Phenomenon, eds. L.O. Takalo, A. Sillanpää, APS Conference Series 159, 172
 Stark A.A., Gammie C.F., Wilson R.W., 1992, ApJS 79, 77
 Stocke J.T., Morris S.L., Gioia I.M., et al., 1991, ApJS 76, 813
 Stocke J.T., Morris S.L., Weymann R.J., Foltz C.B., 1992, ApJ 396, 487
 Tananbaum H., Avni Y., Branduardi G., et al., 1979, ApJ 234, L9
 Trümper J., 1983, Adv. Space Res. Vol. 2, No. 4, 241
 Urry C. M., Padovani P., 1995, PASP 107, 803
 Vigotti M., Merighi R., Vettolani G., Lahulla J.F., Lopez-Arroyo M., 1990, A&AS 83, 205
 Voges W., 1992, In: Proc. of the ISY Conference "Space Science", ESA ISY-3, ESA Publications, p.9
 Voges W., Aschenbach B., Boller Th., et al., 1999, A&A 349, 389
 White R.L., Becker R.H., Helfand D.J., Gregg M.D., 1997, ApJ 475, 479
 White R.L., Becker R.H., Gregg M.D., et al., 2000, ApJ in press (W00)
 Wilkes B.J., Tananbaum H., Worrall D., et al., 1994, ApJ Suppl 92, 53
 Williams O.R., Turner M.J.L., Stewart G.C., et al., 1992, ApJ 389, 157
 Windhorst R.A., Kron R.G., Koo D.C., 1984, A&AS 58, 39
 Worrall D.M., Wilkes B.J., 1990, ApJ 360, 396
 Worrall D.M., Giommi P., Tananbaum H., Zamorani G., 1987, ApJ 313, 596
 Yuan W., Brinkmann W., Siebert J., 1998, A&A 330, 108

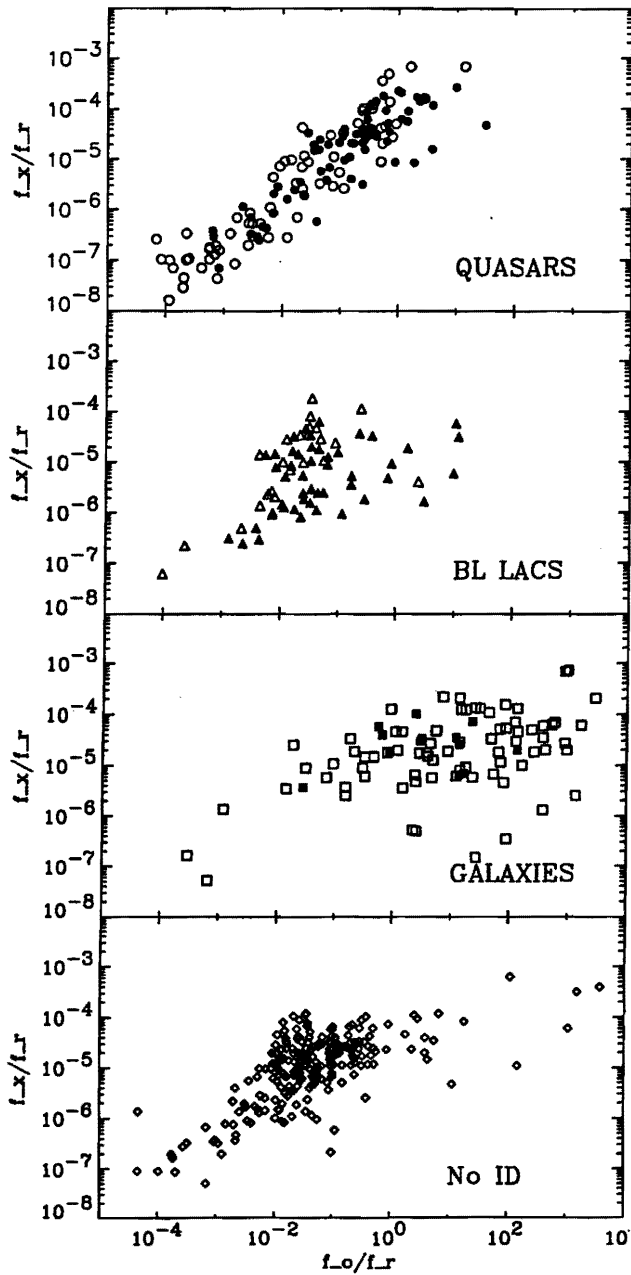


Fig. 10. Logarithmic flux ratios f_x/f_r versus f_{opt}/f_r for quasars (top panel), BL Lac objects, galaxies, and spectroscopically unclassified objects (bottom panel). Open and filled symbols represent previously and newly classified sources, respectively.

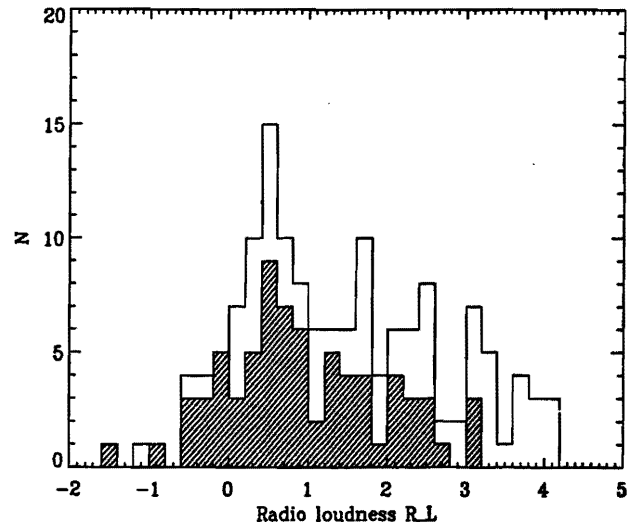


Fig. 11. Distribution of quasars as function of their radio-loudness $\log R$. The top line represents all quasars, the hatched region indicates the newly classified quasars.

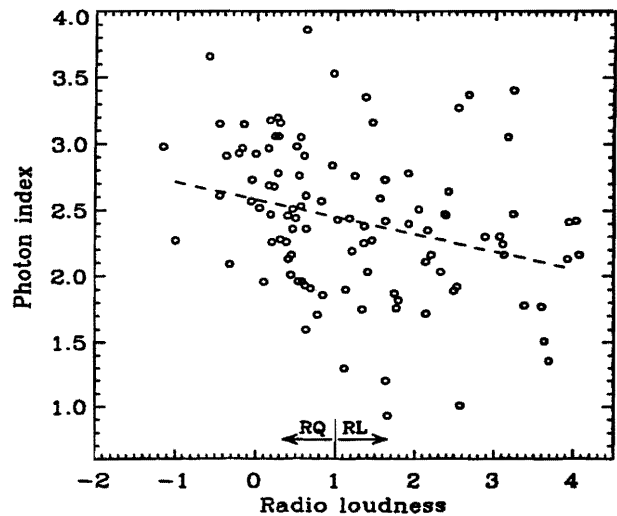


Fig. 12. X-ray photon indices of the quasars as a function of their radio-loudness R . The vertical line at $\log R = 1$ indicates the formal separation between radio-quiet and radio-loud objects. The dashed line represents the regression line.

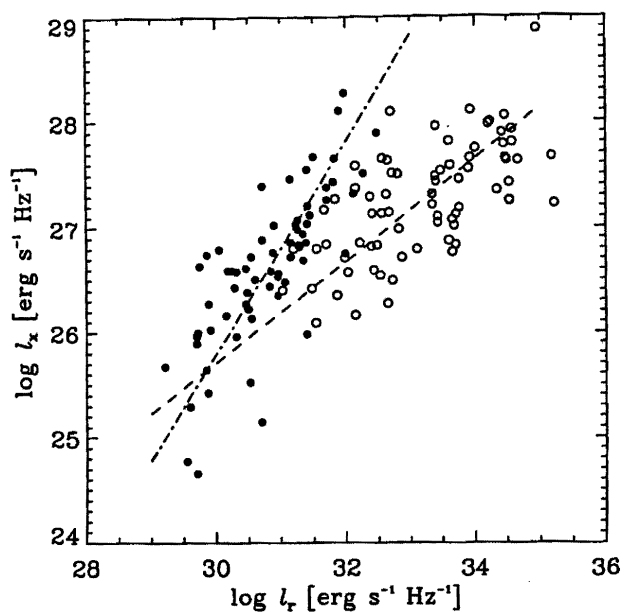


Fig. 13. The quasars' monochromatic X-ray luminosity as a function of the radio luminosity. Filled dots represent radio-quiet objects ($\log R \leq 1$), open dots radio-loud quasars ($\log R > 1$). The ODR regression lines are plotted for the radio-quiet (dashed line) and radio-loud quasars (dash-dotted line).

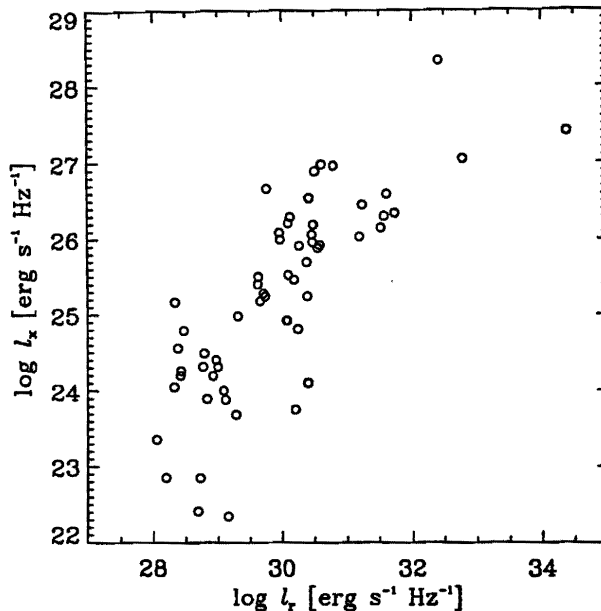


Fig. 15. The monochromatic X-ray luminosity of galaxies as a function of the radio luminosity.

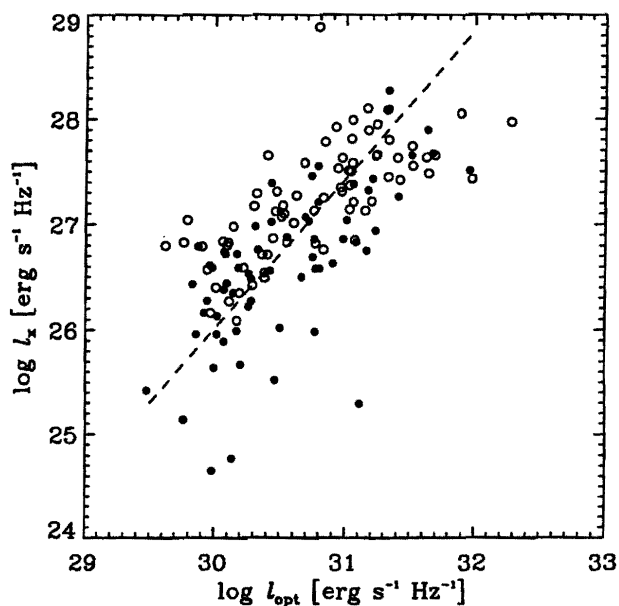


Fig. 14. The monochromatic X-ray luminosity of the FIRST-RASS quasars as function of the optical luminosity. Filled dots represent radio-quiet objects ($\log R \leq 1$), open dots radio-loud quasars ($\log R > 1$). The ODR regression line for the radio-quiet sources is plotted as dashed line.

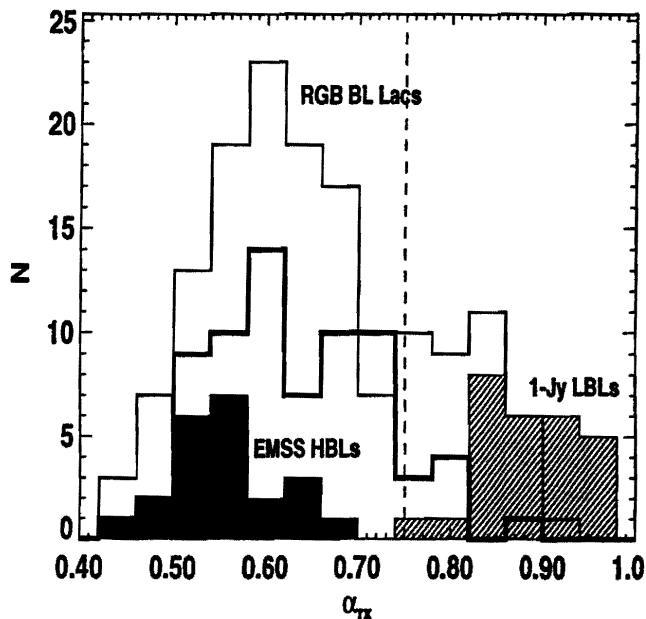


Fig. 16. Histogram of various BL Lac samples as function of the broad-band radio to X-ray spectral index α_{rx} . The thick line represents the BL Lacs of the current sample; the dashed line indicates the classical division between HBLs and LBLs.

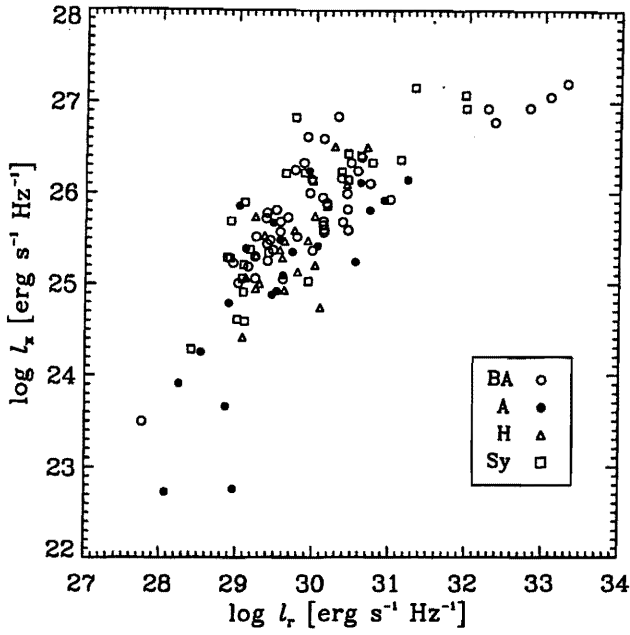


Fig. 17. The monochromatic X-ray luminosity of AGN as function of their 5 GHz radio luminosity. The various classes are identified with different symbols.

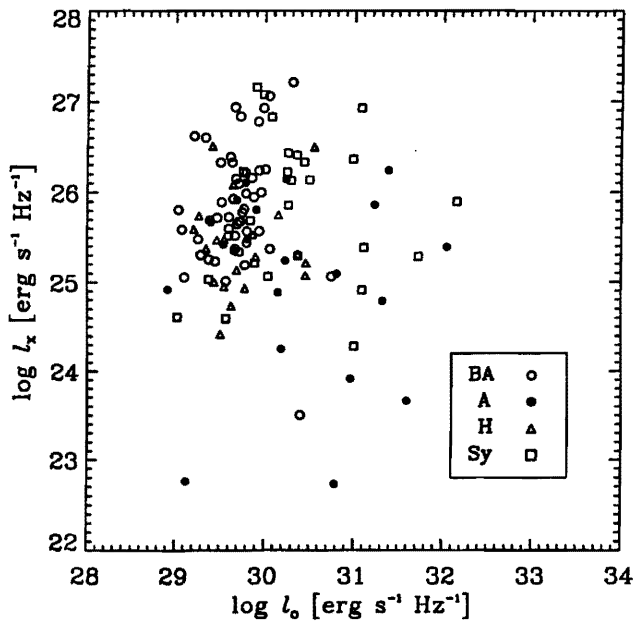


Fig. 18. The monochromatic X-ray luminosity as a function of their optical luminosity for the various AGN classes.

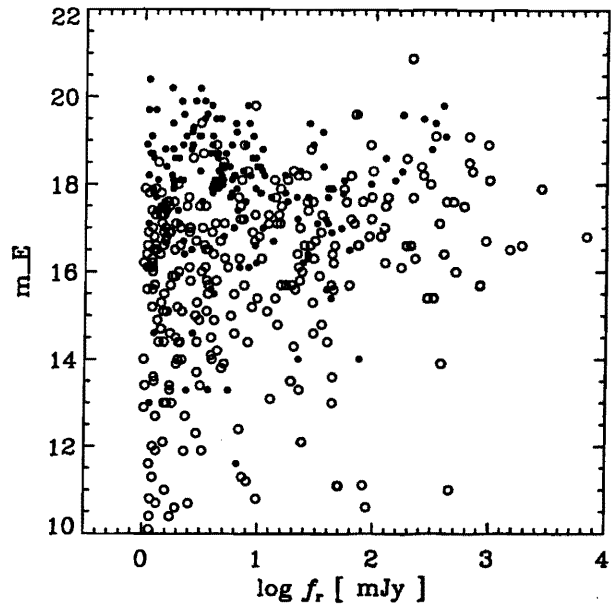


Fig. 19. E - magnitude vs. radio flux density for all sources. Open circles are known objects, solid circles represent objects currently unclassified.

Table 1: ROSAT sources with single FIRST matches

ROSAT name (1)	FIRST position (2)	Δ_{XR} (3)	Name	type (4)	Ref (5)	z (6)	f_r (7)	F_x (8)	Γ (9)	m_E (10)	cl (11)	m_O (12)	cl (13)	$A(E)$ (14)	Δ_{RO} (15)
RXSJ0002.0-1030	00 02 03.00	-10 30 38.5		A	New	0.106	1.41	1.20±0.32	2.90 ^{+0.41} _{-0.45}	15.3	1	14.9	1	...	0.8
RXSJ0005.1-0133	00 05 07.07	-01 32 45.3	LBQS 0002 - 0149	QSO	ned	1.71	61.89	0.57±0.23	3.27 ^{+0.74} _{-1.21}	18.2	-1	18.8	-1	...	0.5
RXSJ0007.2+0053	00 07 10.00	+00 53 28.6	LBQS0004 + 0036	QSO	ned	0.317	1.54	2.08±0.36	2.51 ^{+0.26} _{-0.28}	17.0	-1	18.1	-1	...	1.1
RXSJ0008.2-0057	00 08 13.18	-00 57 51.7		BA	New	0.139	5.35	1.08±0.29	2.82 ^{+0.40} _{-0.43}	16.1	1	18.5	1	...	1.8
RXSJ0011.5+0058	00 11 30.40	+00 57 52.0					173.75	0.53±0.22	...	19.6	-1	19.9	-1	...	0.2
RXSJ0019.5-0929	00 19 26.72	-09 29 58.4					1.03	0.37±0.18	3.12 ^{+0.69} _{-0.98}
RXSJ0022.0+0006	00 22 00.93	+00 06 58.3		B?	New	0.306	2.64	1.83±0.33	2.37 ^{+0.38} _{-0.27}	18.6	-1	20.8	-1	...	0.6
RXSJ0023.0-0009	00 23 00.51	-00 09 17.5	ABELL 0025	Cl	ned		1.75	0.41±0.17	...	15.9	2	19.3	1	...	0.3
RXSJ0024.7+0032	00 24 43.19	+00 32 20.1	LBQS0022 + 0015	QSO			15.53	0.86±0.24	2.65 ^{+0.39} _{-0.44}
RXSJ0026.1-0005	00 26 08.38	-00 05 46.6		B?	New	0.107	1.02	0.41±0.16	0.77 ^{+0.67} _{-0.67}	17.9	1	18.7	1	...	0.5
RXSJ0026.3+0120	00 26 15.91	+01 20 38.0					1.33	0.85±0.22	1.95 ^{+0.49} _{-0.41}
RXSJ0030.7-1057	00 30 42.69	-10 57 06.8					7.76	0.56±0.20	2.03 ^{+0.75} _{-0.56}	19.8	1	21.6	-1	...	0.5
RXSJ0032.7-0103	00 32 39.43	-01 02 54.7					3.06	0.47±0.16	2.61 ^{+0.53} _{-0.54}
RXSJ0034.7-0054	00 34 43.94	-00 54 13.1	PMNJ0034 - 0054	id		0.656	67.19	0.69±0.18	2.23 ^{+0.40} _{-0.37}	19.6	1	20.0	-1	...	0.1
RXSJ0035.9-0912	00 35 52.96	-09 11 50.6		?		1.004	91.03	0.49±0.23	...	18.9	-1	20.0	-1	...	0.7
RXSJ0038.3-0122	00 38 16.45	-01 22 04.1	87GB[BWE91]003	rad			17.33	0.44±0.19
RXSJ0041.8-0918	00 41 50.48	-09 18 11.4		G	ned	0.056	36.43	51.26±1.83	1.66 ^{+0.08} _{-0.07}	8.7	1	9.1	1	...	0.9
RXSJ0042.6-1103	00 42 34.14	-11 03 28.7					3.26	0.72±0.21	1.97 ^{+0.50} _{-0.42}
RXSJ0043.3+0051	00 43 19.70	+00 51 15.3	[HB89]0040 + 005	QSO	ned	2.00	1.10	1.12±0.29	2.36 ^{+0.38} _{-0.37}	17.8	-1	19.4	-1	...	0.7
RXSJ0045.4+0117	00 45 23.51	+01 17 27.4					1.44	0.58±0.23	2.02 ^{+0.54} _{-0.49}
RXSJ0046.2-0044	00 46 13.77	-00 45 08.5					2.14	0.76±0.29	1.89 ^{+0.87} _{-0.59}
RXSJ0050.7-0928	00 50 41.31	-09 29 05.5		B	ned		806.42	4.39±0.46	2.78 ^{+0.17} _{-0.18}	15.7	-1	17.3	-1	...	0.2
RXSJ0054.7+0000	00 54 41.19	+00 01 11.0	LBQS0052 - 0015	QSO	ned	0.648	3.03	1.08±0.28	2.84 ^{+0.37} _{-0.41}	17.5	1	18.3	-1	...	0.5
RXSJ0056.1-0115	00 56 09.38	-01 15 37.2	ABELL 0119	Cl	ned		2.00	2.35±0.44
RXSJ0057.5-0932	00 57 29.07	-09 32 58.9		QSO	New	0.559	1.96	0.60±0.26	3.53 ^{+0.60} _{-0.57}	18.0	-1	18.3	-1	...	0.9
RXSJ0058.1-0024	00 58 08.21	-00 24 18.1					3.31	0.87±0.26	2.38 ^{+0.48} _{-0.46}	19.5	-1	20.4	-1	...	0.2
RXSJ0059.3-0920	00 59 17.48	-09 19 53.9					30.63	0.48±0.20	1.51 ^{+1.51} _{-0.73}	...	0	20.2	-1	...	0.1
RXSJ0059.3-0150	00 59 16.93	-01 50 17.8					13.22	1.92±0.38	2.28 ^{+0.36} _{-0.31}	16.7	1	18.5	1	...	0.5
RXSJ0103.2-0913	01 03 14.22	-09 13 21.9					7.54	0.48±0.21	2.45 ^{+0.93} _{-0.75}
RXSJ0105.1-0214	01 05 05.49	-02 14 22.8					3.05	0.65±0.22	...	20.2	1	19.8	-1	...	1.2
RXSJ0106.7-1033	01 06 44.13	-10 34 10.6		id		0.468	129.84	1.61±0.38	3.37 ^{+0.35} _{-0.41}	17.7	-1	17.7	-1	...	0.4
RXSJ0106.8+0103	01 06 49.39	+01 03 22.4		H?	New	0.254	1.81	0.78±0.23	2.08 ^{+0.56} _{-0.46}	17.6	1	18.9	1	...	0.6
RXSJ0109.7+0059	01 09 39.03	+00 59 49.9		BA	New	0.093	1.38	1.59±0.33	2.00 ^{+0.36} _{-0.31}	16.4	1	17.5	1	...	1.3
RXSJ0112.0-0043	01 12 04.07	-00 43 51.8		G	New	0.179	2.53	1.10±0.27	...	15.8	2	17.5	1	...	0.9
RXSJ0113.1-0852	01 13 08.62	-08 52 37.1					2.61	0.48±0.22	...	18.9	-1	19.3	-1	...	0.3
RXSJ0116.6-0230	01 16 36.30	-02 30 00.9	AY Cet	S	Smb		2.55	92.51±2.29	3.16 ^{+0.03} _{-0.04}
RXSJ0118.9-0100	01 18 53.64	-01 00 06.6	UGC00842	B	New	0.045	1.24	0.80±0.25	1.88 ^{+0.75} _{-0.51}	13.5	-1	14.1	1	...	1.3
RXSJ0120.4-0004	01 20 23.15	-00 04 44.4	NPM1G - 00.0049	G	New	0.077	12.94	0.50±0.20	0.75 ^{+0.85} _{-0.40}	13.1	2	15.5	2	...	1.8
RXSJ0121.0-0015	01 21 00.78	-00 15 19.2	PMNJ0121 - 0015	rad			99.88	0.43±0.17	0	21.7	-1	...	1.0

continued on next page

ROSAT name (1)	FIRST position (2)	Δ_{XR} (3)	Name (4)	type (4)	Ref (5)	f_r (6)	F_z (7)	Γ (8)	m_E (9)	cl (10)	mo (11)	cl (12)	$A(E)$ (13)	Δ_{RO} (14)
RXSJ0122.0-0102	01 21 59.81	-01 02 24.5	[HB89]0119-013	Sy	ned	0.054	3.86	3.50±0.45	14.1	1	15.3	1	...	0.4
RXSJ0122.8+0042	01 22 50.31	+00 42 44.5	1ES0120+004	S	New	2.17	31.91±1.27	3.02 ^{+0.07} _{-0.07}	8.2	2	9.4	-1	...	1.9
RXSJ0125.3-0018	01 25 17.19	-00 18 29.9	[HB89]0122-005	QSO	ned	334.40	0.37±0.16	...	19.1	-1	19.5	-1	...	1.2
RXSJ0125.5-0005	01 25 28.86	-00 05 56.2	[HB89]0122-003	QSO	ned	1476.47	1.66±0.31	2.47 ^{+0.33} _{-0.31}	16.5	-1	17.3	-1	...	0.4
RXSJ0130.3+0119	01 30 16.84	+01 19 37.4				2.38	0.93±0.25
RXSJ0135.4-0043	01 35 21.68	-00 44 01.3	BA	New	0.097	1.18	0.86±0.25	2.51 ^{+0.44} _{-0.41}	16.2	-1	17.5	1	...	1.0
RXSJ0140.7-0758	01 40 40.89	-07 58 49.3				20.10	8.40±0.62	2.02 ^{+0.12} _{-0.11}
RXSJ0140.7-0823	01 40 42.28	-08 23 18.0				47.62	0.39±0.15
RXSJ0140.7-0904	01 40 45.15	-09 05 05.7				3.71	0.84±0.20	1.24 ^{+0.73} _{-0.44}
RXSJ0143.8-0126	01 43 47.18	-01 26 10.3				1.72	0.59±0.24	2.39 ^{+0.72} _{-0.67}	20.2	0	21.1	-1	...	0.5
RXSJ0146.7-0821	01 46 40.71	-08 21 15.9				1.31	0.87±0.22	1.97 ^{+0.36} _{-0.45}
RXSJ0149.3-0111	01 49 18.89	-01 11 12.4				1.49	0.52±0.18	2.05 ^{+0.69} _{-0.56}	17.6	2	...	0	...	1.0
RXSJ0152.6-0143	01 52 37.08	-01 43 58.6	QSO	New	0.850	1.56	0.49±0.18	2.26 ^{+0.61} _{-0.55}	16.8	-1	17.5	-1	...	0.5
RXSJ0159.8+0023	01 59 50.25	+00 23 41.0	PG0157+001	Sy	ned	22.39	3.77±0.47	2.97 ^{+0.19} _{-0.20}	13.3	2	14.5	1	...	0.5
RXSJ0201.1+0034	02 01 06.19	+00 33 59.9		B	ned	11.89	6.36±0.59	2.40 ^{+0.13} _{-0.14}	17.1	1	18.5	-1	...	0.5
RXSJ0201.5-0926	02 01 31.68	-09 26 14.5				4.50	0.36±0.15	0	21.7	-1	...	1.1
RXSJ0201.7-0139	02 01 45.58	-01 40 12.7		A	New	0.209	1.35±0.31	1.62 ^{+0.64} _{-0.46}	15.7	2	20.2	1	...	1.9
RXSJ0202.2-0700	02 02 14.78	-07 00 30.3		G?	ned	3.19	0.56±0.17	0.80 ^{+0.67} _{-0.43}
RXSJ0202.9-0223	02 02 52.26	-02 23 21.1				43.06	1.82±0.31	2.21 ^{+0.25} _{-0.24}
RXSJ0204.0-0905	02 03 60.00	-09 06 21.2		G	New	0.050	0.38±0.14	1.65 ^{+0.61} _{-0.49}	10.4	1	11.6	2	...	0.5
RXSJ0206.3-0017	02 06 15.99	-00 17 29.3		A	ned	0.042	3.31	6.52±0.59	7.7	1	9.4	1	...	0.6
RXSJ0209.5-0438	02 09 30.76	-04 38 26.8	UGC01597	QSO	New	1.128	203.06	0.65±0.22	16.6	-1	17.2	-1	...	0.6
RXSJ0211.4-1003	02 11 23.00	-10 03 08.4				2.04	0.55±0.20	2.84 ^{+0.51} _{-0.56}
RXSJ0212.3-0222	02 12 16.86	-02 21 55.9				10.37	0.78±0.22	2.19 ^{+0.42} _{-0.40}	18.3	1	19.6	1	...	0.1
RXSJ0214.0-0253	02 13 56.41	-02 53 25.1				29.36	1.43±0.30	1.67 ^{+0.34} _{-0.31}
RXSJ0214.0+0042	02 13 59.80	+00 42 26.6	NGC0863	BA	New	0.182	3.89	2.76±0.56	16.9	1	18.0	1	...	0.8
RXSJ0214.6-0046	02 14 33.56	-00 46 00.1		A	ned	0.026	6.91	51.03±3.16	8.7	1	9.8	-1	...	1.7
RXSJ0214.8-0356	02 14 46.44	-03 56 31.7				6.77	1.61±0.30	1.83 ^{+0.29} _{-0.26}
RXSJ0216.7-0443	02 16 40.74	-04 44 05.0				90.79	0.52±0.19
RXSJ0218.0-0940	02 18 00.08	-09 40 28.5				1.64	0.66±0.25	2.38 ^{+0.59} _{-0.59}
RXSJ0220.3-0728	02 20 14.52	-07 28 59.2				1.30	0.63±0.24
RXSJ0220.8-0842	02 20 48.48	-08 42 50.4				55.04	1.60±0.35	2.82 ^{+0.31} _{-0.34}
RXSJ0223.8-0836	02 23 47.51	-08 36 55.8				1.33	0.60±0.22	2.17 ^{+0.64} _{-0.56}
RXSJ0225.1-0950	02 25 05.29	-09 50 11.6		Cl	ned	2.21	0.76±0.24	1.88 ^{+0.63} _{-0.50}
RXSJ0230.1-0859	02 30 05.52	-08 59 52.7	MRK1044	Sy	ned	0.016	1.32	42.79±2.57
RXSJ0238.2-0924	02 38 13.70	-09 24 32.0				2.97	0.65±0.26	1.15 ^{+1.13} _{-1.13}	19.1	1	20.5	-1	...	0.3
RXSJ0240.3-0719	02 40 16.85	-07 20 14.3				3.94	0.64±0.32
RXSJ0241.9+0009	02 41 57.38	+00 09 44.7				1.58	1.20±0.45	3.32 ^{+0.56} _{-0.74}
RXSJ0242.7+0057	02 42 40.31	+00 57 27.7	[CLA95]024005.	QSO	ned	0.569	3.44	3.89±0.69	16.5	-1	16.8	-1	...	1.0
RXSJ0302.1+0046	03 02 08.96	+00 46 28.0				1.10	1.29±0.56	2.98 ^{+1.81} _{-0.84}	20.4	-1	22.0	-1	...	0.7

continued on next page

ROSAT name (1)	FIRST position (2)	Δ_{XR} (3)	Name	type (4)	Ref	z (5)	f_r (6)	F_x (7)	Γ (8)	m_E (9)	cl (10)	m_O (11)	cl (12)	A(E) (13)	Δ_{RO} (14)
RXSJ0304.5-0054	03 04 33.97	-00 54 04.2	15	B?	id	0.33	19.35	1.67±0.55	...	18.3	1	19.8	-1	...	0.4
RXSJ0306.7+0003	03 06 39.61	+00 03 43.5	9	H	New	0.108	3.85	2.17±0.59	1.94 ^{+1.02} _{-0.61}	14.5	1	16.4	1	...	0.9
RXSJ0316.0-0226	03 16 00.77	-02 25 39.3	29	A	New	0.007	81.60	0.57±0.23	...	11.1	-1	...	0	...	1.0
RXSJ0720.3+2349	07 20 18.64	+23 49 04.0	6	BA	New	0.152	5.47	5.67±0.69	1.73 ^{+0.51} _{-0.38}	12.9	2	17.5	2	0.15	2.6
RXSJ0720.7+3028	07 20 40.47	+30 28 48.5	19	BA	New	0.100	1.07	3.40±0.52	2.71 ^{+0.34} _{-0.29}	15.6	1	17.0	1	0.17	1.1
RXSJ0722.3+3030	07 22 17.56	+30 30 50.2	3	BA	New	0.100	5.69	4.07±0.56	2.03 ^{+0.44} _{-0.34}	14.9	1	16.2	1	0.17	0.6
RXSJ0729.5+2436	07 29 27.97	+24 36 23.3	8	H	New	0.163	8.02	5.13±0.76	1.60 ^{+0.40} _{-0.31}	14.2	2	18.2	1	0.16	1.9
RXSJ0729.9+3046	07 29 52.30	+30 46 45.1	14	QSO	ned	0.15	1.48	0.51±0.22	...	17.0	-1	17.6	-1	0.18	0.7
RXSJ0732.4+3137	07 32 20.45	+31 37 57.6	15	Cl	ned	0.171	4.75	9.17±0.75	1.43 ^{+0.26} _{-0.22}	13.8	2	...	0	0.15	0.3
RXSJ0737.0+2846	07 37 01.87	+28 46 46.0	9	B	id	0.273	15.23	1.41±0.33	2.95 ^{+0.40} _{-0.40}	18.1	1	19.5	-1	0.13	0.1
RXSJ0738.7+3040	07 38 41.41	+30 40 26.3	24	B	id	0.273	4.82	0.52±0.20	...	18.4	2	21.4	1	0.12	1.8
RXSJ0740.1+2406	07 40 03.90	+24 06 15.6	6	S	sigma Gem	...	3.60	1.85±0.38	2.23 ^{+0.41} _{-0.35}
RXSJ0743.3+2853	07 43 18.65	+28 53 02.2	4	S	Smb	...	1.99	191.43±3.45	2.87 ^{+0.04} _{-0.03}
RXSJ0745.8+2848	07 45 48.28	+28 48 37.1	15	QSO	New	0.158	1.24	0.77±0.25	3.15 ^{+0.45} _{-0.55}	16.4	1	17.5	1	0.10	1.0
RXSJ0746.0+2226	07 45 59.19	+22 26 50.9	16	QSO	New	0.158	27.47	0.57±0.23	...	18.8	-1	20.4	1	0.16	0.3
RXSJ0746.4+2549	07 46 25.90	+25 49 02.2	15	rad	406.99	0.77±0.24	1.86 ^{+0.86} _{-0.56}	19.1	-1	20.0	-1	0.10	0.5
RXSJ0746.5+3503	07 46 28.37	+35 04 21.9	30	rad	1.94	0.46±0.20
RXSJ0746.7+2735	07 46 40.43	+27 34 59.2	4	G	ned	0.029	214.28	0.32±0.15
RXSJ0747.0+4132	07 47 02.08	+41 32 10.0	4	G	ned	0.029	1.22	2.04±0.37	...	8.1	2	10.3	2	0.11	10.3
RXSJ0747.6+2456	07 47 38.39	+24 56 37.6	11	BA	New	0.130	2.47	0.61±0.22	...	16.1	1	17.2	-1	0.15	1.7
RXSJ0748.6+2400	07 48 36.11	+24 00 24.1	13	QSO	ned	0.410	694.04	2.52±0.44	1.51 ^{+0.67} _{-0.46}	18.3	-1	19.5	-1	0.16	0.5
RXSJ0749.2+2313	07 49 14.03	+23 13 17.1	6	B?	New	0.175	42.13	0.53±0.24	...	15.7	1	18.3	1	0.16	0.2
RXSJ0749.8+3454	07 49 48.18	+34 54 43.8	7	QSO	W00	0.133	1.31	2.46±0.43	2.61 ^{+0.40} _{-0.32}	15.8	-1	16.3	1	0.14	0.9
RXSJ0750.2+3726	07 50 11.01	+37 26 49.2	30	QSO	W00	...	3.66	0.59±0.23	1.76 ^{+0.31} _{-0.21}	12.3	2	...	0	0.18	3.3
RXSJ0750.8+4130	07 50 47.36	+41 30 33.1	9	H	W00	0.082	2.06	0.56±0.21	1.96 ^{+0.61} _{-0.51}	17.1	-1	17.4	-1	0.12	0.1
RXSJ0752.8+2617	07 52 45.63	+26 17 35.1	7	B	New	0.096	1.13	3.71±0.49	3.13 ^{+0.33} _{-0.23}	16.0	-1	17.0	-1	0.09	0.6
RXSJ0754.6+3911	07 54 37.08	+39 10 47.6	18	QSO	ned	0.80	43.63	0.89±0.28	3.65 ^{+0.39} _{-0.28}	14.3	1	15.9	1	0.13	0.4
RXSJ0754.8+3033	07 54 48.83	+30 33 55.1	9	QSO	ned	0.80	44.75	1.61±0.36	1.76 ^{+0.33} _{-0.38}	17.3	-1	17.8	-1	0.15	0.5
RXSJ0755.4+3726	07 55 23.10	+37 26 18.2	19	H	New	0.113	2.05	1.45±0.33	0.76 ^{+0.42} _{-0.31}	...	0	22.0	-1	0.13	1.3
RXSJ0755.9+3526	07 55 51.32	+35 26 35.2	3	rad	1.26	0.82±0.26	...	16.6	1	17.5	1	0.13	0.4
RXSJ0756.1+3834	07 56 07.04	+38 34 00.5	15	G	New	0.072	59.82	1.28±0.29	...	16.4	1	20.7	1	0.14	1.2
RXSJ0756.5+4102	07 56 30.42	+41 02 10.5	9	G	New	0.072	9.71	0.74±0.25	2.28 ^{+1.11} _{-0.66}	12.0	2	14.0	2	0.12	0.7
RXSJ0758.0+3641	07 57 59.20	+36 42 17.4	29	rad	1.02	0.76±0.26	2.65 ^{+0.77} _{-0.61}
RXSJ0758.0+3913	07 58 03.17	+39 13 15.9	12	QSO	ned	0.210	6.44	0.46±0.20	...	17.8	1	20.4	1	0.16	0.4
RXSJ0758.3+4219	07 58 19.70	+42 19 35.3	3	H	New	0.093	2.07	3.68±0.50	3.15 ^{+0.23} _{-0.23}	14.9	1	15.6	1	0.13	1.1
RXSJ0758.7+4145	07 58 38.14	+41 45 12.3	15	G?	New	0.133	2.14	0.45±0.19	2.42 ^{+0.86} _{-0.65}	15.6	1	17.2	1	0.11	0.3
RXSJ0759.7+4149	07 59 39.39	+41 50 23.8	30	Sy	ned	0.025	1.03	0.80±0.26	1.54 ^{+0.68} _{-0.44}	13.7	2	17.0	2	0.10	1.5
RXSJ0800.3+2636	08 00 20.98	+26 36 48.3	6	rad	1.81	1.45±0.40	...	9.6	1	8.8	1	0.11	1.4
RXSJ0800.7+3217	08 00 42.01	+32 17 27.1	24	rad	73.73	0.47±0.22	...	14.9	2	19.7	1	0.17	0.5
RXSJ0807.5+3401	08 07 30.73	+34 00 41.6	23	rad	9.41	1.87±0.44	1.80 ^{+0.60} _{-0.43}	16.0	2	19.9	2	0.11	0.5

continued on next page

ROSAT name (1)	FIRST position (2)	Δ_{XR} (3)	Name	type (4)	Ref	z (5)	f_r (6)	F_z (7)	Γ (8)	m_E (9)	cl (10)	m_O (11)	cl (12)	A(E) (13)	Δ_{RO} (14)
RXSJ0807.9+3832	08 07 52.28	+38 32 10.9	IRASF08045 + 384	H	New	0.067	1.30	1.21±0.32	2.25 ^{+0.60} _{-0.47}	13.8	1	15.8	1	0.14	0.4
RXSJ0808.9+3249	08 08 55.47	+32 49 06.0					2.47	19.16±1.37	3.70 ^{+0.13} _{-0.13}
RXSJ0808.9+4052	08 08 56.65	+40 52 44.9	[HB89]0805 + 410	QSO		1.420	589.58	1.05±0.28	...	17.9	1	19.0	-1	0.14	0.6
RXSJ0810.2+3847	08 10 09.94	+38 47 56.9					26.68	1.17±0.33	2.43 ^{+0.63} _{-0.48}	19.8	-1	22.0	-1	0.12	0.5
RXSJ0810.4+2342	08 10 26.04	+23 41 56.5		H	W00	0.133	1.39	0.98±0.35	2.41 ^{+0.88} _{-0.80}	17.7	-1	18.3	-1	0.13	0.5
RXSJ0811.0+4133	08 10 58.98	+41 34 02.6	B30807 + 417	rad			169.98	0.65±0.26	...	18.7	-1	19.0	-1	0.13	0.3
RXSJ0812.5+2820	08 12 31.26	+28 20 56.2		G?	ned		3.09	0.86±0.27	2.68 ^{+0.49} _{-0.49}	19.7	-1	20.5	-1	0.09	0.3
RXSJ0814.4+2941	08 14 25.89	+29 41 15.7		id		0.372	4.83	1.79±0.52	2.59 ^{+0.34} _{-0.34}	18.8	-1	18.8	-1	0.10	0.2
RXSJ0815.3+2736	08 15 20.66	+27 36 16.9	RXJ08153 + 2735	QSO		0.911	3.62	1.69±0.47	2.28 ^{+0.50} _{-0.43}	16.0	-1	16.5	-1	0.09	0.1
RXSJ0817.0+3436	08 17 00.41	+34 35 56.4					21.80	0.62±0.23	...	13.2	1	14.5	1	0.14	4.8
RXSJ0817.6+2423	08 17 38.34	+24 23 30.1		QSO	W00	0.28	5.02	1.76±0.45	1.91 ^{+0.77} _{-0.49}	16.5	-1	17.1	-1	0.11	0.3
RXSJ0817.9+3243	08 17 51.00	+32 43 40.5					10.10	0.84±0.27	...	19.0	-1	19.3	-1	0.11	0.6
RXSJ0818.3+4222	08 18 16.01	+42 22 45.6	B30814 + 425	B	ned	0.245	944.26	0.64±0.30	...	19.3	-1	20.3	-1	0.17	0.6
RXSJ0819.3+2707	08 19 16.80	+27 07 33.9	IRAS08162 + 271	IRs			5.97	1.27±0.39	2.62 ^{+0.51} _{-0.48}	18.5	1	20.7	-1	0.10	0.3
RXSJ0819.5+3348	08 19 31.07	+33 48 36.3					3.41	0.47±0.21
RXSJ0822.0+2531	08 22 02.14	+25 31 15.6					1.23	0.54±0.22	2.48 ^{+0.82} _{-0.63}	14.6	1	16.8	1	0.08	3.1
RXSJ0822.2+2538	08 22 14.49	+25 38 32.0	87GB081913.8 + 2	QSO	New	1.733	264.37	0.82±0.24	3.05 ^{+0.42} _{-0.46}	18.7	-1	18.5	-1	0.08	1.0
RXSJ0823.1+4215	08 23 08.29	+42 15 20.6		BA	New	0.056	1.98	2.30±0.46	2.12 ^{+0.46} _{-0.35}	13.4	1	15.7	1	0.12	1.0
RXSJ0823.9+3947	08 23 55.65	+39 47 47.5					3.06	1.30±0.34	...	19.4	-1	20.8	-1	0.11	0.2
RXSJ0825.8+2704	08 25 47.37	+27 04 21.9	[HB89]0822 + 272	QSO	ned	2.06	94.61	0.71±0.25	...	18.6	-1	18.7	-1	0.10	0.3
RXSJ0828.2+4153	08 28 14.18	+41 53 52.6	B30824 + 420	rad			37.74	2.04±0.37	1.58 ^{+0.56} _{-0.41}	15.4	2	18.9	1	0.11	1.2
RXSJ0829.7+4154	08 29 42.68	+41 54 36.9		BA	New	0.126	4.01	2.17±0.40	1.55 ^{+0.43} _{-0.34}	16.5	1	17.9	1	0.11	0.3
RXSJ0832.3+2919	08 32 17.35	+29 19 09.6	HD 72146	S	Smb		5.39	18.86±1.52	2.50 ^{+0.13} _{-0.14}	8.7	2	...	0	0.11	4.8
RXSJ0832.4+3707	08 32 25.34	+37 07 36.6	FIRSTJ083225.3	Sy	ned	0.091	11.78	9.30±1.01	2.61 ^{+0.20} _{-0.18}	15.6	1	16.7	-1	0.10	0.2
RXSJ0832.8+2853	08 32 46.98	+28 53 12.7	FBQSJ0832 + 2853	QSO	ned	0.226	1.64	2.20±0.56	2.16 ^{+0.62} _{-0.44}	17.1	1	18.0	-1	0.11	0.9
RXSJ0832.9+3300	08 32 51.47	+33 00 10.8					3.47	3.03±0.50	1.52 ^{+0.54} _{-0.38}	20.3	-1	21.4	-1	0.13	0.7
RXSJ0834.8+3928	08 34 47.60	+39 28 17.7		G	New	0.172	3.50	0.71±0.29	...	15.8	1	17.4	2	0.11	0.8
RXSJ0835.9+2957	08 35 52.38	+29 57 16.1	IRASF08328 + 300	H	New	0.077	2.90	1.46±0.37	...	13.8	1	14.7	1	0.10	0.8
RXSJ0836.4+2728	08 36 22.90	+27 28 52.5	[HB89]0833 + 276	QSO	ned	0.765	300.48	0.42±0.18	...	18.3	-1	19.0	-1	0.11	0.5
RXSJ0837.6+2547	08 37 37.03	+25 47 50.1		BA	New	0.080	1.19	1.43±0.34	...	16.3	1	18.1	1	0.11	0.9
RXSJ0838.2+2453	08 38 10.95	+24 53 42.9	NGC2622	G	ned	0.029	62.86	4.63±0.61	1.44 ^{+0.35} _{-0.28}	8.4	1	9.6	1	0.11	2.1
RXSJ0840.6+3924	08 40 38.55	+39 24 48.7		G	New	0.119	1.69	0.55±0.20	2.27 ^{+0.70} _{-0.54}	14.2	1	17.1	1	0.12	0.5
RXSJ0842.1+4018	08 42 03.74	+40 18 31.4	87GB083846.8 + 4	QSO	New	0.152	20.21	4.72±0.52	2.43 ^{+0.19} _{-0.17}	15.5	2	16.8	1	0.09	0.5
RXSJ0842.9+2927	08 42 55.96	+29 27 27.2	FIRSTJ084255.9	G	ned	0.193	19.93	3.22±0.51	1.53 ^{+0.43} _{-0.33}	13.6	2	18.4	1	0.19	1.8
RXSJ0844.9+2804	08 44 52.27	+28 04 09.8					2.59	1.18±0.42	...	19.4	1	21.8	-1	0.14	1.7
RXSJ0845.6+2738	08 45 35.98	+27 38 47.7		QSO	New	0.572	2.42	1.05±0.41	...	17.7	-1	18.0	-1	0.15	1.3
RXSJ0845.9+2945	08 45 57.09	+29 45 33.0					3.71	1.36±0.39	2.02 ^{+0.52} _{-0.42}	18.9	-1	21.7	-1	0.13	0.7
RXSJ0846.8+2514	08 46 47.58	+25 14 08.0					8.54	1.41±0.41	3.05 ^{+0.44} _{-0.48}	18.9	-1	19.3	-1	0.09	0.5
RXSJ0847.3+3732	08 47 16.05	+37 32 17.9	[HB89]0844 + 377	QSO	ned	0.451	1.69	1.92±0.36	2.36 ^{+0.34} _{-0.31}	17.3	-1	17.6	-1	0.09	0.3
RXSJ0849.8+3246	08 49 46.33	+32 46 11.5					10.71	0.69±0.28	...	17.0	1	19.9	1	0.09	0.4

continued on next page

ROSAT name (1)	FIRST position (2)	Δ_{XR} (3)	Name	type (4)	Ref (5)	f_r (6)	F_z (7)	Γ (8)	m_E (9)	cl (10)	m_O (11)	cl (12)	$A(E)$ (13)	Δ_{RO} (14)
RXSJ0850.6+3455	08 50 36.18 +34 55 22.8	21		B	New	0.149	1.16±0.31	2.68 ^{+0.49} _{-0.49}	14.6	1	17.5	1	0.10	0.2
RXSJ0852.6+4208	08 52 33.09 +42 08 53.3	19				4.67	1.04±0.30	1.91 ^{+0.46} _{-0.40}
RXSJ0859.8+2745	08 59 46.36 +27 45 34.8	13	HS0856 + 2757	G	ned	0.246	0.52±0.21	...	16.9	1	17.4	1	0.08	0.2
RXSJ0900.6+4114	09 00 38.50 +41 13 56.0	14				2.66	1.35±0.32	1.86 ^{+0.50} _{-0.40}	13.4	2	...	0	0.06	3.2
RXSJ0901.1+3222	09 01 08.46 +32 22 08.9	10		rad		65.39	0.46±0.18	1.45 ^{+1.07} _{-0.64}
RXSJ0903.3+4056	09 03 14.71 +40 55 59.7	11				26.13	4.07±0.60	2.78 ^{+0.52} _{-0.24}	16.1	1	18.4	1	0.04	0.3
RXSJ0908.2+4223	09 08 09.15 +42 23 47.5	15				2.04	0.39±0.18
RXSJ0908.3+3551	09 08 16.55 +35 51 32.0	3		BA	New	0.138	1.25±0.28	2.26 ^{+0.28} _{-0.27}	16.4	1	17.2	1	0.07	0.4
RXSJ0908.5+3026	09 08 29.50 +30 26 39.5	16		G	New	0.112	0.68±0.21	...	13.0	2	15.8	2	0.07	1.3
RXSJ0908.7+3235	09 08 38.45 +32 35 34.4	15	IC2439	G	ned	0.014	0.55±0.19	1.75 ^{+0.62} _{-0.49}	9.7	1	11.4	1	0.05	0.8
RXSJ0908.9+3353	09 08 50.15 +33 52 47.3	21				1.97	5.66±0.52	3.02 ^{+0.15} _{-0.16}
RXSJ0909.0+2311	09 09 00.62 +23 11 13.0	1		B	id	0.223	0.91±0.33	2.99 ^{+0.54} _{-0.87}	16.4	1	...	0	0.13	0.7
RXSJ0909.4+2743	09 09 24.53 +27 44 04.0	19		rad		52.97	1.15±0.39	1.71 ^{+0.56} _{-0.56}
RXSJ0912.2+2759	09 12 11.21 +27 59 27.9	29				2.55	1.15±0.33	3.40 ^{+0.40} _{-0.52}	18.9	-1	19.4	-1	0.07	0.4
RXSJ0912.8+2854	09 12 47.80 +28 54 06.6	24		BA	W00	0.182	1.85±0.39	1.89 ^{+0.38} _{-0.34}	16.8	1	17.5	-1	0.07	0.2
RXSJ0913.6+4224	09 13 39.82 +42 24 33.6	27				1.05	0.37±0.14	1.67 ^{+0.57} _{-0.52}	19.5	-1	...	0	0.05	0.4
RXSJ0915.8+2509	09 15 48.10 +25 08 58.8	28		rad		330.00	0.72±0.24	1.47 ^{+1.36} _{-0.67}	19.7	1	...	0	0.09	0.3
RXSJ0915.9+2933	09 15 52.40 +29 33 24.1	11		B	ned	324.36	9.50±0.73	2.18 ^{+0.12} _{-0.12}	15.4	-1	15.9	-1	0.07	0.2
RXSJ0916.7+3927	09 16 43.79 +39 27 08.3	7				3.93	0.37±0.14	...	18.4	1	...	0	0.04	0.6
RXSJ0916.8+3854	09 16 48.89 +38 54 28.0	30		QSO	ned	1.269	0.31±0.12	...	18.6	2	19.2	-1	0.05	0.4
RXSJ0918.6+3156	09 18 33.85 +31 56 20.5	16				1.26	0.99±0.24	1.82 ^{+0.33} _{-0.31}	17.7	1	18.8	-1	0.05	0.7
RXSJ0919.0+2616	09 19 02.23 +26 16 11.9	5		QSO	ned	0.009	0.32±0.15	...	8.8	-1	8.0	-1	0.09	1.3
RXSJ0919.4+3347	09 19 27.27 +33 47 27.1	26		G	ned	0.020	0.41±0.17	0	13.2	1	0.04	1.6
RXSJ0919.8+3422	09 19 49.14 +34 23 03.7	21				2.15	0.46±0.16	2.21 ^{+0.44} _{-0.47}	18.4	1	18.4	-1	0.04	0.3
RXSJ0920.0+2331	09 20 02.13 +23 30 53.1	11				4.36	0.49±0.21	...	18.1	-1	18.5	-1	0.11	0.2
RXSJ0920.1+3829	09 20 06.40 +38 29 22.7	30				1.08	0.60±0.17	1.70 ^{+0.51} _{-0.43}
RXSJ0920.2+3910	09 20 15.69 +39 10 13.7	21				8.06	0.84±0.20	1.80 ^{+0.36} _{-0.34}	20.2	-1	21.3	-1	0.05	0.3
RXSJ0921.3+2854	09 21 15.42 +28 54 43.6	1				1.73	1.22±0.28	1.60 ^{+0.47} _{-0.38}	18.2	-1	19.3	-1	0.06	1.1
RXSJ0923.7+2254	09 23 43.00 +22 54 32.7	4		Sy	ned	0.033	34.64±1.37	2.15 ^{+0.07} _{-0.08}	8.3	1	7.8	2	0.11	1.9
RXSJ0925.9+4004	09 25 54.72 +40 04 14.2	5		QSO	W00	0.47	2.48±0.31	2.25 ^{+0.19} _{-0.18}	17.1	-1	17.3	-1	0.03	0.5
RXSJ0927.0+3902	09 27 03.02 +39 02 20.7	3		QSO	ned	0.695	3.13±0.34	2.16 ^{+0.18} _{-0.32}
RXSJ0927.1+3741	09 27 05.35 +37 42 06.8	10				4.38	0.76±0.19	2.37 ^{+0.37} _{-0.44}	18.6	-1	19.3	-1	0.04	0.5
RXSJ0927.3+2301	09 27 18.51 +23 01 12.2	9		G	ned	0.025	4.64±0.51	2.07 ^{+0.19} _{-0.19}	10.7	-1	9.8	1	0.09	1.6
RXSJ0929.2+2537	09 29 15.54 +25 36 58.2	27		QSO	New	0.539	0.76±0.22	...	18.6	-1	18.7	-1	0.07	0.4
RXSJ0930.9+3933	09 30 56.84 +39 33 35.9	8		B		187.98	1.39±0.25	1.68 ^{+0.26} _{-0.24}	20.2	-1	21.1	-1	0.04	0.8
RXSJ0931.8+2937	09 31 47.77 +29 37 42.3	15		A	New	0.140	0.50±0.24	2.48 ^{+0.68} _{-0.80}	15.9	1	17.4	1	0.06	0.5
RXSJ0933.8+3851	09 33 51.83 +38 51 14.8	16				1.18	0.72±0.22	1.50 ^{+0.50} _{-0.43}	16.9	1	20.2	1	0.04	0.5
RXSJ0935.5+2617	09 35 27.12 +26 17 09.9	6		QSO	New	0.122	2.71±0.37	2.09 ^{+0.19} _{-0.19}	15.3	1	16.3	-1	0.06	1.3
RXSJ0937.1+3615	09 37 03.01 +36 15 37.4	20		BA	W00	0.18	1.30±0.22	2.83 ^{+0.23} _{-0.28}	16.4	1	17.5	-1	0.04	0.2
RXSJ0937.6+2244	09 37 34.59 +22 44 10.7	19				37.05	0.60±0.21	2.07 ^{+0.51} _{-0.46}	17.2	1	21.0	1	0.07	1.5

continued on next page

ROSAT name (1)	FIRST position (2)	Δ_{XR} (3)	Name	type (4)	Ref	z (5)	f_r (6)	F_z (7)	Γ (8)	m_E (9)	cl (10)	m_O (11)	cl (12)	A(E) (13)	Δ_{RO} (14)
RXSJ0938.7+3105	09 38 43.68 +31 05 35.3	29					33.98	0.55±0.18	1.68 ^{+0.49} _{-0.42}
RXSJ0938.9+2433	09 38 58.68 +24 33 29.1	28					1.07	0.47±0.15	1.62 ^{+0.37} _{-0.46}
RXSJ0939.3+4200	09 39 15.34 +41 59 48.5	18					1.34	0.14±0.07
RXSJ0940.5+3502	09 40 29.95 +35 01 47.0	24					1.31	0.36±0.13	...	18.5	-1	18.8	-1	0.03	0.6
RXSJ0942.1+2341	09 42 04.77 +23 41 07.1	11	CGCG122 - 055	G	ned	0.021	5.78	2.19±0.33	2.09 ^{+0.24} _{-0.22}	11.0	1	10.4	2	0.07	0.6
RXSJ0942.4+3004	09 42 23.51 +30 04 27.5	14					41.56	0.40±0.15	0.94 ^{+0.94} _{-0.53}	16.7	1	18.7	1	0.06	1.1
RXSJ0943.4+2835	09 43 24.33 +28 35 40.2	13					1.39	0.48±0.16	...	17.8	-1	18.2	-1	0.05	0.1
RXSJ0944.0+2852	09 44 00.34 +28 52 29.1	15					1.07	0.33±0.13
RXSJ0944.1+3214	09 44 07.02 +32 14 44.3	10					2.05	0.25±0.11	...	18.2	-1	20.2	-1	0.05	0.3
RXSJ0944.7+2251	09 44 39.00 +22 52 10.0	19					1.25	0.35±0.15	...	17.3	-1	18.7	-1	0.08	0.7
RXSJ0949.4+2628	09 49 22.68 +26 28 35.0	14					1.20	0.31±0.13	1.83 ^{+0.63} _{-0.55}	18.9	-1	18.7	-1	0.06	0.9
RXSJ0949.6+2329	09 49 35.15 +23 29 31.5	26	87GB094644.2 + 2	rad			10.97	0.82±0.24	2.26 ^{+0.50} _{-0.48}	18.3	-1	19.2	-1	0.09	0.7
RXSJ0949.6+3126	09 49 35.28 +31 26 34.3	24					1.44	0.41±0.15
RXSJ0950.7+3830	09 50 40.87 +38 30 46.8	12					5.21	0.53±0.15	1.57 ^{+0.51} _{-0.42}
RXSJ0951.4+2635	09 51 22.54 +26 35 14.1	3				1.24	1.48	0.34±0.14	2.78 ^{+0.61} _{-0.96}	16.3	-1	16.3	-1	0.06	0.4
RXSJ0952.2+3936	09 52 14.71 +39 36 15.7	12					2.64	1.74±0.28	2.19 ^{+0.21} _{-0.22}	19.6	-1	20.2	-1	0.04	0.9
RXSJ0955.1+3550	09 55 07.88 +35 51 00.8	7					7.56	1.31±0.23	1.99 ^{+0.23} _{-0.25}	19.5	1	20.9	-1	0.03	1.2
RXSJ0957.8+3030	09 57 45.81 +30 30 24.1	13					1.17	0.75±0.20	...	18.6	1	20.2	-1	0.05	0.2
RXSJ0958.0+2640	09 58 00.85 +26 40 12.3	9	87GB095511.1 + 2	rad			70.10	0.51±0.19	1.73 ^{+1.63} _{-0.86}	19.7	-1	19.4	-1	0.05	2.1
RXSJ0958.9+3345	09 58 53.59 +33 45 52.1	19					5.24	0.25±0.11
RXSJ1001.3+3844	10 01 16.35 +38 44 54.0	12					1.09	0.32±0.12	2.37 ^{+0.43} _{-0.54}	18.7	-1	19.1	-1	0.04	0.4
RXSJ1001.7+4212	10 01 45.22 +42 12 56.2	4					1.78	0.54±0.14	2.71 ^{+0.35} _{-0.39}	18.3	-1	18.7	-1	0.04	0.5
RXSJ1002.6+3242	10 02 36.55 +32 42 24.1	10	NGC3099	G	ned	0.051	7.61	2.73±0.38	0.55 ^{+0.43} _{-0.33}	10.6	2	12.6	2	0.04	1.6
RXSJ1002.9+3240	10 02 54.54 +32 40 38.9	13	FIRSTJ100254.5	QSO	ned	0.83	9.09	1.10±0.23	1.30 ^{+0.40} _{-0.31}	17.0	-1	16.9	-1	0.04	0.5
RXSJ1003.0+3757	10 03 02.74 +37 57 51.5	17					2.15	0.56±0.17	...	19.5	2	20.1	-1	0.05	1.3
RXSJ1004.7+3751	10 04 44.63 +37 52 13.1	17	87GB100148.8 + 3	rad			21.04	0.95±0.19	1.81 ^{+0.27} _{-0.26}	18.2	1	19.9	-1	0.05	1.9
RXSJ1005.1+3414	10 05 07.90 +34 14 24.1	6					3.40	1.52±0.25	2.01 ^{+0.21} _{-0.21}	16.4	1	17.0	-1	0.03	0.4
RXSJ1005.4+4058	10 05 22.98 +40 58 34.5	7					1.29	0.75±0.17	2.47 ^{+0.25} _{-0.31}	16.7	-1	17.9	-1	0.03	0.3
RXSJ1005.5+2247	10 05 28.14 +22 46 58.5	14					4.06	0.53±0.21	...	15.5	1	19.6	1	0.10	0.7
RXSJ1006.7+2854	10 06 38.82 +25 54 44.9	6	B21003 + 26	G	ned	0.116	50.64	3.56±0.50	0.60 ^{+0.52} _{-0.36}	11.5	2	15.5	2	0.10	2.2
RXSJ1006.8+2653	10 06 47.25 +26 53 43.6	18					3.80	1.04±0.27	...	15.2	2	19.0	2	0.08	0.3
RXSJ1006.9+3454	10 06 56.42 +34 54 45.1	6	FIRSTJ100656.4	B	ned		6.81	2.19±0.31	2.52 ^{+0.19} _{-0.21}	17.9	-1	18.2	-1	0.03	1.2
RXSJ1007.9+3039	10 07 53.28 +30 40 02.3	11					1.08	0.78±0.22	2.16 ^{+0.40} _{-0.39}	16.2	1	17.7	1	0.06	0.4
RXSJ1010.3+3249	10 10 14.90 +32 49 41.9	13				0.13	4.21	0.78±0.19	1.33 ^{+0.42} _{-0.34}	17.9	1	21.1	-1	0.05	0.8
RXSJ1010.9+3247	10 10 50.42 +32 47 25.0	21					1.03	0.56±0.18	2.35 ^{+0.42} _{-0.48}
RXSJ1012.7+4229	10 12 44.29 +42 29 57.0	2					69.99	7.64±0.44	1.84 ^{+0.69} _{-0.83}	16.8	1	18.3	-1	0.04	0.2
RXSJ1013.4+2212	10 13 25.43 +22 12 29.0	3	IRASF10106 + 222	QSO	W00	0.27	1.09	2.19±0.33	3.20 ^{+0.23} _{-0.27}	17.1	-1	17.7	-1	0.07	0.4
RXSJ1013.9+2449	10 13 53.42 +24 49 16.4	20	[HB89]1011 + 250	QSO	ned	1.636	500.27	1.08±0.25	1.01 ^{+0.47} _{-0.36}	16.0	-1	16.8	-1	0.11	0.5
RXSJ1016.3+4108	10 16 16.82 +41 08 12.2	7					14.98	5.73±0.41	1.96 ^{+0.76} _{-0.70}	17.4	1	19.1	-1	0.05	0.2
RXSJ1016.8+4210	10 16 45.09 +42 10 25.5	9	IRASF10137 + 422	A?	ned		1.52	5.01±0.37	1.84 ^{+0.10} _{-0.11}	12.8	2	14.1	2	0.04	4.4

continued on next page

ROSAT name (1)	FIRST position (2)	Δ_{XR} (3)	Name	type (4)	Ref	z (5)	f_r (6)	F_x (7)	Γ (8)	m_E (9)	cl (10)	m_O (11)	cl (12)	A(E) (13)	Δ_{RO} (14)
RXSJ1018.6+3128	10 18 34.03	+31 28 34.0	18	B?	New	0.161	4.25	1.56±0.31	2.02 ^{+0.29} _{-0.28}	16.0	1	18.6	1	0.06	0.3
RXSJ1019.0+3752	10 19 00.43	+37 52 40.4	11	BA	New	0.135	3.21	9.70±0.53	2.03 ^{+0.08} _{-0.07}	16.6	1	17.2	1	0.04	0.5
RXSJ1019.5+2626	10 19 31.86	+26 26 43.4	5				1.12	0.70±0.21	2.00 ^{+0.46} _{-0.41}	18.9	1	21.0	-1	0.08	1.1
RXSJ1021.5+3806	10 21 28.89	+38 06 43.4	14				4.57	0.35±0.14	19.7	-1	20.8	-1	0.03	0.2
RXSJ1021.7+2355	10 21 41.20	+23 55 23.0	23	G?	ned		1.32	1.88±0.31	1.02 ^{+0.43} _{-0.33}	8.1	1	11.6	1	0.06	0.2
RXSJ1022.5+3041	10 22 30.32	+30 41 05.2	13	QSO	ned	1.316	907.01	0.43±0.17	2.24 ^{+0.66} _{-0.58}	16.9	-1	17.6	-1	0.07	0.3
RXSJ1023.0+3007	10 23 01.22	+30 07 06.0	21				1.37	0.46±0.17	2.69 ^{+0.49} _{-0.61}
RXSJ1023.7+3001	10 23 39.75	+30 00 57.8	16	B	id		7.81	1.23±0.27	2.40 ^{+0.30} _{-0.39}	18.5	-1	20.4	-1	0.07	0.3
RXSJ1024.9+2332	10 24 53.63	+23 32 34.0	9	B	id		121.33	0.39±0.15	1.03 ^{+0.73} _{-0.47}	16.2	1	18.6	-1	0.05	0.2
RXSJ1025.1+4143	10 25 04.21	+41 43 32.4	1	QSO?	ned		6.97	0.68±0.16	2.31 ^{+0.36} _{-0.36}	18.5	-1	18.7	-1	0.03	0.4
RXSJ1025.9+4013	10 25 53.60	+40 12 43.5	17	QSO	W00	0.405	1.07	0.74±0.20	2.57 ^{+0.32} _{-0.41}	16.2	2	17.2	-1	0.03	0.5
RXSJ1027.4+3554	10 27 25.70	+35 54 31.4	16	G	ned		1.92	0.27±0.12	12.9	1	13.8	1	0.04	0.3
RXSJ1027.5+3526	10 27 32.40	+35 26 21.8	20				10.08	1.99±0.33	2.81 ^{+0.21} _{-0.26}	0	19.4	-1	0.03	0.2
RXSJ1031.6+2847	10 31 34.39	+28 47 02.2	9	QSO?	ned	0.06	1.01	6.28±0.49	2.48 ^{+0.11} _{-0.12}	14.3	2	15.5	2	0.06	2.4
RXSJ1033.3+4222	10 33 17.98	+42 22 36.7	12				26.02	0.40±0.14	16.6	1	18.5	1	0.02	0.7
RXSJ1033.8+3708	10 33 46.42	+37 08 25.7	15				3.69	0.82±0.22	1.59 ^{+0.42} _{-0.37}
RXSJ1034.0+3555	10 33 59.48	+35 55 09.5	15	BA	W00	0.168	2.06	0.68±0.18	2.65 ^{+0.33} _{-0.40}	16.1	1	16.5	-1	0.06	0.9
RXSJ1034.6+3938	10 34 38.60	+39 38 28.2	6	Sy	ned	0.042	23.98	36.21±1.20	3.47 ^{+0.08} _{-0.20}	11.9	1	12.2	1	0.04	0.3
RXSJ1035.0+3041	10 35 00.16	+30 41 38.2	9	G	ned	0.138	6.83	3.60±0.39	1.61 ^{+0.20} _{-0.19}	12.9	2	16.7	2	0.05	0.5
RXSJ1037.4+3259	10 37 25.75	+33 00 07.5	26				7.01	0.26±0.11	1.28 ^{+1.18} _{-0.62}
RXSJ1038.1+2331	10 38 08.65	+23 31 33.3	8	A	id	0.225	4.58	0.54±0.19	15.9	1	18.4	-1	0.06	0.9
RXSJ1039.7+2422	10 39 41.97	+24 22 40.3	21	rad			53.61	0.53±0.18	1.48 ^{+0.83} _{-0.55}	17.7	-1	18.8	-1	0.06	0.3
RXSJ1039.8+2752	10 39 49.60	+27 52 46.2	21				1.07	0.60±0.21	2.31 ^{+0.43} _{-0.44}
RXSJ1041.8+3901	10 41 49.15	+39 01 19.9	13	G?	ned		22.44	1.42±0.22	1.92 ^{+0.22} _{-0.23}	15.9	1	18.9	1	0.03	0.2
RXSJ1043.1+2408	10 43 09.03	+24 08 35.5	14	B	W00	0.56	359.68	1.25±0.28	2.05 ^{+0.41} _{-0.38}	16.3	-1	17.8	-1	0.08	0.4
RXSJ1043.7+2404	10 43 43.28	+24 04 47.3	11	rad			38.90	0.61±0.21	17.1	1	21.9	1	0.08	0.6
RXSJ1044.5+2718	10 44 27.76	+27 18 06.6	7	QSO	New	0.076	1.23	3.68±0.44	2.27 ^{+0.18} _{-0.18}	14.3	1	15.0	1	0.08	0.3
RXSJ1047.1+3515	10 47 03.30	+35 15 21.0	15	Sy	ned	0.370	1.32	0.70±0.18	1.72 ^{+0.46} _{-0.40}	19.3	-1	20.0	-1	0.05	0.9
RXSJ1048.1+3138	10 48 04.96	+31 38 26.8	17				1.92	0.70±0.21	1.23 ^{+1.13} _{-0.56}
RXSJ1048.3+2222	10 48 16.56	+22 22 40.1	10	QSO	W00	0.33	1.17	1.47±0.29	17.3	-1	18.3	-1	0.06	1.2
RXSJ1049.6+2742	10 49 38.83	+27 42 13.0	2				9.16	0.51±0.21	16.3	1	18.7	1	0.05	0.5
RXSJ1049.9+3516	10 49 56.56	+35 16 43.0	2				4.64	1.66±0.35	3.11 ^{+0.30} _{-0.38}	18.9	-1	19.6	-1	0.05	0.4
RXSJ1050.3+3650	10 50 21.41	+36 50 55.9	16				2.19	0.27±0.12	17.1	1	20.9	-1	0.04	0.1
RXSJ1051.2+3850	10 51 13.63	+38 50 15.4	1	id		0.216	4.95	1.14±0.22	2.22 ^{+0.24} _{-0.26}	17.4	1	18.5	-1	0.04	1.0
RXSJ1051.4+3943	10 51 25.38	+39 43 25.7	5				9.14	4.22±0.37	2.20 ^{+0.13} _{-0.12}	18.3	-1	19.1	-1	0.04	1.2
RXSJ1054.5+3855	10 54 31.90	+38 55 21.7	11	B	W00	1.37	72.06	1.15±0.21	1.59 ^{+0.26} _{-0.25}	16.7	-1	17.0	-1	0.05	0.3
RXSJ1057.1+3119	10 57 05.16	+31 19 07.8	17				13.84	0.53±0.19	17.6	-1	18.2	-1	0.07	0.2
RXSJ1057.4+2303	10 57 23.10	+23 03 18.9	6				6.28	5.43±0.62	2.18 ^{+0.16} _{-0.16}	17.8	-1	19.3	-1	0.05	0.3
RXSJ1057.5+2950	10 57 30.86	+29 50 07.6	2				16.65	0.43±0.17
RXSJ1058.0+2937	10 57 57.67	+29 37 14.2	19				5.17	0.79±0.24	1.92 ^{+0.46} _{-0.39}	0	20.6	-1	0.05	0.4

continued on next page

ROSAT name (1)	FIRST position (2)	Δ_{XR} (3)	Name	type (4)	Ref	z (5)	f_r (6)	F_z (7)	Γ (8)	m_E (9)	cl (10)	m_O (11)	cl (12)	A(E) (13)	Δ_{RO} (14)
RXSJ1058.2+3353	10 58 08.72 +33 53 02.8	16					12.61	0.50±0.17	...	18.3	2	21.6	2	0.05	0.3
RXSJ1058.5+2817	10 58 29.90 +28 17 46.4	8	87GB105545.1 + 2	B	W00		77.89	0.42±0.17	...	17.4	-1	17.9	-1	0.06	0.4
RXSJ1100.4+4019	11 00 21.08 +40 19 27.7	6		B	W00		14.88	7.64±0.52	2.48 ^{+0.10} _{-0.11}	17.5	-1	18.2	-1	0.02	0.3
RXSJ1100.4+4210	11 00 21.01 +42 10 53.1	11		B?	W00	0.323	11.95	0.39±0.13	1.88 ^{+0.42} _{-0.44}	17.4	-1	19.1	-1	0.03	0.3
RXSJ1101.4+4108	11 01 24.72 +41 08 47.4	8					22.46	0.62±0.18	2.41 ^{+0.32} _{-0.38}	18.4	-1	19.1	-1	0.03	0.5
RXSJ1103.2+2758	11 03 11.25 +27 58 21.4	7	NGC3504	G	ned	0.005	87.07	0.50±0.20	1.90 ^{+0.70} _{-0.62}	8.8	1	9.8	1	0.07	4.9
RXSJ1103.2+4142	11 03 11.02 +41 42 19.0	23	CGCG213 - 021	G			6.81	1.48±0.27	...	9.4	2	...	0	0.03	2.7
RXSJ1103.9+2611	11 03 57.30 +26 11 19.8	17					3.04	1.61±0.48	2.44 ^{+0.39} _{-0.48}	...	0	22.1	1	0.05	0.7
RXSJ1104.7+4123	11 04 44.00 +41 23 05.1	7					6.56	0.34±0.13	...	12.5	1	14.9	1	0.02	7.1
RXSJ1105.5+3114	11 05 30.73 +31 14 36.8	12					1.54	0.53±0.20	...	18.5	2	...	0	0.08	2.0
RXSJ1106.3+2624	11 06 19.07 +26 24 18.5	28					11.74	0.92±0.31
RXSJ1109.4+4225	11 09 26.68 +42 25 57.9	6	IRASF11066 + 424	IRS			2.23	0.29±0.12	...	16.5	1	18.9	1	0.04	0.4
RXSJ1111.5+3452	11 11 30.89 +34 52 03.5	9					5.72	7.24±0.83	2.27 ^{+0.17} _{-0.16}	18.6	-1	19.5	-1	0.05	0.2
RXSJ1112.1+2608	11 12 07.96 +26 08 03.8	17					8.71	0.92±0.25	...	19.1	-1	20.2	-1	0.05	0.5
RXSJ1112.4+3950	11 12 24.18 +39 50 34.1	22					1.68	1.83±0.35	2.27 ^{+0.26} _{-0.27}
RXSJ1116.1+3710	11 16 03.44 +37 10 35.9	18					1.76	0.54±0.21	...	18.6	-1	20.9	-1	0.04	0.6
RXSJ1117.3+3016	11 17 16.66 +30 16 13.6	17					3.81	0.81±0.27	2.78 ^{+0.41} _{-0.56}	19.7	-1	20.6	-1	0.05	0.5
RXSJ1117.7+2548	11 17 40.41 +25 48 46.5	14		B	W00	0.360	9.92	0.97±0.25	3.05 ^{+0.36} _{-0.51}	17.2	-1	18.0	-1	0.05	0.3
RXSJ1118.5+4025	11 18 30.28 +40 25 53.9	4	PG1115 + 407	QSO	ned	0.154	1.04	7.88±0.67	2.98 ^{+0.13} _{-0.15}	13.9	1	14.9	1	0.04	1.6
RXSJ1118.8+3751	11 18 48.80 +37 50 55.1	29					1.20	0.61±0.23
RXSJ1119.1+4130	11 19 07.08 +41 30 14.6	4	FIRSTJ111907.0	Vis			2.39	3.16±0.42	1.39 ^{+0.24} _{-0.21}	13.8	2	...	0	0.08	7.5
RXSJ1120.8+4212	11 20 48.06 +42 12 12.4	8	87GB111803.1 + 4	B	ned	0.124	24.63	13.59±0.80	2.39 ^{+0.10} _{-0.09}	16.8	-1	17.2	-1	0.05	0.4
RXSJ1121.8+4051	11 21 51.27 +40 51 46.6	6	NPM1G + 41.0266	A	ned		1.16	2.37±0.40	1.97 ^{+0.24} _{-0.23}	11.6	2	13.4	2	0.05	0.7
RXSJ1124.1+3808	11 24 04.31 +38 08 10.6	8					1.14	1.03±0.32	2.31 ^{+0.48} _{-0.53}	12.9	-1	15.8	-1	0.06	4.8
RXSJ1127.5+2908	11 27 27.21 +29 08 29.2	9					5.55	0.52±0.18	2.19 ^{+0.37} _{-0.54}	...	0	20.5	-1	0.06	0.5
RXSJ1128.5+4024	11 28 25.62 +40 24 40.1	26					1.98	0.69±0.24	...	19.1	-1	19.2	-1	0.05	0.6
RXSJ1128.6+3530	11 28 34.32 +35 30 14.2	15					52.52	1.01±0.32	1.43 ^{+0.78} _{-0.47}	18.3	1	...	0	0.06	0.8
RXSJ1128.8+2310	11 28 51.00 +23 10 36.6	4		BA	New	0.117	1.18	1.20±0.22	2.10 ^{+0.23} _{-0.22}	15.7	1	17.4	1	0.04	0.7
RXSJ1129.8+3429	11 29 47.07 +34 28 42.4	22					1.10	0.52±0.22	...	17.6	1	19.4	1	0.07	1.1
RXSJ1129.8+3011	11 29 48.26 +30 11 26.9	19					1.51	0.48±0.19
RXSJ1130.1+4116	11 30 04.73 +41 16 19.8	23	FIRSTJ113004.7	QSO	ned	0.72	1.86	0.57±0.21	1.96 ^{+0.57} _{-0.50}	15.9	-1	16.2	-1	0.05	0.1
RXSJ1130.7+3031	11 30 42.42 +30 31 34.5	17	87GB1112803.6 + 3	QSO			214.15	0.77±0.25	2.30 ^{+0.35} _{-0.35}	17.6	-1	18.1	-1	0.06	1.3
RXSJ1131.1+3114	11 31 09.55 +31 14 03.7	10	[HB89]1128 + 315	QSO	ned	0.289	121.84	9.49±0.78	2.51 ^{+0.12} _{-0.12}	15.7	-1	16.2	-1	0.06	2.2
RXSJ1131.2+2632	11 31 09.21 +26 32 08.4	5	RXJ11311 + 2632	Sy	ned	0.244	2.00	1.87±0.29	2.65 ^{+0.22} _{-0.25}	15.5	1	16.3	-1	0.05	1.1
RXSJ1131.4+3334	11 31 20.94 +33 34 47.0	6					6.74	1.86±0.35	1.52 ^{+0.31} _{-0.27}	16.5	1	19.9	1	0.06	0.7
RXSJ1133.4+2228	11 33 26.17 +22 28 53.0	9					1.29	0.31±0.12
RXSJ1133.5+3027	11 33 27.88 +30 27 10.4	7					1.54	0.35±0.16
RXSJ1134.5+4147	11 34 27.80 +41 47 21.7	30	FIRSTJ113427.8	QSO	W00	0.818	3.34	1.17±0.32	1.60 ^{+0.69} _{-0.51}	16.7	-1	17.2	-1	0.06	0.7
RXSJ1135.5+3153	11 35 26.68 +31 53 33.2	8		G	New	0.231	27.52	1.11±0.28	1.68 ^{+0.44} _{-0.37}	16.2	1	19.6	1	0.07	1.0
RXSJ1136.7+3727	11 36 39.18 +37 26 51.6	17					17.53	0.54±0.21	...	17.1	1	18.3	-1	0.07	0.5

continued on next page

ROSAT name (1)	FIRST position (2)	Δ_{XR} (3)	Name (4)	type (4)	Ref (5)	z (5)	f_r (6)	F_x (7)	Γ (8)	m_E (9)	cl (10)	m_O (11)	cl (12)	$A(E)$ (13)	Δ_{RO} (14)
RXSJ1136.8+3141	11 36 46.05 +31 41 07.3	9					1.76	0.52±0.20	18.8	-1	20.0	-1	0.06	0.6
RXSJ1136.8+2551	11 36 50.13 +25 50 52.5	21		B	New	0.155	13.94	0.80±0.20	15.9	1	17.5	1	0.06	0.2
RXSJ1137.6+2349	11 37 35.93 +23 49 30.6	18					2.15	0.50±0.18	2.03 ^{+0.53} _{-0.51}
RXSJ1139.4+3129	11 39 21.91 +31 29 30.7	18					1.51	0.65±0.22
RXSJ1139.7+3154	11 39 42.52 +31 54 33.7	12	NGC3786	G	ned	0.008	10.61	0.53±0.22	8.4	1	9.3	2	0.06	3.2
RXSJ1140.1+4115	11 40 03.37 +41 15 04.6	4	IRASF11374 + 413	BA	New	0.071	1.51	1.05±0.31	12.1	2	13.8	2	0.05	0.8
RXSJ1140.2+2441	11 40 13.92 +24 41 49.5	1	NGC3798	QSO	New	0.012	1.76	1.05±0.22	1.27 ^{+0.64} _{-0.43}	8.7	1	0	0.09	1.4
RXSJ1142.5+2503	11 42 31.76 +25 03 37.6	7		QSO	New	0.185	1.00	2.31±0.33	2.73 ^{+0.21} _{-0.23}	16.6	1	16.7	1	0.06	1.1
RXSJ1144.5+2307	11 44 32.11 +23 06 54.1	12		G	ned		1.35	0.91±0.22	1.00 ^{+0.47} _{-0.38}	8.9	2	0	0.08	2.4
RXSJ1144.7+3936	11 44 43.19 +39 36 38.7	2	NPM1G + 39.0269	G	ned		1.22	1.42±0.29	2.34 ^{+0.28} _{-0.13}	12.0	2	14.7	2	0.05	3.0
RXSJ1145.2+3047	11 45 10.26 +30 47 17.5	14	[HB89]1142 + 310	Sy	ned	0.059	3.03	6.96±0.54	2.89 ^{+0.13} _{-0.14}	14.4	1	15.5	1	0.06	0.4
RXSJ1145.4+3347	11 45 23.44 +33 47 44.0	12					5.82	0.51±0.19	2.41 ^{+0.43} _{-0.48}
RXSJ1146.6+3200	11 46 36.78 +32 00 03.6	11	87GB114400.9 + 3	rad			122.03	0.50±0.17	18.3	-1	18.6	-1	0.05	0.7
RXSJ1150.6+4154	11 50 34.77 +41 54 40.1	8	FIRSTJ115034.7	QSO	W00	1.01	21.60	3.70±0.53	3.35 ^{+0.27} _{-0.38}	16.4	-1	17.1	-1	0.05	0.2
RXSJ1150.7+3411	11 50 43.91 +34 11 17.2	11	NPM1G + 34.0233	H	New	0.071	1.57	0.81±0.19	1.88 ^{+0.36} _{-0.34}	13.6	1	14.9	1	0.05	1.2
RXSJ1151.0+2531	11 50 58.83 +25 31 45.8	22	RXJ11509 + 2531	Sy	ned	0.087	9.23	2.72±0.35	2.62 ^{+0.19} _{-0.20}	17.0
RXSJ1151.1+2321	11 51 06.74 +23 21 28.3	29					4.42	0.55±0.17	2.62 ^{+0.41} _{-0.49}	18.5	-1	19.6	-1	0.06	0.3
RXSJ1152.4+2823	11 52 20.46 +28 23 15.1	12	ABELL1403	Cl	ned		3.22	0.86±0.25	1.36 ^{+0.65} _{-0.47}
RXSJ1152.5+3209	11 52 27.51 +32 09 59.3	5	87GB114949.8 + 3	Sy	ned	0.374	29.02	3.35±0.38	2.52 ^{+0.17} _{-0.18}	17.0	-1	17.4	-1	0.06	0.7
RXSJ1152.7+3406	11 52 44.86 +34 06 39.0	5					1.75	0.36±0.14	2.25 ^{+0.51} _{-0.53}	19.2	-1	0	0.05	0.0
RXSJ1152.9+3307	11 52 51.91 +33 07 19.0	3	87GB115018.0 + 3	QSO	W00	1.40	187.17	0.50±0.17	2.46 ^{+0.47} _{-0.56}	15.8	-1	16.3	-1	0.05	0.5
RXSJ1153.0+2930	11 52 58.78 +29 30 14.9	19	FBQSJ1152 + 2930	QSO	ned	1.23	122.66	0.72±0.26	17.1	-1	18.3	-1	0.05	0.3
RXSJ1153.4+3557	11 53 26.23 +35 56 53.9	15	KUG1150 + 362	G	ned		2.15	0.36±0.16	12.0	1	13.0	1	0.06	0.2
RXSJ1153.5+3617	11 53 26.70 +36 17 26.3	18	87GB115051.8 + 3	QSO	W00	1.35	61.74	1.36±0.27	1.72 ^{+0.32} _{-0.28}	16.6	-1	17.2	-1	0.06	0.4
RXSJ1155.3+2324	11 55 18.61 +23 24 22.0	11	[GJP96]3	G	ned	0.142	1.26	0.95±0.59	1.04 ^{+0.11} _{-0.11}	8.1	2	0	0.07	11.0
RXSJ1157.0+3245	11 57 00.69 +32 44 58.3	19	87GB115425.5 + 3	rad			91.43	0.48±0.19	2.06 ^{+0.48} _{-0.45}	17.6	-1	18.0	-1	0.07	1.5
RXSJ1157.1+2602	11 57 05.96 +26 02 28.1	2		G?	id	0.301	9.99	0.48±0.16	18.1	-1	18.6	-1	0.06	1.0
RXSJ1157.2+2821	11 57 09.54 +28 22 00.8	13	FBQSJ1157 + 2822	G?			26.01	0.98±0.21	2.06 ^{+0.29} _{-0.29}	17.0	1	19.8	-1	0.06	0.5
RXSJ1158.4+2219	11 58 24.30 +22 19 13.7	8		S	W00		1.85	0.34±0.15	2.87 ^{+0.67} _{-0.53}	16.9	-1	17.6	-1	0.07	0.8
RXSJ1158.5+2514	11 58 31.76 +25 14 44.5	18					1.18	0.85±0.19	1.92 ^{+0.32} _{-0.37}	18.2	1	19.9	-1	0.06	0.4
RXSJ1159.5+2914	11 59 31.84 +29 14 43.9	6	[HB89]1156 + 295	QSO	ned	0.729	1855.80	1.41±0.23	1.78 ^{+0.27} _{-0.24}	16.1	-1	17.1	-1	0.05	0.3
RXSJ1203.7+2836	12 03 44.09 +28 36 22.5	22					2.18	3.68±0.37	2.08 ^{+0.14} _{-0.15}
RXSJ1204.7+3110	12 04 43.34 +31 10 38.2	15	UGC07064	A	ned	0.025	5.10	0.35±0.13	9.7	-1	10.7	1	0.05	1.1
RXSJ1205.8+3510	12 05 49.89 +35 10 45.3	13	PG1203 + 354	Sy	ned	0.053	1.40	2.84±1.01	1.94 ^{+0.54} _{-0.51}	12.8	1	13.6	1	0.06	1.0
RXSJ1206.6+2810	12 06 38.89 +28 10 26.8	30	NGC4104GROUP	Cl	ned	0.028	2.78	1.67±0.27	1.99 ^{+0.21} _{-0.22}	10.5	1	0	0.06	1.7
RXSJ1207.8+3148	12 07 44.66 +31 48 51.5	7					2.85	0.82±0.21
RXSJ1209.1+2651	12 09 08.41 +26 51 31.9	18					1.19	0.29±0.12	17.7	1	18.2	-1	0.05	1.2
RXSJ1209.4+4119	12 09 22.80 +41 19 41.5	14	B31206 + 416	B	W00		397.21	1.10±0.23	2.39 ^{+0.29} _{-0.32}	16.8	-1	17.5	-1	0.04	0.3
RXSJ1209.8+3217	12 09 45.24 +32 17 00.9	10	FIRSTJ120945.2	Sy	ned	0.145	1.66	8.69±0.98	3.31 ^{+0.22} _{-0.27}	16.7	-1	17.1	-1	0.05	0.7
RXSJ1211.0+2613	12 10 59.95 +26 13 03.6	21					1.37	0.42±0.15	1.98 ^{+0.51} _{-0.47}

continued on next page

ROSAT name (1)	FIRST position (2)	Δ_{XR} (3)	Name	type (4)	Ref	z (5)	f_r (6)	F_z (7)	Γ (8)	m_E (9)	cl (10)	m_O (11)	cl (12)	A(E) (13)	Δ_{RO} (14)
RXSJ1211.4+4053	12 11 23.38 +40 53 42.0	25					13.78	0.63±0.19	2.18 ^{+0.44} _{-0.42}
RXSJ1211.6+3901	12 11 34.25 +39 00 53.7	9	FIRSTJ121134.2	G	ned		12.13	0.36±0.15
RXSJ1211.8+3611	12 11 44.43 +36 11 57.1	29					4.83	0.33±0.14	...	17.9	-1	18.2	-1	0.06	0.3
RXSJ1212.0+2242	12 11 58.63 +22 42 32.6	8					16.46	6.99±0.55	2.16 ^{+0.13} _{-0.12}	18.5	-1	19.6	-1	0.08	0.5
RXSJ1212.8+4104	12 12 48.51 +41 04 12.1	25					1.80	0.54±0.18	...	18.4	2	20.7	1	0.05	0.5
RXSJ1213.1+3410	12 13 07.55 +34 10 34.1	5					9.74	0.85±0.28	1.54 ^{+0.50} _{-0.44}
RXSJ1213.7+4227	12 13 42.81 +42 27 42.7	19		QSO	New	0.073	2.91	0.51±0.18	...	14.5	1	16.1	1	0.04	0.9
RXSJ1214.1+2903	12 14 07.53 +29 03 29.3	9					1.25	0.34±0.13	...	19.8	-1	...	0	0.05	0.2
RXSJ1215.8+2938	12 15 47.23 +29 38 30.5	16					1.41	0.24±0.10	...	17.3	1	18.4	1	0.05	0.7
RXSJ1216.9+3754	12 16 51.78 +37 54 38.8	12	IRASF12144 + 381	Sy	ned	0.062	1.18	0.49±0.16	...	14.8	1	...	0	0.07	0.3
RXSJ1217.4+3056	12 17 21.42 +30 56 30.6	6	FBQSJ1217 + 3056	QSO	ned	0.307	8.69	2.86±0.33	2.44 ^{+0.17} _{-0.19}	16.8	1	17.4	-1	0.04	0.1
RXSJ1217.9+3007	12 17 52.08 +30 07 00.5	5	[HB89]1215 + 303	B	ned	0.237	375.97	40.67±1.24	2.47 ^{+0.05} _{-0.05}	13.9	2	15.5	-1	0.06	0.4
RXSJ1218.3+3223	12 18 15.75 +32 23 44.3	13					1.45	0.27±0.13
RXSJ1218.4+2948	12 18 26.52 +29 48 46.5	10	NGC4253	Sy	ned	0.013	38.16	68.48±1.65	2.16 ^{+0.04} _{-0.03}	9.6	-1	10.5	1	0.05	1.5
RXSJ1219.9+2825	12 19 51.67 +28 25 21.5	13	CGCG158 - 075	G	ned	0.026	7.90	0.70±0.19	...	11.9	2	14.1	1	0.06	0.5
RXSJ1220.1+3111	12 20 04.38 +31 11 48.1	11					26.21	0.29±0.13	1.40 ^{+0.87} _{-0.60}	17.6	-1	18.0	-1	0.05	0.1
RXSJ1220.1+2916	12 20 06.82 +29 16 50.7	11	NGC4278	Sy	ned	0.002	389.38	0.54±0.17	...	10.4	2	...	0	0.07	1.4
RXSJ1221.2+3522	12 21 14.48 +35 22 40.2	17					7.22	0.42±0.14	1.98 ^{+0.39} _{-0.41}	...	0	21.4	-1	0.03	0.6
RXSJ1221.4+3010	12 21 21.94 +30 10 37.1	5	PG1218 + 304	B	ned	0.179	60.66	23.02±1.13	2.10 ^{+0.08} _{-0.07}	15.6	1	16.7	-1	0.06	0.1
RXSJ1222.2+3541	12 22 11.44 +35 40 58.1	15					6.25	0.37±0.13	2.76 ^{+0.42} _{-0.65}	19.0	-1	19.5	-1	0.03	0.5
RXSJ1222.8+4021	12 22 45.56 +40 21 26.8	4					1.83	0.59±0.16	2.37 ^{+0.36} _{-0.49}
RXSJ1224.4+2436	12 24 24.18 +24 36 23.5	5	87GB122151.4 + 2	B	ned	0.218	21.93	2.57±0.31	2.22 ^{+0.18} _{-0.18}	16.8	-1	17.5	-1	0.06	0.1
RXSJ1224.8+3832	12 24 50.19 +38 32 48.5	14	87GB122220.7 + 3	rad			34.51	0.83±0.19	2.36 ^{+0.28} _{-0.31}	19.7	1	19.9	-1	0.03	1.0
RXSJ1225.2+3213	12 25 13.13 +32 14 01.7	11	87GB122241.8 + 3	A	New	0.059	43.80	2.34±0.26	0.79 ^{+0.25} _{-0.21}	10.7	2	13.5	1	0.06	1.3
RXSJ1226.4+3244	12 26 24.22 +32 44 29.4	4		BA	W00	0.242	1.49	4.90±0.41	2.58 ^{+0.12} _{-0.13}	16.4	1	17.1	-1	0.05	0.5
RXSJ1226.7+4026	12 26 41.97 +40 26 33.2	15					7.50	0.33±0.13	...	17.9	-1	18.7	-1	0.04	0.5
RXSJ1227.8+3214	12 27 49.15 +32 14 59.0	1					6.54	0.91±0.18	...	16.9	-1	18.8	-1	0.05	0.2
RXSJ1228.8+3706	12 28 47.42 +37 06 12.3	5	NGP9F268 - 03413	G	ned	1.515	381.76	0.31±0.11	2.00 ^{+0.46} _{-0.48}
RXSJ1230.2+2518	12 30 14.10 +25 18 07.1	3	87GB122746.7 + 2	B		0.135	225.99	3.43±0.34	2.15 ^{+0.15} _{-0.14}	16.0	-1	17.0	-1	0.05	0.2
RXSJ1231.3+3352	12 31 20.33 +33 52 39.6	24	NGP9F268 - 14307	G?	ned		6.72	0.27±0.11	...	15.6	1	19.0	1	0.05	0.3
RXSJ1231.9+3530	12 31 55.98 +35 30 15.1	6	IRASF12295 + 354	BA	W00	0.131	3.50	0.95±0.20	...	14.9	-1	16.0	1	0.04	0.1
RXSJ1233.3+3428	12 33 16.09 +34 29 00.2	1					4.64	0.35±0.12	2.51 ^{+0.41} _{-0.49}	17.9	-1	18.9	-1	0.04	0.1
RXSJ1235.3+2334	12 35 14.99 +23 34 45.1	26					1.13	0.74±0.19
RXSJ1236.4+3859	12 36 23.03 +39 00 01.1	6	87GB123357.2 + 3	B	W00		34.94	0.49±0.14	2.10 ^{+0.34} _{-0.34}	17.6	-1	18.7	-1	0.04	0.5
RXSJ1236.8+2309	12 36 46.12 +23 10 04.4	9	NGP9F378 - 03302	G?	ned		4.80	0.47±0.15	...	18.3	-1	19.4	-1	0.04	0.3
RXSJ1237.1+3020	12 37 05.59 +30 20 05.2	3	FIRSTJ123705.5	B	ned		3.23	6.54±0.43	1.84 ^{+0.10} _{-0.10}	18.8	-1	19.8	-1	0.04	0.7
RXSJ1237.5+2737	12 37 32.00 +27 37 53.0	6					4.48	0.49±0.15	0	21.3	-1	0.05	1.2
RXSJ1238.0+3616	12 38 02.52 +36 16 39.7	6		QSO?	ned		4.20	1.99±0.26	2.23 ^{+0.17} _{-0.18}	18.9	-1	19.9	-1	0.04	0.5
RXSJ1238.9+3942	12 38 52.15 +39 42 27.6	26					10.36	0.69±0.18	2.48 ^{+0.36} _{-0.33}	19.2	1	19.7	-1	0.04	0.5
RXSJ1239.0+3609	12 39 00.69 +36 09 24.6	12		QSO?	ned		13.53	1.43±0.22	2.40 ^{+0.20} _{-0.20}	...	0	20.2	1	0.04	0.2

continued on next page

ROSAT name (1)	FIRST position (2)	Δ_{XR} (3)	Name	type (4)	Ref	z (5)	f_r (6)	F_x (7)	Γ (8)	m_E (9)	cl (10)	m_O (11)	cl (12)	$A(E)$ (13)	Δ_{RO} (14)
RXSJ1239.2+4049	12 39 15.04 +40 49 56.1	6	87GB123651.2 + 4	QSO	W00	1.315	56.64	0.26±0.12	...	17.8	-1	18.7	-1	0.05	0.8
RXSJ1239.4+4132	12 39 22.73 +41 32 51.6	7					9.19	2.36±0.29	1.83 ^{+0.17} _{-0.18}	19.1	1	20.0	-1	0.06	0.4
RXSJ1240.2+2425	12 40 09.14 +24 25 31.1	9	87GB123740.5 + 2	QSO	W00	0.83	30.16	0.65±0.16	1.20 ^{+0.48} _{-0.40}	16.4	-1	16.9	-1	0.04	0.3
RXSJ1240.7+2310	12 40 44.50 +23 10 45.8	30	87GB123815.8 + 2	rad			40.76	0.58±0.20	...	17.7	-1	18.5	-1	0.06	0.2
RXSJ1241.4+3132	12 41 21.70 +31 32 03.6	5		A	W00	0.072	2.83	0.73±0.16	2.52 ^{+0.28} _{-0.34}	17.0	-1	18.2	1	0.04	0.1
RXSJ1241.7+3440	12 41 41.40 +34 40 31.1	3	FIRSTJ124141.3	B	ned		7.24	2.25±0.27	1.93 ^{+0.15} _{-0.16}	19.0	-1	20.1	-1	0.05	0.4
RXSJ1241.8+3202	12 41 45.72 +32 02 56.4	5	MCG + 05 - 30 - 060	Sy	ned	0.053	2.00	0.64±0.15	...	15.0	1	16.8	1	0.04	0.3
RXSJ1242.5+2906	12 42 33.06 +29 06 41.7	16					2.23	0.87±0.18	1.18 ^{+0.35} _{-0.29}
RXSJ1243.2+3627	12 43 12.69 +36 27 43.9	3	TON0116	B	W00		113.31	16.96±0.68	2.52 ^{+0.07} _{-0.08}	16.3	-1	16.8	-1	0.03	0.5
RXSJ1245.2+3356	12 45 11.27 +33 56 10.2	11	FIRSTJ124511.2	QSO	ned	0.717	1.88	0.32±0.12	...	16.6	-1	17.2	-1	0.04	0.3
RXSJ1246.2+4108	12 46 12.15 +41 08 12.7	6	IRAS12438 + 412	QSO	New	0.067	4.99	0.46±0.13	...	14.1	1	15.4	1	0.04	0.9
RXSJ1247.4+3925	12 47 25.40 +39 25 37.2	9		QSO?	ned		1.58	0.90±0.17	2.20 ^{+0.25} _{-0.27}	18.0	-1	18.6	-1	0.03	0.3
RXSJ1249.8+3708	12 49 46.76 +37 07 48.0	24					5.65	0.41±0.13	...	18.9	-1	19.7	-1	0.04	0.7
RXSJ1249.8+3554	12 49 47.58 +35 54 47.0	10					9.23	0.20±0.09
RXSJ1251.7+2404	12 51 42.27 +24 04 35.1	10		A?	ned		1.62	0.67±0.18	1.94 ^{+0.34} _{-0.33}	17.4	-1	17.9	-1	0.03	0.7
RXSJ1253.0+3826	12 53 00.91 +38 26 26.0	3					5.46	5.42±0.39	1.86 ^{+0.11} _{-0.10}	18.7	1	20.1	-1	0.05	0.8
RXSJ1255.2+2804	12 55 09.84 +28 04 17.8	3	ABELL1656P	G/Cl			2.09	0.32±0.11	2.12 ^{+0.43} _{-0.32}	20.0	1	20.7	-1	0.02	0.3
RXSJ1257.1+2649	12 57 08.40 +26 49 25.8	11					4.12	1.02±0.18	2.23 ^{+0.34} _{-0.27}	19.7	2	21.1	-1	0.03	0.1
RXSJ1257.3+3647	12 57 16.58 +36 47 15.2	7	[HB89]1254 + 370	B	W00	0.28	65.93	0.72±0.17	3.41 ^{+0.39} _{-0.63}	16.6	-1	17.4	-1	0.04	0.4
RXSJ1257.5+2412	12 57 31.92 +24 12 40.0	6	RXJ12575 + 2412	B	ned	0.141	9.61	11.96±0.60	2.14 ^{+0.08} _{-0.07}	15.0	2	...	0	0.03	2.9
RXSJ1258.1+2329	12 58 07.46 +23 29 21.9	20		QSO	W00	1.184	4.16	0.43±0.15	...	16.8	-1	17.6	-1	0.05	0.5
RXSJ1258.6+2736	12 58 35.17 +27 35 46.1	28	NGC4853	A	id	0.025	1.24	0.61±0.16	0.96 ^{+0.46} _{-0.37}	9.3	-1	9.8	1	0.03	2.0
RXSJ1259.5+3333	12 59 26.74 +33 33 39.7	13					4.33	0.48±0.17	...	18.9	-1	19.4	-1	0.03	0.2
RXSJ1259.6+3848	12 59 39.32 +38 48 56.1	16		G	ned	0.033	1.06	0.28±0.11	0	11.4	2	0.04	0.2
RXSJ1259.7+2808	12 59 44.12 +28 09 08.3	30	IC4003	rad			4.22	5.55±0.41	1.39 ^{+0.17} _{-0.16}
RXSJ1259.8+3423	12 59 48.79 +34 23 22.6	3	1257 + 28W06	QSO	ned	1.375	10.56	0.62±0.17	...	16.1	-1	17.0	-1	0.03	0.1
RXSJ1301.8+4056	13 01 45.67 +40 56 24.8	5	[HB89]1257 + 346	B	W00		25.53	1.45±0.21	2.54 ^{+0.21} _{-0.23}	17.8	-1	18.8	-1	0.05	0.3
RXSJ1303.6+3647	13 03 35.64 +36 47 28.2	14	87GB125926.5 + 4				1.38	0.19±0.08	...	17.6	1	20.8	1	0.04	0.4
RXSJ1303.9+2937	13 03 53.78 +29 37 34.9	28					5.40	0.32±0.11
RXSJ1305.4+2219	13 05 24.84 +22 19 14.0	10					7.14	0.56±0.17	2.12 ^{+0.45} _{-0.45}	18.0	-1	18.4	-1	0.05	0.3
RXSJ1305.5+3855	13 05 31.07 +38 55 22.8	8					12.60	1.06±0.19	2.41 ^{+0.24} _{-0.27}
RXSJ1305.7+2408	13 05 44.56 +24 08 40.7	2					6.18	0.82±0.17	1.62 ^{+0.30} _{-0.27}	19.1	-1	20.2	-1	0.06	0.4
RXSJ1305.9+3054	13 05 50.67 +30 54 15.3	27	B21303 + 31B	G	ned	0.182	49.08	2.59±0.27	1.73 ^{+0.17} _{-0.16}	11.1	2	...	0	0.03	2.4
RXSJ1307.8+2925	13 07 49.25 +29 25 48.3	12	FIRSTJ130749.2	G	ned	0.241	2.80	0.60±0.14	1.42 ^{+0.37} _{-0.32}	14.9	1	19.7	2	0.03	0.9
RXSJ1308.7+2736	13 08 40.62 +27 35 39.4	25					10.71	0.24±0.09
RXSJ1310.5+2808	13 10 28.16 +28 08 35.6	12	[HB89]1308 + 284	QSO	ned	0.520	1.23	0.61±0.15	0	18.1	-1	0.02	0.3
RXSJ1310.9+3703	13 10 56.23 +37 03 33.1	4	NGC5005	A	ned	0.003	35.90	0.72±0.15	0.90 ^{+0.38} _{-0.31}
RXSJ1312.3+3515	13 12 17.76 +35 15 21.3	4	PG1309 + 355	QSO	ned	0.184	43.92	1.57±0.21	2.38 ^{+0.17} _{-0.19}	15.2	1	15.9	-1	0.03	0.2
RXSJ1312.9+2402	13 12 56.61 +24 03 10.2	21					2.30	0.39±0.12	...	18.8	-1	20.4	-1	0.04	0.6
RXSJ1313.2+3753	13 13 14.27 +37 53 57.2	5		QSO	W00	0.66	2.48	0.57±0.14	2.61 ^{+0.31} _{-0.40}	16.8	-1	17.2	-1	0.04	0.4

continued on next page

ROSAT name (1)	FIRST position (2)	Δ_{XR} (3)	Name	type (4)	Ref	z (5)	f_r (6)	F_x (7)	Γ (8)	m_E (9)	cl (10)	m_O (11)	cl (12)	A(E) (13)	Δ_{RO} (14)
RXSJ1314.7+2348	13 14 43.80	+23 48 26.8	5 87GB131219.8 + 2	B	W00		168.97	1.66±0.20	2.86 ^{+0.17} _{-0.20}	15.7	-1	16.7	-1	0.03	0.1
RXSJ1315.8+3624	13 15 51.56	+36 24 36.7	13 NPM1G + 36.0301	G	ned		1.35	0.40±0.11	...	13.8	1	15.3	2	0.03	0.7
RXSJ1316.9+3014	13 16 54.59	+30 14 54.3	4 FIRSTJ131654.5	UvE			3.33	1.64±0.21	2.76 ^{+0.20} _{-0.25}	20.2	-1	20.2	-1	0.03	0.4
RXSJ1317.3+3925	13 17 18.65	+39 25 28.0	25 4C + 39.38	G	ned	1.56	473.47	0.27±0.10	1.84 ^{+0.44} _{-0.44}	17.8	-1	18.6	-1	0.04	0.3
RXSJ1317.5+3630	13 17 32.78	+36 30 59.8	5 QSO	QSO	New	0.466	21.20	0.64±0.13	...	18.4	-1	18.3	-1	0.03	0.6
RXSJ1320.3+3308	13 20 14.81	+33 08 37.7	21 NGC5098NED02	G	ned	0.036	25.91	2.02±0.24	0.65 ^{+0.26} _{-0.21}	...	0	12.2	2	0.04	1.3
RXSJ1320.5+3121	13 20 28.93	+31 21 07.3	20 CGCG160 - 204	G	ned	0.046	1.70	0.34±0.11	2.15 ^{+0.41} _{-0.47}	9.8	1	12.0	2	0.03	1.8
RXSJ1320.7+3516	13 20 41.31	+35 16 09.3	7				9.38	0.32±0.11	...	18.6	-1	18.4	2	0.02	0.0
RXSJ1320.9+3354	13 20 55.09	+33 54 12.1	13 87GB131838.7 + 3	G?	ned		38.53	1.06±0.16	1.69 ^{+0.22} _{-0.22}	13.8	1	17.1	2	0.04	7.4
RXSJ1321.5+3852	13 21 32.30	+38 52 49.3	1	S	New		1.06	14.12±0.54	1.48 ^{+0.66} _{-0.66}	7.3	1	...	0	0.03	1.4
RXSJ1323.1+3948	13 23 04.27	+39 48 54.8	14				10.20	0.21±0.08	...	18.1	-1	19.2	-1	0.04	0.5
RXSJ1323.6+3816	13 23 36.42	+38 16 41.4	8	BA	New	0.215	1.26	0.45±0.12	1.80 ^{+0.31} _{-0.32}	18.2	1	...	0	0.03	1.7
RXSJ1325.3+2422	13 25 15.08	+24 22 52.5	30 NGP9F380 - 04339	G	ned		1.17	0.59±0.19	1.33 ^{+0.45} _{-0.36}	10.8	2	13.8	2	0.04	2.3
RXSJ1325.5+3201	13 25 29.08	+32 01 13.6	10				1.86	0.11±0.06
RXSJ1325.7+4139	13 25 45.31	+41 38 57.2	22				1.19	0.77±0.17
RXSJ1325.8+3413	13 25 47.65	+34 13 20.9	24	id		1.934	4.59	0.29±0.10	1.75 ^{+0.40} _{-0.40}	18.1	-1	17.8	-1	0.03	0.5
RXSJ1328.9+3148	13 28 56.21	+31 48 14.2	6				4.29	0.32±0.10	1.74 ^{+0.40} _{-0.39}	18.9	-1	19.3	-1	0.03	0.4
RXSJ1330.6+2509	13 30 37.70	+25 09 10.9	16 [HB89]1328 + 254	QSO	ned	1.055	6826.39	0.45±0.16	2.42 ^{+0.43} _{-0.60}	16.6	1	18.3	-1	0.03	0.5
RXSJ1330.6+3104	13 30 35.59	+31 04 36.3	22 NGP9F324 - 01312	G?	ned		1.70	0.35±0.10	...	13.4	2	17.3	2	0.03	4.8
RXSJ1330.8+2413	13 30 46.83	+24 13 58.4	13				1.75	2.10±0.31	1.69 ^{+0.20} _{-0.19}	...	0	9.0	-1	0.04	3.5
RXSJ1330.8+3318	13 30 49.17	+33 19 04.0	23				1.66	0.46±0.13	2.27 ^{+0.30} _{-0.35}
RXSJ1331.8+2916	13 31 46.73	+29 16 37.8	7				2.51	4.89±0.38	2.37 ^{+0.11} _{-0.15}
RXSJ1331.8+3031	13 31 48.51	+30 31 47.6	8				260.94	0.25±0.10	2.04 ^{+0.55} _{-0.53}	19.8	1	20.1	-1	0.04	0.3
RXSJ1333.8+4141	13 33 45.46	+41 41 28.2	13				2.47	0.58±0.13	2.02 ^{+0.28} _{-0.30}	17.2	-1	18.3	-1	0.02	0.5
RXSJ1334.3+2919	13 34 18.98	+29 19 11.6	22	BA	W00	0.22	3.86	0.39±0.15	...	19.2	-1	20.2	-1	0.03	0.1
RXSJ1334.4+3044	13 34 22.48	+30 44 12.4	9 87GB133204.6 + 3	QSO	ned	1.352	54.15	0.31±0.11	2.47 ^{+0.44} _{-0.63}	18.2	-1	18.8	-1	0.04	0.6
RXSJ1334.4+3441	13 34 25.23	+34 41 26.1	12 NGC5223	G	ned	0.024	1.57	0.92±0.17	1.06 ^{+0.29} _{-0.25}	7.2	-1	...	0	0.04	0.5
RXSJ1334.8+3710	13 34 47.78	+37 10 56.7	5 BHCv _n	S	Smb		4.02	29.44±0.79	1.85 ^{+0.04} _{-0.04}
RXSJ1335.1+3412	13 35 06.49	+34 12 34.0	8 NGP9F270 - 11277	G	ned		1.53	0.25±0.08	1.62 ^{+0.47} _{-0.44}	16.3	1	18.5	1	0.02	0.4
RXSJ1336.2+2320	13 36 12.17	+23 19 57.8	12 NGP9F380 - 07547	G	ned		7.66	1.08±0.22	1.94 ^{+0.26} _{-0.27}
RXSJ1336.6+4209	13 36 36.66	+42 09 34.1	26	QSO	ned	0.224	2.89	0.28±0.10	...	15.3	2	17.0	2	0.02	1.6
RXSJ1337.3+2423	13 37 18.72	+24 23 03.4	3 [HB89]1334 + 246	QSO	ned	0.108	19.18	29.48±1.01	2.97 ^{+0.08} _{-0.08}	12.7	1	14.0	1	0.03	0.3
RXSJ1337.8+3350	13 37 47.65	+33 50 24.0	7				3.43	0.21±0.07	1.50 ^{+0.50} _{-0.50}
RXSJ1338.7+4122	13 38 44.46	+41 22 11.9	23				2.90	0.31±0.10	2.04 ^{+0.48} _{-0.48}
RXSJ1343.6+3601	13 43 34.38	+36 01 44.4	11 87GB134120.1 + 3	rad			31.51	0.29±0.09	2.72 ^{+0.39} _{-0.58}	16.8	1	19.6	1	0.03	0.2
RXSJ1343.7+4102	13 43 42.46	+41 02 56.6	5				2.77	0.43±0.12	2.28 ^{+0.31} _{-0.37}	20.5	-1	21.2	-1	0.01	0.6
RXSJ1344.0+2712	13 43 57.51	+27 12 41.0	12 NGP9F324 - 09335	G	ned	0.077	1.50	0.74±0.17	1.02 ^{+0.58} _{-0.39}	15.6	1	17.4	1	0.03	0.1
RXSJ1344.3+3907	13 44 19.33	+39 06 38.6	24	G	New	0.295	1.42	0.53±0.11	1.04 ^{+0.44} _{-0.35}	14.7	2	...	0	0.02	1.5
RXSJ1345.1+4047	13 45 03.12	+40 47 44.8	8				2.92	0.93±0.18	1.91 ^{+0.25} _{-0.25}
RXSJ1345.4+2310	13 45 25.19	+23 10 37.9	15				1.50	0.49±0.19	1.88 ^{+0.50} _{-0.50}	18.9	-1	21.1	-1	0.04	0.7

continued on next page

ROSAT name (1)	FIRST position (2)	Δ_{XR} (3)	Name	type (4)	Ref	z (5)	f_r (6)	F_x (7)	Γ (8)	m_E (9)	cl (10)	m_O (11)	cl (12)	A(E) (13)	Δ_{RO} (14)
RXSJ1434.8+3805	14 34 47.09	13					148.24	0.32±0.10	1.97 ^{+0.39} _{-0.41}	18.4	1	20.5	2	0.02	0.3
RXSJ1435.2+3132	14 35 09.52	15					39.26	1.21±0.22	...	18.3	-1	18.9	-1	0.04	0.7
RXSJ1436.0+3308	14 36 02.53	29	IRAS14339 + 332	H	New	0.094	6.08	0.28±0.11	...	15.0	1	16.4	1	0.04	0.1
RXSJ1437.0+2640	14 37 01.50	7					8.07	0.45±0.17	2.61 ^{+0.51} _{-0.58}	16.5	2	18.6	2	0.06	0.4
RXSJ1437.5+4128	14 37 27.92	27					19.13	1.13±0.19	2.62 ^{+0.22} _{-0.24}
RXSJ1437.8+2439	14 37 48.59	7	[HB89]1435 + 248	QSO	ned	1.01	252.95	0.45±0.17	...	18.7	-1	19.7	-1	0.11	1.0
RXSJ1438.5+3539	14 38 30.24	7					3.81	1.32±0.18	2.58 ^{+0.22} _{-0.29}	18.2	-1	19.1	-1	0.03	0.4
RXSJ1439.3+3932	14 39 17.50	6	PG1437 + 398	B	ned		42.35	16.06±0.60	2.33 ^{+0.06} _{-0.07}	16.5	1	18.4	-1	0.03	0.4
RXSJ1439.4+3904	14 39 24.44	13					2.58	0.49±0.12	1.62 ^{+0.34} _{-0.33}	16.6	1	19.9	1	0.03	0.4
RXSJ1440.1+3707	14 40 03.63	29					4.36	0.88±0.17	1.68 ^{+0.25} _{-0.25}	13.1	1	...	0	0.03	1.2
RXSJ1442.1+3526	14 42 07.47	10	PG1440 + 356	Sy	ned	0.079	3.94	49.85±1.07	3.08 ^{+0.06} _{-0.07}	12.8	1	13.8	1	0.03	0.1
RXSJ1442.2+4252	14 42 12.93	10	B31440 + 430	rad			5.51	0.42±0.13	1.83 ^{+0.46} _{-0.42}	18.1	-1	19.1	-1	0.04	0.5
RXSJ1442.7+2920	14 42 39.66	7	IRASF14405 + 293	G	ned		1.90	0.36±0.12	1.69 ^{+0.51} _{-0.47}	13.1	1	14.4	1	0.04	0.5
RXSJ1442.7+2623	14 42 40.81	7					3.17	1.17±0.24	2.64 ^{+0.26} _{-0.30}	15.2	-1	16.3	1	0.06	0.7
RXSJ1444.3+3808	14 44 17.24	21	B31442 + 383	rad			91.65	0.14±0.06
RXSJ1444.5+3022	14 44 30.95	5	87GB144222.3 + 3	rad			163.05	0.41±0.13	2.43 ^{+0.40} _{-0.32}
RXSJ1446.5+4127	14 46 32.55	6					35.70	0.32±0.10	1.74 ^{+0.49} _{-0.45}	19.0	-1	20.3	-1	0.04	0.4
RXSJ1447.5+3455	14 47 33.05	4	IRASF14455 + 350	QSO	W00	0.661	14.02	3.00±0.29	3.16 ^{+0.21} _{-0.26}	16.9	-1	17.4	1	0.04	0.2
RXSJ1448.0+3608	14 48 00.58	5	[WB92]1446 + 362	B?	W00		29.65	6.67±0.44	2.66 ^{+0.12} _{-0.13} 16.21	-1	16.8	-1	0.03	0.3	
RXSJ1449.4+3218	14 49 24.45	10	IRASF14473 + 323	G	ned		8.63	0.58±0.12	...	14.1	1	16.1	1	0.04	0.3
RXSJ1449.5+2746	14 49 32.75	10	87GB144719.7 + 2	rad			51.46	6.79±0.50	1.48 ^{+0.13} _{-0.13}	16.6	1	18.7	-1	0.08	0.5
RXSJ1450.2+3150	14 50 07.23	28					1.77	0.38±0.12	...	17.8	-1	18.0	-1	0.03	0.6
RXSJ1450.6+4127	14 50 36.61	6					21.27	0.26±0.10	1.44 ^{+0.65} _{-0.48}	17.5	2	21.2	1	0.05	1.9
RXSJ1451.0+3117	14 50 58.71	13					12.69	0.59±0.14	1.32 ^{+0.40} _{-0.33}
RXSJ1451.1+2709	14 51 08.81	8	PG1448 + 273	Sy	ned	0.065	3.43	14.83±0.77	2.56 ^{+0.08} _{-0.08}	...	0	14.6	1	0.08	0.2
RXSJ1451.5+3402	14 51 31.92	9					25.35	0.23±0.09	...	18.2	-1	18.0	-1	0.06	0.4
RXSJ1451.6+3357	14 51 32.35	15					3.91	0.15±0.07	...	19.3	-1	...	0	0.05	1.1
RXSJ1452.6+3257	14 52 36.20	14					2.01	0.22±0.08	0	20.9	-1	0.05	1.2
RXSJ1452.8+3833	14 52 49.22	17	87GB145051.2 + 3	rad			73.01	0.48±0.17	2.11 ^{+0.39} _{-0.44}
RXSJ1453.1+2554	14 53 05.59	28					1.07	3.28±0.39	1.51 ^{+0.39} _{-0.24}
RXSJ1454.5+2956	14 54 32.31	4	[HB89]1452 + 301	QSO	ned	0.58	650.82	0.72±0.17	2.13 ^{+0.31} _{-0.33}	19.3	-1	18.7	-1	0.05	0.6
RXSJ1455.5+3250	14 55 28.19	30	VV274	G	ned		3.29	0.33±0.11	2.28 ^{+0.37} _{-0.39}	12.0	1	11.5	1	0.05	0.7
RXSJ1456.6+3152	14 56 35.77	8					1.60	0.45±0.14	...	17.2	1	18.0	1	0.04	0.2
RXSJ1456.6+3852	14 56 34.34	19					5.67	0.29±0.11	1.43 ^{+0.87} _{-0.55}	17.9	1	...	0	0.03	0.3
RXSJ1457.3+2220	14 57 15.09	9	MS1455.0 + 2232	G	ned	0.258	4.07	5.65±0.61	1.22 ^{+0.25} _{-0.24}	14.9	1	18.5	1	0.12	0.6
RXSJ1457.5+3347	14 57 30.13	10					3.04	0.31±0.10	0.88 ^{+0.38} _{-0.44}	18.3	-1	19.1	-1	0.04	0.1
RXSJ1457.5+3417	14 57 32.35	10					2.03	0.38±0.12	...	18.0	-1	18.7	-1	0.03	0.4
RXSJ1458.1+3434	14 58 04.05	4					2.19	0.32±0.11	2.39 ^{+0.41} _{-0.49}	19.8	-1	20.1	-1	0.04	0.9
RXSJ1458.4+2833	14 58 19.66	28					11.07	0.51±0.17
RXSJ1459.8+3141	14 59 48.68	9					5.33	0.21±0.09	0.51 ^{+0.35} _{-0.49}

continued on next page

ROSAT name (1)	FIRST position (2)	Δ_{XR} (3)	Name	type (4)	Ref	z (5)	f_r (6)	F_x (7)	Γ (8)	m_E (9)	cl (10)	m_O (11)	cl (12)	A(E) (13)	Δ_{RO} (14)
RXSJ1500.0+3337	14 59 58.47	+33 37 01.6	3 87GB145756.1 + 3	QSO	W00	0.645	7.22	1.56±0.21	2.19 ^{+0.17} _{-0.18}	17.1	-1	17.2	-1	0.04	0.5
RXSJ1500.8+3212	15 00 47.51	+32 12 31.7	22 NPM1G + 32.0412	G	ned		1.14	0.63±0.16	1.01 ^{+0.85} _{-0.47}	11.6	2	13.6	2	0.04	8.3
RXSJ1501.0+2238	15 01 01.84	+22 38 06.5	6 MS1458.8 + 2249	B	ned	0.235	28.74	7.40±0.72	2.74 ^{+0.16} _{-0.16}	15.3	-1	16.6	-1	0.13	0.2
RXSJ1501.1+4222	15 01 06.66	+42 22 35.2	8				1.15	0.52±0.14	2.02 ^{+0.34} _{-0.34}	19.4	-1	0	0.04	0.8
RXSJ1502.5+3947	15 02 28.98	+39 47 28.0	18 B31500 + 399B	rad			385.61	0.38±0.11	1.40 ^{+0.51} _{-0.41}	20.2	2	0	0.03	1.9
RXSJ1502.7+3752	15 02 39.15	+37 52 28.2	7				1.35	0.52±0.12	1.85 ^{+0.30} _{-0.30}
RXSJ1504.5+2854	15 04 26.71	+28 54 30.5	9 B21502 + 29	G?	ned		549.11	0.98±0.22	1.78 ^{+0.39} _{-0.35}	18.3	-1	18.5	-1	0.06	0.8
RXSJ1504.5+3024	15 04 26.75	+30 24 05.4	23				5.01	0.83±0.18	2.42 ^{+0.31} _{-0.33}	19.6	1	21.9	-1	0.05	0.4
RXSJ1508.9+4055	15 08 56.86	+40 55 26.0	25				2.97	0.30±0.11
RXSJ1510.3+4221	15 10 17.84	+42 21 54.4	5 B31508 + 425	rad			182.65	0.25±0.09	1.24 ^{+0.88} _{-0.54}
RXSJ1510.7+3127	15 10 39.59	+31 27 16.0	2 87GB150837.3 + 3	rad			74.26	0.64±0.18	2.19 ^{+0.38} _{-0.39}	18.9	-1	18.9	-1	0.05	0.3
RXSJ1510.7+3335	15 10 41.18	+33 35 04.5	12				3.54	4.06±0.36	1.90 ^{+0.14} _{-0.13}	15.8	1	17.7	1	0.05	0.7
RXSJ1510.7+3648	15 10 41.28	+36 48 55.0	15	G?	ned		1.34	0.67±0.13	0.80 ^{+0.34} _{-0.26}	15.7	1	18.9	1	0.04	1.4
RXSJ1513.6+3241	15 13 35.45	+32 41 41.6	1 IRASF15116 + 325	IrS			1.05	0.39±0.15	17.6	1	18.1	1	0.04	1.4
RXSJ1514.1+3126	15 14 02.92	+31 26 13.0	10				3.45	0.89±0.21	2.01 ^{+0.34} _{-0.33}	0	21.9	-1	0.05	0.1
RXSJ1514.3+4135	15 14 21.18	+41 35 03.4	28				5.24	0.80±0.24
RXSJ1514.4+3636	15 14 22.44	+36 36 20.7	22 FIRSTJ151422.4	G	ned	2.723	1.71	0.62±0.13	1.22 ^{+0.46} _{-0.36}	17.6	1	0	0.06	0.7
RXSJ1515.3+2922	15 15 17.32	+29 22 25.7	24				26.79	0.40±0.16	1.52 ^{+1.40} _{-0.70}	19.4	1	19.8	-1	0.08	0.3
RXSJ1515.7+3510	15 15 41.10	+35 10 47.4	11				8.79	1.27±0.20	1.72 ^{+0.25} _{-0.22}
RXSJ1515.9+2426	15 15 56.19	+24 26 20.3	13	B	New	0.228	23.68	0.64±0.26	17.0	1	19.1	-1	0.13	0.3
RXSJ1516.0+3305	15 15 57.90	+33 06 06.9	14				1.71	0.44±0.15	2.32 ^{+0.51} _{-0.57}	13.3	1	16.3	-1	0.05	3.5
RXSJ1516.6+2918	15 16 35.25	+29 18 22.0	23 FIRSTJ151641.5	G			2.77	0.64±0.22	2.10 ^{+0.53} _{-0.48}
RXSJ1517.5+2856	15 17 28.50	+28 56 16.0	12 FBQSJ1517 + 2856	QSO	ned	0.208	1.39	0.39±0.16	17.2	-1	17.8	-1	0.07	0.5
RXSJ1518.3+2927	15 18 19.51	+29 27 12.8	20				1.72	0.66±0.21	1.20 ^{+0.90} _{-0.54}
RXSJ1518.6+4045	15 18 38.92	+40 45 00.1	13 NPM1G + 40.0388	A?	ned		44.17	0.82±0.19	1.41 ^{+0.46} _{-0.35}	13.0	2	15.1	1	0.05	0.4
RXSJ1519.6+2838	15 19 36.15	+28 38 27.9	26 FBQSJ1519 + 2838	QSO	ned	0.270	2.08	0.76±0.25	2.98 ^{+0.50} _{-0.61}	16.6	-1	17.3	-1	0.07	0.5
RXSJ1524.1+2952	15 24 08.40	+29 52 55.2	7 FIRSTJ152408.3	G	ned	0.114	1.13	6.01±0.57	1.18 ^{+0.34} _{-0.27}
RXSJ1524.4+3237	15 24 23.97	+32 37 58.3	13				1.34	0.37±0.14
RXSJ1524.4+3516	15 24 26.05	+35 15 59.6	18				3.94	0.64±0.19	1.69 ^{+0.38} _{-0.34}	17.3	1	21.0	-1	0.05	0.5
RXSJ1525.8+2825	15 25 48.41	+28 25 35.4	17	BA	New	0.160	16.94	1.45±0.34	2.84 ^{+0.34} _{-0.38}	16.4	2	17.2	1	0.08	1.6
RXSJ1528.3+3222	15 28 16.59	+32 22 59.7	4				1.59	1.05±0.25	3.26 ^{+0.43} _{-0.71}
RXSJ1528.7+2825	15 28 40.67	+28 25 30.8	5 [HB89]1526 + 285	QSO	ned	0.45	1.13	4.50±0.55	3.06 ^{+0.18} _{-0.21}	16.7	-1	16.7	-1	0.06	0.9
RXSJ1529.2+3812	15 29 13.57	+38 12 17.6	11				10.34	1.09±0.23	2.79 ^{+0.29} _{-0.36}	19.9	-1	19.9	-1	0.04	0.2
RXSJ1532.0+3016	15 32 02.24	+30 16 28.9	3 87GB152959.0 + 3	B?	New	0.066	58.91	6.12±0.58	1.93 ^{+0.14} _{-0.14}	12.4	2	14.6	2	0.08	0.7
RXSJ1532.9+3021	15 32 53.79	+30 20 59.5	4	A?	ned		15.21	3.87±0.51	0.99 ^{+0.30} _{-0.23}	16.2	2	18.6	2	0.08	3.6
RXSJ1533.4+3416	15 33 24.25	+34 16 40.2	8	B	W00		27.14	4.87±0.48	2.55 ^{+0.14} _{-0.15}	17.1	-1	17.7	-1	0.06	0.2
RXSJ1534.8+3716	15 34 47.20	+37 15 54.8	17 87GB153254.4 + 3	B	W00	0.143	21.75	0.38±0.15	16.3	1	18.3	-1	0.05	0.2
RXSJ1535.5+3922	15 35 29.05	+39 22 46.7	6	B	W00	0.257	19.20	2.25±0.29	2.54 ^{+0.19} _{-0.22}	16.8	1	18.5	-1	0.05	0.1
RXSJ1535.8+4322	15 35 47.13	+43 22 45.4	11				8.52	0.85±0.18	2.05 ^{+0.33} _{-0.32}	18.7	-1	19.1	-1	0.07	0.7
RXSJ1538.3+4105	15 38 18.66	+41 05 48.4	17 B31536 + 412	rad			26.03	0.65±0.20	17.6	-1	18.0	-1	0.07	1.0

continued on next page

ROSAT name (1)	FIRST position (2)	Δ_{XR} (3)	Name	type (4)	Ref	z (5)	f_r (6)	F_x (7)	Γ (8)	m_E (9)	cl (10)	m_O (11)	cl (12)	A(E) (13)	Δ_{RO} (14)
RXSIJ1539.8+3043	15 39 50.77	+30 43 03.9	FIRSTJ153950.7	G	ned	0.097	5.81	7.73±0.85	1.53 ^{+0.20} _{-0.18}	11.3	2	...	0	0.07	3.5
RXSIJ1539.8+3349	15 39 52.23	+33 49 31.1	FIRSTJ153952.2	Sy	ned	0.33	2.31	0.78±0.25	1.98 ^{+0.51} _{-0.45}	15.5	1	17.6	1	0.09	2.0
RXSIJ1539.8+4143	15 39 51.38	+41 43 25.6		B?	New	0.120	19.12	0.35±0.14	2.78 ^{+0.55} _{-0.73}	12.7	2	...	0	0.07	0.3
RXSIJ1543.8+4013	15 43 48.60	+40 13 24.9		QSO	W00	0.32	3.24	2.22±0.32	2.76 ^{+0.21} _{-0.24}	16.4	-1	17.3	-1	0.04	0.2
RXSIJ1548.3+3511	15 48 17.92	+35 11 28.4	[HB89]1546 + 353	QSO	W00	0.48	140.94	0.82±0.28	...	17.7	-1	18.4	-1	0.06	0.7
RXSIJ1550.3+2950	15 50 21.43	+29 50 28.1					15.17	0.40±0.19	...	17.3	1	19.1	1	0.07	0.3
RXSIJ1551.6+3548	15 51 35.63	+35 48 51.6		H	New	0.093	5.31	0.86±0.27	1.92 ^{+0.43} _{-0.41}	13.8	2	16.5	1	0.05	1.1
RXSIJ1551.8+3259	15 51 47.42	+33 00 07.9		QSO	W00	1.424	1.78	1.69±0.36	2.53 ^{+0.29} _{-0.32}	17.5	-1	18.0	-1	0.07	0.8
RXSIJ1552.2+3159	15 52 10.33	+31 59 08.7					1.92	1.09±0.29	1.95 ^{+0.52} _{-0.44}
RXSIJ1553.7+2417	15 53 40.70	+24 18 00.0					1.16	1.14±0.29	2.05 ^{+0.66} _{-0.48}	17.8	1	18.6	1	0.12	0.3
RXSIJ1554.2+2414	15 54 12.07	+24 14 26.9					7.83	2.12±0.35	2.10 ^{+0.37} _{-0.29}	18.6	-1	20.3	-1	0.13	0.3
RXSIJ1554.3+3238	15 54 17.43	+32 38 38.1					2.11	1.73±0.35	...	13.6	1	15.7	1	0.07	0.8
RXSIJ1556.1+2426	15 56 03.87	+24 26 53.8	CG1329	A	ned		58.48	0.32±0.14	2.37 ^{+0.68} _{-0.54}	8.8	1	11.2	1	0.16	1.4
RXSIJ1558.3+2551	15 58 18.75	+25 51 24.6	CGCG137 - 003	G	ned	0.043	2.50	4.17±0.45	2.04 ^{+0.24} _{-0.20}	15.4	1	16.4	1	0.17	0.5
RXSIJ1558.7+2534	15 58 44.00	+25 34 11.0	MRK0864	A	ned	0.072	2.26	15.83±0.83	3.08 ^{+0.68} _{-0.68}	7.9	-1	...	0	0.20	9.1
RXSIJ1558.9+3323	15 58 55.16	+33 23 18.8	MS Ser	S	Smb		142.96	0.43±0.16	...	16.9	-1	18.3	-1	0.08	0.5
RXSIJ1559.2+3501	15 59 09.63	+35 01 47.7	[HB89]1556 + 335	QSO	ned	1.646	3.51	8.72±0.65	2.71 ^{+0.12} _{-0.12}	8.1	1	8.7	1	0.07	0.6
RXSIJ1602.3+3050	16 02 18.09	+30 51 09.3	UGC10120	Sy	ned	0.032	54.12	1.39±0.27	2.29 ^{+0.32} _{-0.31}	17.8	-1	...	0	0.07	0.7
RXSIJ1602.6+2645	16 02 39.63	+26 46 06.0	FIRSTJ160218.0	B	ned		36.34	0.68±0.20	2.50 ^{+0.51} _{-0.48}	18.6	1	20.5	2	0.12	0.7
RXSIJ1603.0+3039	16 02 57.36	+30 38 52.0	FBQSJ1602 + 3038	QSO	ned	0.81	1.23	0.58±0.18	3.05 ^{+0.41} _{-0.49}	17.8	-1	18.6	-1	0.08	0.2
RXSIJ1603.0+4212	16 02 58.87	+42 12 02.7					6.23	3.73±0.49	1.88 ^{+0.18} _{-0.18}	19.1	-1	20.0	-1	0.03	0.4
RXSIJ1604.8+3344	16 04 46.51	+33 45 21.8					5.97	1.15±0.24	1.96 ^{+0.31} _{-0.28}	16.5	1	19.3	1	0.07	0.6
RXSIJ1605.2+3239	16 05 08.87	+32 39 22.4		H	New	0.091	1.07	0.55±0.17	2.35 ^{+0.42} _{-0.41}	16.4	1	18.2	1	0.10	0.3
RXSIJ1605.3+3756	16 05 15.50	+37 56 43.9	B31603 + 380	rad			118.93	1.57±0.26	2.97 ^{+0.25} _{-0.31}
RXSIJ1606.5+3713	16 06 30.54	+37 13 39.6					3.38	0.26±0.12	...	18.6	-1	18.7	-1	0.03	0.6
RXSIJ1607.7+2541	16 07 40.61	+25 41 14.2					18.35	5.51±0.48	2.34 ^{+0.17} _{-0.15}	13.4	1	15.3	1	0.17	6.5
RXSIJ1607.8+3450	16 07 46.04	+34 50 48.8		H	New	0.054	1.83	0.42±0.13	...	15.0	1	16.3	1	0.06	0.5
RXSIJ1609.4+2405	16 09 25.56	+24 05 17.6					1.18	0.27±0.13	...	18.8	-1	20.2	-1	0.19	0.4
RXSIJ1610.8+3303	16 10 47.73	+33 03 37.7	RXJ16107 + 3303	Sy	ned	0.097	6.86	3.46±0.29	2.42 ^{+0.12} _{-0.13}	14.4	1	15.5	-1	0.05	0.5
RXSIJ1611.7+3812	16 11 39.24	+38 12 41.7	NPM1G + 38.0357	G	ned		6.86	0.47±0.13	2.72 ^{+0.37} _{-0.53}	12.5	2	14.2	1	0.04	0.6
RXSIJ1612.0+3110	16 11 59.54	+31 10 41.6					7.62	0.56±0.14	1.12 ^{+0.61} _{-0.43}	16.9	1	19.7	1	0.09	0.4
RXSIJ1612.3+3911	16 12 17.18	+39 11 03.1					1.23	0.27±0.10	2.33 ^{+0.50} _{-0.73}	14.8	2	17.0	2	0.02	7.0
RXSIJ1613.7+3412	16 13 41.06	+34 12 47.8	[HB89]1611 + 343	QSO	ned	1.401	3532.04	0.64±0.14	2.41 ^{+0.27} _{-0.30}	17.7	-1	18.0	-1	0.05	0.3
RXSIJ1614.2+2604	16 14 13.20	+26 04 16.1	PG1612 + 261	QSO	ned	0.131	17.69	9.87±0.63	2.52 ^{+0.11} _{-0.10}	13.3	2	...	0	0.14	4.9
RXSIJ1614.7+3351	16 14 40.98	+33 51 31.6	sig CrB	S	Smb		5.52	134.78±1.63	1.98 ^{+0.02} _{-0.02}
RXSIJ1614.7+2312	16 14 41.69	+23 12 40.7		QSO	W00	0.295	4.55	1.03±0.24	...	16.8	-1	18.0	-1	0.31	0.2
RXSIJ1614.8+3745	16 14 46.96	+37 46 07.3	87GB161259.6 + 3	QSO	W00	1.52	49.26	0.31±0.09	2.03 ^{+0.39} _{-0.41}	16.1	-1	16.7	-1	0.04	0.1
RXSIJ1615.7+3308	16 15 40.36	+33 09 04.1					2.98	0.37±0.12	2.52 ^{+0.45} _{-0.53}	17.6	1	19.1	1	0.05	0.7
RXSIJ1616.2+2241	16 16 08.49	+22 41 07.4					12.46	1.39±0.27	...	16.9	1	19.2	1	0.32	1.2
RXSIJ1616.6+3755	16 16 32.88	+37 56 03.6					3.12	1.42±0.17	1.64 ^{+0.17} _{-0.17}	18.0	1	20.1	1	0.05	0.4

continued on next page

ROSAT name (1)	FIRST position (2)	Δ_{XR} (3)	Name	type (4)	Ref	z (5)	f_r (6)	F_z (7)	Γ (8)	m_E (9)	cl (10)	m_O (11)	cl (12)	A(E) (13)	Δ_{RO} (14)
RXSI1616.9+3621	16 16 55.57 +36 21 34.4	5	87GB161506.4 + 3	rad			309.10	0.17±0.07	2.34 ^{+0.46} _{-0.39}	18.5	-1	18.7	-1	0.03	0.4
RXSI1618.0+4123	16 18 00.41 +41 23 31.3	27	NPM1G + 41.0426	G	ned		1.10	0.71±0.15	1.14 ^{+0.37} _{-0.37}	10.8	2	13.4	2	0.03	0.5
RXSI1618.4+2907	16 18 20.93 +29 07 46.9	22					1.15	0.27±0.11	17.2	1	20.1	1	0.16	0.5
RXSI1619.0+3030	16 19 02.51 +30 30 51.5	15	FBQSI1619 + 3030	QSO	ned	1.286	66.82	0.51±0.14	1.87 ^{+0.45} _{-0.38}	16.4	2	17.6	-1	0.08	0.7
RXSI1619.7+2543	16 19 40.56 +25 43 23.4	14	RXJ16196 + 2543	Sy	ned	0.268	1.66	0.78±0.21	3.34 ^{+0.36} _{-0.41}	15.6	2	16.7	1	0.13	2.6
RXSI1620.1+3230	16 20 07.86 +32 30 27.8	3					4.14	0.26±0.09 ^{+0.10} _{-0.10}	0	21.4	1	0.06	0.6
RXSI1620.2+4008	16 20 13.08 +40 08 28.1	30					1.52	3.65±0.24	2.28 ^{+0.10} _{-0.10}
RXSI1620.5+2953	16 20 31.12 +29 53 27.6	13	FIRSTJ162031.1	G	ned	0.095	4.39	6.04±0.43	11.8	2	0	0.11	4.1
RXSI1620.7+3435	16 20 44.36 +34 35 11.1	7					6.91	0.61±0.13	1.91 ^{+0.27} _{-0.27}	18.6	-1	20.4	-1	0.06	0.2
RXSI1621.2+3745	16 21 11.29 +37 46 04.9	9	4C + 37.46	B?	ned		631.78	1.54±0.16	1.96 ^{+0.14} _{-0.14}	18.9	-1	21.3	-1	0.04	0.5
RXSI1622.5+4006	16 22 29.33 +40 06 43.5	12	87GB162048.8 + 4	id		0.69	27.50	0.48±0.10	2.40 ^{+0.34} _{-0.38}	18.1	-1	18.3	-1	0.03	0.6
RXSI1623.1+3909	16 23 07.60 +39 09 32.5	6	[HB89]1621 + 392	QSO	ned	1.98	189.57	0.57±0.11	2.78 ^{+0.39} _{-0.38}	15.9	1	16.1	1	0.03	0.8
RXSI1623.3+4116	16 23 19.93 +41 17 02.8	26	FIRSTJ162319.9	QSO	ned	1.62	3.23	0.32±0.09	3.16 ^{+0.40} _{-0.64}	16.4	-1	17.2	-1	0.02	0.1
RXSI1623.3+4022	16 23 18.92 +40 22 58.3	3	FIRSTJ162318.9	QSO	W00	0.91	8.63	0.27±0.08	1.90 ^{+0.36} _{-0.38}	17.3	-1	17.8	-1	0.02	0.5
RXSI1623.5+3559	16 23 30.57 +35 59 33.1	6	[HB89]1621 + 361	QSO	ned	0.87	259.58	0.24±0.09	17.8	-1	18.2	-1	0.03	0.4
RXSI1623.5+2841	16 23 32.30 +28 41 28.7	12					2.79	0.42±0.14	2.51 ^{+0.47} _{-0.49}
RXSI1624.2+2604	16 24 09.40 +26 04 30.3	10	IRASF16221 + 261	Sy	ned	0.040	2.07	5.71±0.48	2.26 ^{+0.14} _{-0.14}	11.8	1	13.1	1	0.15	3.0
RXSI1625.0+4230	16 24 58.41 +42 31 07.5	12					2.50	0.85±0.13	3.25 ^{+0.39} _{-0.41}	18.2	-1	18.8	1	0.03	0.2
RXSI1625.0+3532	16 25 01.44 +35 33 02.7	21					1.04	0.38±0.10	1.63 ^{+0.37} _{-0.33}	17.9	1	20.7	1	0.05	0.7
RXSI1625.2+2650	16 25 14.24 +26 50 27.5	16	[HB89]1623 + 269	QSO	ned	0.779	368.12	0.71±0.20	3.40 ^{+0.41} _{-0.50}	18.0	-1	0	0.08	1.3
RXSI1625.5+2705	16 25 30.85 +27 05 44.2	7	B21623 + 27A	G	ned	0.525	99.73	1.48±0.29	2.73 ^{+0.30} _{-0.29}	18.6	1	18.7	1	0.08	2.7
RXSI1625.7+4118	16 25 42.16 +41 18 41.1	15	B31624 + 414	rad			70.61	0.29±0.09	2.80 ^{+0.35} _{-0.53}	19.1	-1	19.4	-1	0.02	0.2
RXSI1625.9+4346	16 25 53.32 +43 47 13.8	20		id		1.04	125.04	0.95±0.14	1.92 ^{+0.18} _{-0.19}	18.0	-1	18.3	-1	0.03	0.4
RXSI1626.1+3359	16 26 07.05 +33 59 16.1	16	FIRSTJ162607.0	QSO	ned	0.204	3.36	1.69±0.22	3.06 ^{+0.22} _{-0.26}	15.6	-1	16.1	-1	0.06	2.3
RXSI1626.4+3513	16 26 25.85 +35 13 41.6	11	FIRSTJ162625.8	B	ned	0.50	17.60	1.35±0.16	1.91 ^{+0.17} _{-0.17}	18.2	-1	18.9	-1	0.06	0.1
RXSI1626.7+4239	16 26 42.53 +42 40 12.2	16	ABELL2192	Cl	ned	0.187	1.60	0.67±0.12	1.51 ^{+0.25} _{-0.23}	14.4	1	18.1	2	0.03	0.3
RXSI1627.4+3507	16 27 26.65 +35 08 15.8	16		A	W00	0.194	1.33	0.30±0.10	2.14 ^{+0.40} _{-0.43}	17.7	1	19.1	-1	0.06	0.0
RXSI1627.7+4055	16 27 41.12 +40 55 37.7	8	NGC6160	G	ned	0.031	1.17	0.78±0.14	0.47 ^{+0.36} _{-0.47}	11.1	1	0	0.01	0.6
RXSI1628.3+3629	16 28 19.38 +36 30 10.9	17					2.89	0.30±0.09	3.24 ^{+0.47} _{-1.00}	20.5	-1	21.3	-1	0.03	0.7
RXSI1629.0+4007	16 29 01.32 +40 07 59.6	6	FIRSTJ162901.3	Sy	ned	0.272	11.97	8.05±0.34	3.27 ^{+0.11} _{-0.13}	17.7	-1	18.0	-1	0.02	0.3
RXSI1629.4+3926	16 29 19.88 +39 25 56.8	23	FIRSTJ162919.8	G	ned		12.93	1.44±0.19	1.54 ^{+0.31} _{-0.30}	11.0	1	0	0.02	10.7
RXSI1629.7+4048	16 29 44.89 +40 48 41.8	5	NGC6173	G	ned	0.029	6.80	0.43±0.10	10.8	1	9.5	1	0.02	3.7
RXSI1630.3+3756	16 30 20.77 +37 56 56.5	27	[HB89]1628 + 380	QSO	ned	0.394	20.00	0.56±0.12	0.93 ^{+0.54} _{-0.35}	17.6	-1	17.4	-1	0.03	0.1
RXSI1631.3+2352	16 31 15.53 +23 52 58.3	15		A	New	0.059	3.68	1.02±0.26	0.06 ^{+0.23} _{-1.23}	14.1	2	16.0	2	0.13	1.2
RXSI1631.4+4216	16 31 24.71 +42 17 02.5	6	[NBK96]16313 + 4	B	ned		6.58	5.94±0.29	1.91 ^{+0.07} _{-0.08}	18.7	-1	19.6	-1	0.02	0.1
RXSI1631.9+3858	16 31 55.53 +38 58 05.1	16					1.97	0.18±0.07	1.47 ^{+0.71} _{-0.56}
RXSI1633.0+2349	16 33 02.68 +23 49 28.6	14		S	W00		3.62	1.94±0.34	1.22 ^{+0.49} _{-0.37}	15.6	-1	16.3	-1	0.21	0.2
RXSI1633.3+3520	16 33 17.83 +35 20 32.4	26	NGC6185	G	ned	0.034	60.36	0.23±0.09	1.51 ^{+0.77} _{-0.56}	9.1	1	8.8	1	0.07	0.7
RXSI1634.4+2410	16 34 22.94 +24 10 11.7	5					1.08	0.88±0.26	0.90 ^{+0.88} _{-0.50}	16.9	1	19.2	1	0.11	1.0
RXSI1635.3+3712	16 35 16.92 +37 12 28.4	6					3.30	0.41±0.13	2.67 ^{+0.42} _{-0.58}	17.2	1	19.9	1	0.04	0.5

continued on next page

ROSAT name (1)	FIRST position (2)	Δ_{XR} (3)	Name	type (4)	Ref (5)	z (5)	f_r (6)	F_x (7)	Γ (8)	m_E (9)	cl (10)	m_O (11)	cl (12)	A(E) (13)	Δ_{RO} (14)
RXSJ1636.9+3535	16 36 55.60	+35 35 36.2					1.03	0.13±0.07	19.2	1	0	0.06	1.2
RXSJ1637.1+4140	16 37 09.33	+41 40 30.6	87GB163528.0+4	QSO	W00	0.76	7.37	0.32±0.10	2.57 ^{+0.36} _{-0.48}	16.8	-1	17.2	-1	0.02	0.1
RXSJ1639.5+3908	16 39 31.80	+39 08 45.4		BA	W00	0.144	1.27	0.71±0.14	1.70 ^{+0.24} _{-0.24}	17.0	1	17.8	-1	0.03	0.2
RXSJ1640.6+3602	16 40 33.24	+36 03 01.6					1.39	0.29±0.11	2.59 ^{+0.46} _{-0.62}
RXSJ1641.8+3934	16 41 47.55	+39 35 03.4	[HB89]1640+396	QSO	ned	0.54	40.63	0.48±0.12	2.16 ^{+0.32} _{-0.37}	18.4	-1	18.4	-1	0.04	0.3
RXSJ1642.6+2726	16 42 38.65	+27 26 37.3		G	New	0.103	3.79	4.19±0.54	12.8	2	14.9	2	0.27	1.9
RXSJ1642.7+2522	16 42 40.41	+25 23 07.6	87GB164034.1+2	QSO	W00	1.71	490.22	0.37±0.18	17.7	-1	17.9	-1	0.16	0.2
RXSJ1644.5+2457	16 44 30.27	+24 57 28.7					2.89	0.57±0.20	2.12 ^{+1.35} _{-0.64}	16.6	1	18.4	1	0.12	0.4
RXSJ1647.0+3850	16 47 02.08	+38 50 05.3					1.04	0.40±0.12	1.52 ^{+0.46} _{-0.40}	15.1	1	18.0	2	0.04	1.9
RXSJ1648.9+3954	16 48 55.91	+39 54 37.0		B?	New	0.070	3.79	0.25±0.10	12.6	2	15.3	2	0.04	0.5
RXSJ1651.2+4212	16 51 09.19	+42 12 53.4		B?	W00		16.33	0.15±0.07	17.7	-1	18.2	-1	0.07	0.3
RXSJ1652.8+4022	16 52 49.93	+40 23 09.9		B?	W00		16.82	0.46±0.15	16.6	-1	17.2	-1	0.05	0.4
RXSJ1652.9+4009	16 52 53.30	+40 09 12.9		B?	New	0.148	29.95	1.63±0.25	13.1	2	16.4	2	0.05	2.0
RXSJ1652.9+3123	16 52 55.93	+31 23 43.9		QSO	W00	0.59	1.16	0.37±0.13	1.96 ^{+0.70} _{-0.56}	17.8	1	17.7	-1	0.08	0.3
RXSJ1653.5+3107	16 53 29.91	+31 07 56.9	87GB165133.2+3	rad			177.12	0.42±0.14	2.37 ^{+0.46} _{-0.47}	13.6	2	0	0.09	6.7
RXSJ1653.9+3945	16 53 52.21	+39 45 36.7	MRK 501	B	ned	0.034	1394.38	62.24±1.33	2.36 ^{+0.03} _{-0.04}	7.6	1	10.8	2	0.05	2.5
RXSJ1655.0+3030	16 55 00.22	+30 30 40.6		QSO	W00	0.40	3.20	0.72±0.17	1.71 ^{+0.98} _{-0.54}	17.2	-1	17.4	-1	0.09	0.4
RXSJ1657.2+3920	16 57 12.59	+39 20 18.2					3.18	0.39±0.14	1.72 ^{+0.56} _{-0.50}	9.9	-1	10.7	-1	0.05	1.2
RXSJ1659.5+3735	16 59 31.93	+37 35 29.0		QSO	W00	0.77	18.31	0.37±0.12	2.73 ^{+0.54} _{-0.92}	17.3	-1	17.2	-1	0.06	0.3
RXSJ1700.1+2703	17 00 04.33	+27 02 48.8	87GB165802.2+2	rad			108.12	0.38±0.15	19.0	-1	19.6	1	0.18	0.6
RXSJ1700.6+3553	17 00 33.38	+35 52 55.5		QSO	New	0.142	1.10	1.71±0.20	2.91 ^{+0.18} _{-0.21}	15.0	1	16.0	1	0.05	1.6
RXSJ1700.6+3414	17 00 36.33	+34 14 14.9		QSO	W00	0.798	1.16	0.55±0.12	2.44 ^{+0.31} _{-0.33}	17.4	-1	17.3	-1	0.06	0.5
RXSJ1700.8+2919	17 00 46.79	+29 19 26.4		S	W00		1.81	2.32±0.29	1.85 ^{+0.29} _{-0.25}	13.3	1	15.0	1	0.12	0.2
RXSJ1700.8+3324	17 00 52.67	+33 24 31.5	NPM1G+29.0397				1.65	0.33±0.10	2.00 ^{+0.42} _{-0.41}	20.0	-1	0	0.06	0.5
RXSJ1701.5+3811	17 01 32.33	+38 11 04.0					3.01	0.31±0.11
RXSJ1702.0+3622	17 02 01.83	+36 22 05.2	IRASF17002+362	H	New	0.098	1.04	1.60±0.20	2.48 ^{+0.18} _{-0.18}	14.6	1	15.7	1	0.06	1.2
RXSJ1702.5+3247	17 02 31.03	+32 47 19.7	FIRSTJ170231.0	QSO	ned	0.164	1.82	9.94±0.49	3.18 ^{+0.08} _{-0.09}	15.9	-1	15.8	-1	0.06	0.4
RXSJ1702.5+3330	17 02 33.14	+33 31 00.1	NPM1G+33.0395	G	ned	0.086	9.04	1.76±0.25	11.9	1	14.1	2	0.07	0.4
RXSJ1702.6+3115	17 02 38.55	+31 15 43.5		B	W00		5.54	0.77±0.18	2.47 ^{+0.38} _{-0.37}	17.7	-1	18.1	-1	0.09	0.1
RXSJ1702.7+3403	17 02 42.51	+34 03 37.3		Cl	ned	0.102	2.41	16.40±0.58	1.49 ^{+0.06} _{-0.06}	10.2	2	12.3	2	0.06	6.1
RXSJ1703.3+3737	17 03 20.15	+37 37 24.9		BA	New	0.065	1.86	3.65±0.29	1.91 ^{+0.13} _{-0.13}	14.2	1	15.8	1	0.07	0.4
RXSJ1703.5+3604	17 03 27.80	+36 04 19.9	MCG+06-37-023	G	ned		4.30	0.85±0.16	9.4	1	11.3	2	0.06	0.7
RXSJ1704.9+2241	17 04 54.76	+22 41 19.6					2.32	0.60±0.20	2.81 ^{+0.61} _{-0.54}	18.7	-1	18.5	-1	0.16	0.2
RXSJ1706.6+3615	17 06 34.16	+36 15 08.0		QSO	W00	0.920	18.85	0.50±0.13	1.82 ^{+0.41} _{-0.36}	17.9	-1	18.4	-1	0.08	0.3
RXSJ1707.6+3749	17 07 39.39	+37 49 43.7					1.80	0.17±0.07	20.3	-1	0	0.08	0.3
RXSJ1708.0+3910	17 07 59.74	+39 10 29.4	IRASF17063+391	H	New	0.127	1.70	0.37±0.11	1.23 ^{+0.66} _{-0.44}	16.1	1	17.3	1	0.13	0.2
RXSJ1708.4+4123	17 08 23.13	+41 23 09.5		QSO	W00	0.84	1.23	0.31±0.10	2.26 ^{+0.47} _{-0.46}	16.8	-1	17.2	-1	0.07	0.5
RXSJ1710.2+3344	17 10 13.43	+33 44 02.8	FIRSTJ171013.4	Sy	ned	0.208	4.05	2.52±0.28	2.77 ^{+0.17} _{-0.19}	15.2	1	16.0	-1	0.07	1.0
RXSJ1710.4+4039	17 10 25.41	+40 40 15.9					9.53	0.37±0.12	1.39 ^{+0.46} _{-0.35}
RXSJ1710.8+4109	17 10 48.60	+41 09 21.9					1.74	0.26±0.10

continued on next page

ROSAT name (1)	FIRST position (2)	Δx (3)	Name	type (4)	Ref	z (5)	f_p (6)	F_z (7)	Γ (8)	m_E (9)	cl (10)	mo (11)	cl (12)	A(E) (13)	$\Delta \rho$ (14)
RXSJ1711.5+3745	17 11 31.55 +37 45 10.6	19					5.13	0.16±0.08
RXSJ1712.2+3934	17 12 11.09 +39 34 03.3	4					2.68	0.51±0.14	...	17.0	-1	18.3	1	0.12	0.3
RXSJ1712.6+3801	17 12 36.58 +38 01 13.3	23	IC1245	G	ned	0.037	2.93	0.86±0.19	1.00±0.47	7.8	1	10.8	1	0.12	2.5
RXSJ1712.8+2931	17 12 48.70 +29 31 17.5	4		B	W00		11.54	0.70±0.19	1.51±0.22	18.0	-1	18.5	-1	0.15	0.8
RXSJ1713.1+3523	17 13 04.48 +35 23 33.4	2		H	W00	0.085	11.13	20.54±0.78	2.97±0.07	15.8	-1	16.9	-1	0.08	0.4
RXSJ1713.4+3256	17 13 22.63 +32 56 28.1	4	87GB17131.7+3	A	W00	0.101	34.97	3.65±0.36	2.21±0.15	15.3	1	16.7	-1	0.14	0.1
RXSJ1714.3+4341	17 14 14.98 +43 41 04.9	16	NGC6329	G	ned	0.027	1.59	1.19±0.17	1.01±0.28	8.9	1	...	0	0.04	2.3
RXSJ1714.7+3036	17 14 45.48 +30 36 28.9	22					1.08	0.47±0.15	...	18.9	-1	19.1	-1	0.12	1.2
RXSJ1716.0+3623	17 15 58.85 +36 23 23.4	15	CGCG198-028	G	ned		1.32	1.02±0.20	1.91±0.38	8.1	1	11.5	1	0.10	0.1
RXSJ1716.0+3112	17 16 01.92 +31 12 13.8	8	IRAS17141+311	Sy	ned	0.111	2.68	6.03±0.46	2.61±0.13	14.6	1	15.3	-1	0.09	0.2
RXSJ1717.1+2931	17 17 06.67 +29 31 16.1	2					1.35	6.04±0.47	1.47±0.13
RXSJ1718.7+3605	17 18 41.45 +36 05 22.0	22					11.43	0.54±0.15	2.50±0.46	18.3	2	20.2	-1	0.12	1.1
RXSJ1718.8+3041	17 18 50.34 +30 42 01.3	17		BA	W00	0.281	1.25	0.74±0.19	3.01±0.42	17.6	-1	18.4	-1	0.11	0.5
RXSJ1719.0+4127	17 19 02.68 +41 27 33.2	4					3.69	0.46±0.13	...	18.7	-1	21.3	1	0.07	0.3
RXSJ1719.5+2934	17 19 30.40 +29 34 13.6	5					1.95	0.89±0.20	3.04±0.35
RXSJ1719.5+2441	17 19 29.77 +24 41 26.6	19	87GB171724.5+2	rad			48.58	0.41±0.16	...	18.5	1	...	0	0.19	0.1
RXSJ1719.6+2510	17 19 34.18 +25 10 58.5	16	RXJ17195+2510	Sy	ned	0.579	12.67	0.90±0.21	1.60±0.48	15.5	1	16.8	-1	0.14	0.3
RXSJ1720.2+2637	17 20 09.89 +26 37 30.8	8	RXJ17201+2637	G?	ned	0.164	5.24	12.57±0.67	1.18±0.37	12.7	2	17.3	2	0.14	1.1
RXSJ1720.7+3430	17 20 40.58 +34 29 56.4	21					9.91	0.60±0.15	3.03±0.38	20.5	1	...	0	0.08	1.7
RXSJ1721.8+3626	17 21 48.04 +36 25 59.4	15	87GB172003.5+3	rad			303.90	0.35±0.13
RXSJ1722.0+4315	17 22 01.91 +43 15 24.0	1					7.00	5.27±0.32	2.00±0.10	18.7	-1	19.7	1	0.07	0.6
RXSJ1722.3+3042	17 22 15.42 +30 42 39.8	11	CGCG170-018	G	ned		5.01	1.63±0.29	1.34±0.52	10.1	2	11.7	2	0.09	1.9
RXSJ1722.4+3207	17 22 27.08 +32 07 58.0	8	FIRSTJ172227.0	G	ned	0.224	3.54	7.96±0.51	1.30±0.15	12.1	2	...	0	0.12	2.7
RXSJ1723.3+3417	17 23 20.80 +34 17 57.9	4	[HB89]1721+343	QSO	ned	0.206	438.57	20.61±0.75	2.35±0.07	14.9	2	15.2	-1	0.10	0.4
RXSJ1723.4+3630	17 23 23.22 +36 30 10.2	1	IRAS17216+363	Sy	ned	0.040	3.42	4.71±0.37	0.99±0.23	12.2	1	...	0	0.14	0.9
RXSJ1723.9+3748	17 23 54.27 +37 48 41.6	6		QSO	W00	0.83	1.70	0.76±0.19	3.86±0.43	17.5	-1	18.4	-1	0.11	0.6
RXSJ1724.2+3303	17 24 14.18 +33 03 04.0	15	[HB89]1722+330	QSO	ned	1.87	368.13	0.43±0.14	1.77±0.61	19.3	-1	20.4	-1	0.12	0.3
RXSJ1724.4+4021	17 24 27.51 +40 20 48.9	15					1.21	0.44±0.13	1.63±0.65
RXSJ1726.5+3957	17 26 32.65 +39 57 01.9	10	[HB89]1724+399	QSO	ned	0.66	475.49	0.81±0.15	2.30±0.29	18.2	-1	18.4	-1	0.10	0.3
RXSJ1729.0+3838	17 28 59.13 +38 38 26.4	9	[HB89]1727+386	QSO	ned	1.39	240.27	0.78±0.16	1.89±0.48	16.7	-1	16.9	-1	0.10	0.5
RXSJ1730.7+3804	17 30 44.79 +38 04 55.2	7					7.30	0.59±0.14	2.05±0.44	15.7	1	...	0	0.10	3.1
RXSJ2101.0-0730	21 01 00.95 -07 30 18.8	26					12.25	0.66±0.25	2.39±1.05
RXSJ2101.1-0547	21 01 09.59 -05 47 47.3	13					2.45	1.66±0.34	1.16±1.05	16.1	2	17.5	2	...	0.0
RXSJ2118.7-0636	21 18 43.25 -06 36 17.9	4		id		0.328	75.53	3.15±0.52	1.91±0.40	17.3	-1	18.7	-1	...	0.3
RXSJ2123.6-0139	21 23 36.04 -01 39 47.4	6					1.26	1.68±0.37	...	19.7	1	20.4	-1	...	0.2
RXSJ2125.0-0813	21 24 59.91 -08 13 27.8	23					1.63	1.68±0.37	1.65±0.41
RXSJ2128.3-0621	21 28 20.16 -06 21 10.3	28					566.40	0.56±0.24	...	20.3	1	21.7	-1	...	0.7
RXSJ2128.4+0135	21 28 23.43 +01 35 40.4	28	4C+01.65NED02	rad			56.97	1.11±0.38
RXSJ2129.7+0005	21 29 39.97 +00 05 21.0	24		S?	New		21.17	7.99±0.88	1.60±0.31	...	0	19.4	2	...	0.7
RXSJ2129.7+0035	21 29 40.69 +00 35 27.8	27					5.81	0.98±0.34	...	19.0	1	20.3	-1	...	0.8

continued on next page

ROSAT name (1)	FIRST position (2)	Δ yr (3)	Name	type (4)	Ref	z (5)	F_r (6)	F_x (7)	Γ (8)	mE (9)	cl (10)	mo (11)	cl (12)	A(E) (13)	Δ ro (14)	
RXSIJ2130.2-0156	21 30 08.02	-01 55 56.5					2.32	0.90±0.32	0	20.6	1	...	0.6	
RXSIJ2134.0+0022	21 34 00.56	+00 22 31.9					4.71	0.43±0.21	1	0	...	1.7	
RXSIJ2135.8+0118	21 35 52.50	+01 18 15.8					895.95	0.64±0.25	18.7	-1	20.0	-1	...	
RXSIJ2136.5-0116	21 36 32.85	-01 16 18.3		QSO	ned		3.34	1.24±0.32	2.17±0.52	19.5	1	22.6	2	...	2.0	
RXSIJ2137.7+0137	21 37 40.20	+01 37 14.0		S	New		2.42	4.52±0.61	3.53±0.32	11.5	-1	13.7	-1	...	1.5	
RXSIJ2140.9+0025	21 40 54.47	+00 25 37.0					1.07	1.28±0.34	1.65±0.40	15.2	1	15.4	1	...	1.9	
RXSIJ2145.7-0143	21 45 39.83	-01 43 01.8					1.88	0.50±0.25	17.0	1	21.6	-1	...	
RXSIJ2151.4-0139	21 51 25.69	-01 38 56.4					9.40	0.78±0.31	0.1	
RXSIJ2153.1-0042	21 53 05.35	-00 42 30.6		B?	New		18.19	6.38±0.76	1.90±0.32	17.6	1	18.8	-1	...	0.6	
RXSIJ2154.5+0038	21 54 27.46	+00 38 31.5					3.88	0.99±0.37	15.0	1	17.9	2	...	
RXSIJ2159.4+0113	21 59 24.09	+01 13 05.3		id		1.00	1.44	1.42±0.39	2.97±0.50	15.5	1	16.6	-1	...	0.3	
RXSIJ2200.5+0036	22 00 31.35	+00 35 41.6		G	New	0.098	1.86	1.17±0.37	16.3	1	18.3	-1	...	
RXSIJ2201.1-0053	22 01 03.12	-00 52 59.6		id		0.213	1.46	3.65±0.60	2.93±0.31	15.9	-1	16.7	-1	...	0.5	
RXSIJ2205.2-0048	22 05 09.45	-00 48 19.7		BA	New	0.098	1.13	2.86±0.55	1.92±0.49	15.3	2	17.1	2	...	1.6	
RXSIJ2211.1-0003	22 11 08.34	-00 03 02.5		B	New		15.12	3.03±0.56	2.71±0.31	16.7	-1	17.8	-1	...	0.2	
RXSIJ2212.4-0142	22 12 25.13	-01 42 07.5		BA	New	0.095	1.20	1.37±0.41	15.1	1	16.9	1	...	
RXSIJ2215.7-0036	22 15 42.32	-00 36 09.2		BA	New	0.099	1.62	2.19±0.52	1.46±1.39	15.4	1	17.3	1	...	0.5	
RXSIJ2225.3+0122	22 25 17.76	+01 22 51.1					1.86	3.29±0.62	1.09±0.64	
RXSIJ2226.0-0145	22 25 58.84	-01 45 12.1		B?	New		8.68	1.37±0.51	19.2	-1	20.9	-1	...	
RXSIJ2228.9-0753	22 28 52.60	-07 53 46.7		id		0.639	131.70	0.97±0.39	18.6	-1	18.5	-1	...	
RXSIJ2228.9-0904	22 28 52.78	-09 04 52.5		A	New	0.07	3.61	1.16±0.41	11.9	1	12.8	1	...	
RXSIJ2232.7-0040	22 32 45.59	-00 40 35.2					16.09	1.19±0.47	2.17±1.64	
RXSIJ2248.3-1015	22 48 17.53	-10 15 47.0		id		0.291	18.20	2.99±0.77	2.27±0.48	16.8	-1	17.0	-1	...	0.3	
RXSIJ2248.4+0009	22 48 24.63	+00 09 21.0		BA	New	0.053	1.64	1.69±0.48	14.4	1	16.4	1	...	
RXSIJ2252.2-0943	22 52 12.60	-09 43 39.9		G	New	0.067	3.96	0.95±0.46	0	13.9	1	...	
RXSIJ2258.2-0115	22 58 10.02	-01 15 13.1		QSO	New	0.117	2.60	3.40±0.56	3.66±0.27	13.8	1	13.3	1	...	2.3	
RXSIJ2258.6-0949	22 58 33.97	-09 49 29.6					240.36	3.58±0.81	1.51±0.59	21.2	-1	0	...	0.9	
RXSIJ2258.9-0018	22 58 52.92	-00 18 57.5					1.28	5.03±0.71	2.63±0.23	0	8.0	2	...	2.7	
RXSIJ2304.3-0816	23 04 17.32	-08 16 46.5					11.01	0.93±0.33	0.47±0.47	16.2	1	17.3	1	...	0.3	
RXSIJ2304.7-0841	23 04 43.49	-08 41 08.5		A	ned	0.047	17.05	36.59±2.85	2.00±0.14	9.6	1	10.4	1	...	1.1	
RXSIJ2308.4-0853	23 08 23.86	-08 54 00.8					1.87	0.43±0.21	2.33±1.56	0	
RXSIJ2311.3-0946	23 11 18.88	-09 46 22.3					3.20	0.99±0.29	2.00±0.48	20.0	1	0.1	
RXSIJ2317.6-1004	23 17 33.17	-10 05 04.2					3.01	0.42±0.18	2.68±0.67	19.0	-1	19.6	-1	...	0.3	
RXSIJ2318.8-0008	23 18 45.82	-00 07 54.6					5.30	0.62±0.29	2.68±0.80	19.4	-1	20.2	-1	...	0.6	
RXSIJ2318.9-0103	23 18 53.82	-01 03 36.7					2.95	1.61±0.39	9.2	1	11.4	1	...	0.6
RXSIJ2318.9+0014	23 18 56.67	+00 14 38.4		G	ned	0.030	18.34	9.49±1.14	1.90±0.25	9.4	1	10.0	1	...	1.0	
RXSIJ2322.3-1037	23 22 14.74	-10 37 24.4		QSO	New	0.031	1.11	1.75±0.35	2.46±0.28	17.2	-1	17.7	-1	...	0.8	
RXSIJ2326.6+0113	23 26 35.10	+01 13 33.4		id		0.745	1.10	0.73±0.26	3.57±0.56	8.6	-1	9.8	-1	...	4.7	
RXSIJ2338.4-0142	23 38 23.23	-01 42 24.7		QSO	New	0.284	1.65	1.21±0.31	2.13±0.63	16.8	1	17.4	-1	...	1.6	
RXSIJ2341.7-0038	23 41 40.88	-00 38 22.8					1.02	0.66±0.26	

ROSAT name (1)	FIRST position (2)	Δx_r (3)	Name (4)	type (4)	Ref (5)	z (5)	f_r (6)	F_x (7)	Γ (8)	m_E (9)	cl (10)	mo (11)	cl (12)	A(E) (13)	ΔRO (14)
RXSJ2344.7-0032	23 44 40.04 -00 32 31.6	10		QSO	ned	0.50	16.69	0.75 ± 0.27	...	17.2	-1	17.7	-1	...	0.3
RXSJ2352.0-0106	23 52 00.38 -01 06 37.2	23					1.04	0.88 ± 0.30	$2.13^{+0.78}_{-0.56}$
RXSJ2352.8+0037	23 52 51.86 +00 38 14.7	30		A		0.273	2.36	0.70 ± 0.25	$1.89^{+1.45}_{-0.71}$	17.4	-1	19.4	-1	...	0.4
RXSJ2359.8+0043	23 59 45.50 +00 44 00.9	19					7.29	0.49 ± 0.19

Table 2: ROSAT sources with multiple FIRST matches

ROSAT Name (1)	F_x ($10^{-12} \text{erg s}^{-1} \text{cm}^{-2}$) (2)	Type (3)	z (4)	Δ_{XR} ($''$) (5)	FIRST Position (J2000) (6)	F_r (mJy) (7)
RXSJ0003.7-1108	0.36±0.17	6	00 03 45.11 -11 08 24.8	204.20
				13	00 03 45.33 -11 08 14.3	106.88
RXSJ0017.6-0051	0.75±0.27	22	00 17 39.34 -00 52 12.2	1.09
				58	00 17 37.60 -00 52 42.3	5.35
RXSJ0026.5-0842	1.31±0.35	QSO	...	20	00 26 31.30 -08 42 34.7	83.33
				29	00 26 31.88 -08 42 39.2	198.32
RXSJ0026.9-0901	0.96±0.32	22	00 26 57.52 -09 01 57.3	13.27
				39	00 26 56.17 -09 01 00.9	4.47
RXSJ0028.4-0027	1.31±0.28	36	00 28 25.89 -00 27 34.1	6.34
				40	00 28 25.90 -00 27 25.7	6.36
				48	00 28 25.82 -00 27 15.4	4.36
				56	00 28 24.74 -00 27 25.1	14.92
				59	00 28 24.41 -00 27 29.3	177.68
RXSJ0029.0-0113	0.43±0.18	G	...	12	00 29 01.01 -01 13 41.7	266.25
				20	00 29 01.59 -01 13 52.3	1.07
				28	00 29 01.79 -01 13 30.6	1.50
RXSJ0030.8+0102	0.28±0.10	50	00 30 52.33 +01 01 48.4	9.21
				60	00 30 52.77 +01 01 39.6	5.57
RXSJ0034.3+0118	0.75±0.25	8	00 34 19.19 +01 18 35.8	2.31
				29	00 34 19.76 +01 18 06.8	159.32
				51	00 34 18.70 +01 19 24.2	32.51
RXSJ0038.3-0207	1.73±0.28	G	0.2196	6	00 38 20.41 -02 07 37.2	824.08
				7	00 38 20.06 -02 07 33.1	254.10
				16	00 38 20.93 -02 07 46.7	761.50
				19	00 38 21.78 -02 07 28.0	9.94
RXSJ0040.2+0126	1.04±0.30	12	00 40 15.37 +01 26 25.2	1.34
				21	00 40 14.91 +01 26 45.5	1.18
				21	00 40 15.56 +01 26 40.5	2.26
				42	00 40 13.51 +01 25 46.4	131.13
				54	00 40 12.60 +01 25 40.5	5.84
RXSJ0045.2-0151	0.67±0.26	46	00 45 12.43 -01 52 32.4	3.90
				53	00 45 10.18 -01 52 13.5	1.02

continued on next page

ROSAT Name (1)	F_x ($10^{-12} \text{erg s}^{-1} \text{cm}^{-2}$) (2)	Type (3)	z (4)	Δ_{XR} ($''$) (5)	FIRST Position (J2000) (6)	F_r (mJy) (7)
RXSJ0046.9+0036	0.32±0.15	47 00 46 53.72 56 00 46 53.38	+00 36 46.8 +00 36 54.5	1.67 1.75
RXSJ0056.3-0936	8.02±0.75	B	0.101	3 00 56 20.08 7 00 56 20.57 11 00 56 20.75 31 00 56 21.32	-09 36 29.8 -09 36 24.6 -09 36 32.4 -09 35 59.7	94.39 6.22 4.47 1.94
RXSJ0056.9-0121	0.97±0.32	36 00 56 58.32 45 00 56 59.04	-01 21 44.9 -01 21 41.1	1.67 3.41
RXSJ0059.1+0006	0.91±0.28	QSO	0.717	9 00 59 06.58 22 00 59 05.74 30 00 59 05.51 34 00 59 04.93 43 00 59 04.72	+00 06 35.0 +00 06 31.6 +00 06 51.7 +00 06 30.8 +00 06 57.3	4.48 8.08 2307.92 1.69 1.93
RXSJ0101.8-0919	0.58±0.23	14 01 01 47.98 50 01 01 51.90	-09 18 58.3 -09 19 15.0	1.10 1.85
RXSJ0105.7+0101	0.54±0.21	10 01 05 47.28 43 01 05 49.61 45 01 05 45.87	+01 00 58.4 +01 01 38.6 +01 00 29.5	1.35 1.98 1.74
RXSJ0110.2-0219	1.78±0.37	QSO/cl	0.958,0.5364	13 01 10 13.20 29 01 10 13.40	-02 19 50.5 -02 20 06.8	90.54 20.17
RXSJ0114.4+0000	0.61±0.21	QSO	0.389	20 01 14 29.19 29 01 14 29.94	+00 00 33.5 +00 00 42.0	83.09 104.46
RXSJ0115.2-0126	1.14±0.30	QSO	1.365	12 01 15 17.11 17 01 15 18.51	-01 27 04.5 -01 27 04.9	1012.22 1.16
RXSJ0117.0+0000	4.24±0.52	BA	0.04	9 01 17 03.60 45 01 17 02.57	+00 00 25.7 -00 00 12.7	1.18 1.02
RXSJ0122.0+0020	1.54±0.33	CI?	...	20 01 22 02.65 53 01 22 05.30	+00 20 04.3 +00 19 52.1	1.09 2.60
RXSJ0129.0-0845	0.93±0.25	40 01 29 01.72 41 01 29 04.77	-08 44 27.9 -08 45 01.3	1.11 3.05

continued on next page

ROSAT Name (1)	F_x ($10^{-12} \text{erg s}^{-1} \text{cm}^{-2}$) (2)	Type (3)	z (4)	Δ_{XR} ($''$) (5)	FIRST Position (J2000) (6)	F_r (mJy) (7)
RXSJ0129.2-0829	0.48±0.20	9 58	01 29 12.50 -08 29 25.3 01 29 10.03 -08 28 51.5	3.48 20.61
RXSJ0130.1-1019	0.33±0.16	23 31	01 30 08.91 -10 19 07.4 01 30 09.44 -10 19 07.4	53.72 7.94
RXSJ0133.8+0113	1.38±0.31	12 34 37	01 33 52.73 +01 13 43.6 01 33 54.19 +01 13 10.6 01 33 53.98 +01 13 06.5	8.53 7.42 15.69
RXSJ0136.1-0957	0.95±0.25	6 29 35	01 36 06.36 -09 57 11.4 01 36 06.14 -09 56 48.1 01 36 05.84 -09 56 42.7	9.57 18.92 17.72
RXSJ0137.2-0911	6.08±0.54	G	...	9 11 17 16	01 37 14.97 -09 11 55.1 01 37 15.45 -09 11 55.6 01 37 15.08 -09 12 03.1 01 37 16.21 -09 11 49.4	5.03 8.27 10.12 9.92
RXSJ0137.7-0211	0.42±0.18	10 12 26	01 37 45.65 -02 11 09.4 01 37 45.97 -02 11 19.0 01 37 44.89 -02 10 52.7	4.15 3.79 46.66
RXSJ0138.1-0145	0.34±0.16	8 16	01 38 08.09 -01 45 18.8 01 38 07.42 -01 45 22.6	177.99 75.20
RXSJ0140.9+0010	0.62±0.30	25 46 58	01 40 57.41 +00 10 54.0 01 40 57.86 +00 09 48.2 01 40 56.45 +00 11 23.7	1.99 1.10 5.37
RXSJ0141.4-0928	0.61±0.18	B	>0.501	19 34 47	01 41 25.82 -09 28 43.7 01 41 28.79 -09 29 16.0 01 41 27.81 -09 29 42.1	493.21 6.26 5.39
RXSJ0146.7-0040	2.75±0.40	BA	0.080	11 28	01 46 44.88 -00 40 42.6 01 46 47.32 -00 40 27.8	1.09 1.39
RXSJ0147.6-0937	0.31±0.14	14 17	01 47 34.14 -09 36 57.0 01 47 34.86 -09 36 47.9	92.92 5.27
RXSJ0151.0-0034	1.16±0.26	2	01 51 05.85 -00 34 26.0	1.75

continued on next page

ROSAT Name (1)	F_x ($10^{-12} \text{erg s}^{-1} \text{cm}^{-2}$) (2)	Type (3)	z (4)	Δ_{XR} ($''$) (5)	FIRST Position (J2000) (6)	F_r (mJy) (7)
				44	01 51 04.11 -00 33 50.3	1.16
				54	01 51 04.19 -00 33 38.4	17.47
RXSJ0152.6-0758	0.59±0.26	15	01 52 38.93 -07 58 48.0	18.05
				31	01 52 39.35 -07 59 12.5	5.52
				45	01 52 39.79 -07 59 25.7	2.06
				52	01 52 39.96 -07 59 32.0	3.37
RXSJ0153.5-0118	2.65±0.40	42	01 53 35.01 -01 18 26.3	3.88
				51	01 53 34.32 -01 18 07.5	54.41
RXSJ0159.8-0849	2.62±0.36	12	01 59 49.35 -08 49 58.9	30.10
				44	01 59 49.34 -08 49 05.8	1.28
RXSJ0201.7-0211	5.01±0.51	Cl	0.196	19	02 01 43.12 -02 11 48.0	11.86
				35	02 01 46.55 -02 11 58.2	28.15
				54	02 01 47.78 -02 11 52.8	14.74
RXSJ0202.2-0107	1.06±0.27	Cl	0.04276	24	02 02 15.94 -01 07 43.7	2.50
				42	02 02 17.24 -01 07 40.0	3.85
RXSJ0202.6+0003	0.51±0.19	30	02 02 34.30 +00 03 12.8	9.54
				31	02 02 34.33 +00 03 01.8	39.27
				45	02 02 34.45 +00 02 34.4	49.10
RXSJ0209.5-0737	0.72±0.22	18	02 09 31.41 -07 36 49.7	39.32
				30	02 09 31.01 -07 36 37.2	137.97
RXSJ0213.7-0256	1.11±0.27	G	0.357	8	02 13 46.91 -02 56 27.5	18.42
				15	02 13 47.01 -02 56 49.8	118.05
				19	02 13 47.11 -02 56 17.4	59.97
RXSJ0215.1-0702	0.54±0.21	8	02 15 07.96 -07 02 02.5	123.14
				14	02 15 07.60 -07 02 08.7	102.43
RXSJ0215.7-0223	0.47±0.19	15	02 15 42.02 -02 22 57.0	359.16
				29	02 15 41.93 -02 22 40.4	33.92
RXSJ0225.1-0035	1.42±0.40	QSO	0.687	5	02 25 08.32 -00 35 30.0	812.90
				8	02 25 07.55 -00 35 34.7	220.49
				23	02 25 06.49 -00 35 35.5	1.75
				44	02 25 10.91 -00 35 21.7	1.17
				50	02 25 05.83 -00 34 52.1	1.34

continued on next page

ROSAT Name (1)	F_x ($10^{-12} \text{erg s}^{-1} \text{cm}^{-2}$) (2)	Type (3)	z (4)	Δ_{XR} ($''$) (5)	FIRST Position (J2000) (6)	F_r (mJy) (7)
				60	02 25 06.12 -00 34 37.0	1.32
RXSJ0228.4-0455	1.05±0.28	47	02 18 26.96 -04 54 50.2	10.92
				48	02 18 27.33 -04 54 37.2	28.74
RXSJ0234.6-0847	24.9±1.36	G	0.0431	3	02 34 37.85 -08 47 16.2	4.80
				21	02 34 36.54 -08 47 16.6	1.02
RXSJ0241.0-0815	0.68±0.35	A	0.005	4	02 41 05.45 -08 15 38.3	1.08
				20	02 41 05.63 -08 15 23.0	25.37
				22	02 41 04.81 -08 15 20.8	967.94
RXSJ0242.6-0000	3.88±2.05	A	0.00379	2	02 42 40.76 -00 00 46.5	2308.48
				9	02 42 41.51 -00 00 45.5	6.12
				45	02 42 43.87 -00 00 37.9	4.52
				47	02 42 37.89 -00 01 00.5	2.20
				54	02 42 44.52 -00 00 48.4	2.13
				55	02 42 42.06 +00 00 05.5	2.73
RXSJ0248.9+0010	0.71±0.34	38	02 48 54.80 +00 10 55.4	38.32
				45	02 48 54.71 +00 10 33.4	2.27
RXSJ0250.8+0002	0.79±0.43	QSO	0.766	4	02 50 48.69 +00 02 08.0	12.62
				5	02 50 49.12 +00 02 10.1	24.22
				12	02 50 48.12 +00 02 02.9	53.07
RXSJ0303.2-0015	1.35±0.54	QSO	0.693	16	03 03 13.06 -00 14 59.5	619.42
				21	03 03 11.04 -00 15 07.4	4.44
				30	03 03 12.12 -00 15 42.3	1.34
				39	03 03 09.83 -00 15 12.6	1.85
				40	03 03 13.37 -00 14 35.4	1.81
				40	03 03 15.07 -00 15 16.0	1.20
				40	03 03 09.82 -00 15 02.2	1.71
				43	03 03 14.98 -00 14 52.3	3.42
				44	03 03 14.21 -00 14 37.2	1.11
				49	03 03 09.14 -00 15 10.7	1.54
				50	03 03 14.05 -00 14 29.4	1.99
				51	03 03 15.64 -00 14 55.7	2.39
RXSJ0315.8+0107	0.59±0.24	3	03 15 53.62 +01 08 02.1	1.38
				18	03 15 55.01 +01 07 55.9	67.63
RXSJ0721.5+2742	0.39±0.22	A	0.064	4	07 21 32.05 +27 42 12.9	87.23
				7	07 21 31.46 +27 42 21.3	3.66
				20	07 21 31.05 +27 42 32.4	1.05

continued on next page

ROSAT Name (1)	F_x ($10^{-12} \text{erg s}^{-1} \text{cm}^{-2}$) (2)	Type (3)	z (4)	Δ_{XR} ($''$) (5)	FIRST Position (J2000) (6)	F_r (mJy) (7)
				24	07 21 32.83 +27 41 55.7	2.63
				41	07 21 30.38 +27 42 51.9	22.93
RXSJ0726.3+3019	0.55±0.23	16	07 26 23.74 +30 20 02.9	23.67
				18	07 26 24.03 +30 19 57.4	16.69
				22	07 26 24.40 +30 19 52.0	14.24
RXSJ0726.8+3102	2.39±0.43	G	0.188	6	07 26 49.99 +31 02 03.6	25.18
				7	07 26 49.72 +31 02 08.1	11.33
				17	07 26 48.99 +31 02 05.5	4.94
				53	07 26 49.42 +31 01 15.8	17.15
RXSJ0729.1+2530	0.72±0.27	24	07 29 06.69 +25 30 28.8	8.29
				33	07 29 05.74 +25 30 34.2	93.93
				42	07 29 04.87 +25 30 41.3	7.18
RXSJ0729.7+2749	0.40±0.20	G	0.086	42	07 29 47.79 +27 49 47.3	1.61
				45	07 29 46.55 +27 49 49.3	1.45
				45	07 29 48.98 +27 49 44.9	4.92
				59	07 29 50.47 +27 49 47.4	5.41
RXSJ0731.8+2804	4.88±0.52	10	07 31 52.74 +28 04 32.6	47.41
				55	07 31 56.18 +28 04 45.2	2.56
RXSJ0732.0+3005	0.77±0.25	15	07 32 01.20 +30 05 36.0	3.95
				22	07 32 00.42 +30 05 44.4	12.00
				30	07 32 03.25 +30 05 19.4	5.27
				33	07 31 59.62 +30 05 51.7	11.96
RXSJ0743.7+2328	0.57±0.21	QSO	0.770	11	07 43 45.05 +23 28 41.2	107.82
				22	07 43 44.53 +23 28 28.8	22.25
RXSJ0745.1+3312	0.77±0.26	G	...	15	07 45 04.97 +33 12 47.2	31.08
				23	07 45 04.81 +33 13 01.2	45.41
RXSJ0745.6+3142	2.83±0.53	QSO/CI	0.46108,0.1917	9	07 45 41.66 +31 42 56.5	614.67
				18	07 45 40.62 +31 43 06.5	12.62
				52	07 45 44.84 +31 42 25.9	51.72
				56	07 45 37.95 +31 43 26.9	40.94
				59	07 45 38.06 +31 43 33.2	13.77
RXSJ0745.8+3558	0.60±0.23	BA	0.272	21	07 45 53.75 +35 57 58.6	9.84
				37	07 45 56.13 +35 58 13.9	132.01

continued on next page

ROSAT Name (1)	F_x ($10^{-12} \text{erg s}^{-1} \text{cm}^{-2}$) (2)	Type (3)	z (4)	Δ_{XR} ($''$) (5)	FIRST Position (J2000) (6)	F_r (mJy) (7)
RXSJ0745.9+3313	0.84±0.27	QSO	0.610	17	07 45 59.31 +33 13 34.5	98.52
				41	07 45 57.72 +33 12 40.0	1.05
RXSJ0753.4+3350	0.84±0.28	QSO	2.07	7	07 53 28.94 +33 50 44.5	10.43
				12	07 53 27.78 +33 50 53.5	17.31
				22	07 53 27.01 +33 50 56.8	43.43
RXSJ0756.9+2919	0.57±0.21	B?	0.067	18	07 56 52.81 +29 19 42.3	1.42
				24	07 56 55.78 +29 19 49.5	1.07
RXSJ0757.9+3920	2.02±0.39	QSO	0.096	9	07 58 00.05 +39 20 29.1	10.80
				40	07 58 03.04 +39 20 46.0	16.02
RXSJ0758.4+3747	0.68±0.23	G	0.04333	10	07 58 28.16 +37 47 11.4	198.59
				14	07 58 26.31 +37 47 21.0	5.77
				16	07 58 28.55 +37 47 09.7	14.76
				50	07 58 24.15 +37 47 46.3	2.59
				60	07 58 32.06 +37 46 53.9	7.74
RXSJ0801.3+3449	0.50±0.21	Cl	0.1495	12	08 01 23.12 +34 49 01.6	8.78
				17	08 01 23.53 +34 49 00.8	1.54
RXSJ0804.2+4232	0.44±0.19	48	08 04 14.24 +42 33 45.6	3.15
				48	08 04 15.27 +42 33 41.5	3.02
RXSJ0808.0+3819	0.53±0.21	34	08 08 04.42 +38 20 01.2	1.09
				43	08 07 59.51 +38 19 49.3	1.82
RXSJ0809.6+3455	8.03±0.92	B?	...	9	08 09 38.87 +34 55 37.1	149.79
				18	08 09 39.11 +34 55 27.7	10.23
				38	08 09 38.31 +34 55 06.2	1.91
				42	08 09 38.57 +34 56 26.4	1.08
RXSJ0810.1+3517	2.31±0.56	Cl	0.0843	41	08 10 08.30 +35 16 47.7	1.83
				51	08 10 07.45 +35 16 44.9	1.18
RXSJ0810.3+4216	3.49±0.54	36	08 10 23.56 +42 16 31.1	3.65
				40	08 10 23.00 +42 16 21.8	3.35
RXSJ0811.0+3558	0.94±0.36	40	08 11 03.93 +35 59 05.1	13.83
				49	08 11 04.55 +35 59 11.7	17.38

continued on next page

ROSAT Name (1)	F_x ($10^{-12}\text{erg s}^{-1}\text{cm}^{-2}$) (2)	Type (3)	z (4)	Δ_{XR} ($''$) (5)	FIRST Position (J2000) (6)	F_r (mJy) (7)
RXSJ0812.3+3827	0.64±0.28	4	08 12 22.44 +38 27 54.3	3.55
				11	08 12 21.55 +38 28 03.2	1.65
				16	08 12 23.26 +38 27 44.9	1.73
RXSJ0819.2+2641	0.61±0.27	17	08 19 16.96 +26 41 57.7	61.15
				17	08 19 16.49 +26 42 03.2	67.35
RXSJ0820.3+3630	0.83±0.28	45	08 20 19.42 +36 30 08.5	3.43
				46	08 20 20.35 +36 30 05.0	13.54
				53	08 20 17.80 +36 30 12.0	6.39
RXSJ0824.9+3916	2.04±0.41	QSO	1.216	8	08 24 55.48 +39 16 41.8	1403.96
				41	08 24 57.66 +39 17 22.1	3.25
				41	08 24 59.50 +39 16 42.5	3.77
RXSJ0825.9+4014	1.22±0.31	22	08 25 56.37 +40 13 44.8	20.21
				35	08 25 55.28 +40 13 32.5	14.45
RXSJ0827.2+4128	5.17±0.52	51	08 27 09.59 +41 28 05.3	4.49
				52	08 27 10.21 +41 27 54.7	1.25
RXSJ0830.2+3213	0.42±0.19	40	08 30 10.46 +32 13 52.4	1.64
				51	08 30 16.11 +32 13 13.4	3.23
RXSJ0830.8+2410	2.53±0.49	QSO	0.94 (2.046?)	10	08 30 52.08 +24 10 59.9	835.48
				19	08 30 51.52 +24 11 12.5	1.52
				27	08 30 52.81 +24 11 14.0	1.66
				47	08 30 48.10 +24 10 57.6	1.12
RXSJ0836.6+4126	1.38±0.39	QSO	1.30	22	08 36 36.89 +41 25 54.9	424.23
				38	08 36 40.91 +41 25 43.9	1.03
RXSJ0837.6+2454	0.59±0.27	QSO	1.122	5	08 37 40.75 +24 54 11.9	18.99
				10	08 37 40.26 +24 54 23.0	422.63
RXSJ0846.9+2457	1.16±0.37	Cl	...	28	08 46 55.21 +24 57 06.2	3.93
				45	08 46 56.52 +24 56 43.2	14.06
RXSJ0848.0+3146	0.92±0.31	G	0.067	27	08 47 59.05 +31 47 08.7	21.68
				51	08 47 58.54 +31 47 33.4	2.87
				55	08 47 59.70 +31 45 53.7	3.02
				57	08 48 01.42 +31 45 52.1	8.12

continued on next page

ROSAT Name (1)	F_x ($10^{-12} \text{erg s}^{-1} \text{cm}^{-2}$) (2)	Type (3)	z (4)	Δ_{XR} (//) (5)	FIRST Position (J2000) (6)	F_r (mJy) (7)
				59	08 48 00.44 +31 45 49.3	7.55
RXSJ0850.1+3604	2.32±0.40	19	08 50 12.82 +36 04 21.6	4.42
				28	08 50 13.51 +36 04 21.8	3.92
				43	08 50 07.77 +36 04 30.2	1.38
				43	08 50 08.45 +36 04 49.1	3.77
				46	08 50 07.52 +36 04 12.3	3.47
				48	08 50 07.49 +36 04 05.8	3.69
RXSJ0850.4+3746	0.34±0.16	G	0.407	9	08 50 25.15 +37 46 50.6	38.61
				14	08 50 24.75 +37 47 10.3	136.28
RXSJ0854.9+3021	0.92±0.28	18	08 55 00.28 +30 21 06.7	2.10
				29	08 55 00.62 +30 20 57.0	2.94
				32	08 54 59.49 +30 20 48.6	2.27
				38	08 54 58.67 +30 20 42.7	1.36
RXSJ0855.9+3713	0.89±0.30	11	08 55 56.17 +37 13 42.5	13.32
				15	08 55 57.64 +37 14 00.3	2.68
				32	08 55 54.65 +37 13 31.5	20.60
				46	08 56 00.86 +37 13 45.8	2.21
RXSJ0856.1+3755	1.76±0.42	55	08 56 10.69 +37 55 10.7	4.12
				58	08 56 10.32 +37 55 04.0	3.66
RXSJ0857.6+3404	0.70±0.27	3	08 57 41.30 +34 04 07.4	825.98
				30	08 57 38.83 +34 04 04.4	404.08
RXSJ0903.4+3750	12.0±0.98	4	09 03 27.03 +37 50 29.5	1.67
				27	09 03 24.57 +37 50 28.6	1.07
RXSJ0905.6+3921	0.44±0.20	24	09 05 37.75 +39 20 40.2	1.39
				43	09 05 39.03 +39 20 28.1	3.99
RXSJ0908.5+4150	0.87±0.29	13	09 08 35.77 +41 50 46.1	153.81
				51	09 08 39.38 +41 50 44.0	1.39
RXSJ0909.9+3105	5.85±0.53	B	0.272	2	09 09 53.76 +31 05 58.2	24.99
				8	09 09 53.35 +31 06 03.2	62.38
RXSJ0910.6+3329	2.37±0.36	B	...	5	09 10 37.06 +33 29 24.5	102.94
				22	09 10 38.41 +33 29 04.6	1.02

continued on next page

ROSAT Name (1)	F_x ($10^{-12} \text{erg s}^{-1} \text{cm}^{-2}$) (2)	Type (3)	z (4)	Δ_{XR} (//) (5)	FIRST Position (J2000) (6)	F_r (mJy) (7)
RXSJ0913.2+3658	1.79±0.29	6	09 13 13.74 +36 58 17.4	1.09
				44	09 13 10.48 +36 57 46.1	7.62
RXSJ0913.7+4056	1.71±0.33	2	09 13 45.87 +40 56 19.6	1.67
				10	09 13 45.47 +40 56 28.5	6.88
				19	09 13 45.08 +40 56 36.7	4.60
RXSJ0918.9+2325	0.66±0.24	QSO	0.69	7	09 18 58.15 +23 25 55.4	26.70
				41	09 18 55.78 +23 26 20.5	1.93
				50	09 18 55.25 +23 26 26.0	5.12
RXSJ0919.0+4016	0.57±0.18	11	09 19 03.86 +40 16 57.4	1.50
				48	09 19 05.87 +40 16 09.2	1.10
RXSJ0922.9+2453	0.51±0.19	5	09 22 56.47 +24 53 23.8	8.99
				44	09 22 59.06 +24 53 56.4	55.74
RXSJ0925.8+3612	0.46±0.15	6	09 25 51.83 +36 12 35.6	205.81
				33	09 25 50.21 +36 13 06.4	1.08
RXSJ0927.8+3430	0.51±0.19	30	09 27 51.11 +34 31 03.5	6.13
				52	09 27 46.90 +34 30 12.8	1.30
RXSJ0932.1+3630	0.65±0.19	9	09 32 09.60 +36 30 02.9	29.71
				27	09 32 08.52 +36 30 29.2	1.75
RXSJ0934.0+3542	0.43±0.15	QSO	1.09	29	09 34 07.63 +35 42 48.6	14.18
				30	09 34 07.31 +35 42 38.2	3.87
RXSJ0936.0+3207	0.58±0.16	QSO	1.15	11	09 36 03.70 +32 07 40.4	3.81
				21	09 36 03.89 +32 07 09.3	27.45
RXSJ0936.2+2624	0.60±0.20	QSO	0.748	12	09 36 14.23 +26 24 08.5	66.45
				13	09 36 13.54 +26 24 16.0	2.29
				29	09 36 12.51 +26 24 30.9	2.55
				41	09 36 11.75 +26 24 38.6	7.71
RXSJ0936.6+2725	0.16±0.080	32	09 36 36.41 +27 25 36.2	245.24
				42	09 36 35.73 +27 25 58.3	12.48
RXSJ0941.0+2948	0.78±0.20	15	09 41 01.74 +29 48 31.9	3.07

continued on next page

ROSAT Name (1)	F_x ($10^{-12} \text{erg s}^{-1} \text{cm}^{-2}$) (2)	Type (3)	z (4)	Δ_{XR} ($''$) (5)	FIRST Position (J2000) (6)	F_r (mJy) (7)
				42	09 40 59.07 +29 49 06.3	2.48
				46	09 41 02.91 +29 48 02.1	2.28
RXSJ0941.0+3854	1.59±0.26	QSO	0.616			
				15	09 41 04.47 +38 53 45.9	41.28
				21	09 41 02.41 +38 54 09.3	108.36
				22	09 41 05.06 +38 53 42.1	62.36
				31	09 41 05.46 +38 53 34.0	76.82
RXSJ0942.5+2336	0.64±0.19			
				2	09 42 31.79 +23 36 13.8	52.49
				10	09 42 31.42 +23 36 06.3	57.61
RXSJ0944.3+2332	0.43±0.18	QSO	0.99			
				47	09 44 21.15 +23 31 49.1	19.96
				50	09 44 20.88 +23 31 41.3	21.21
				54	09 44 19.63 +23 31 27.0	1.11
				60	09 44 18.88 +23 31 20.0	11.16
RXSJ0945.1+3900	0.46±0.16			
				31	09 45 07.21 +39 00 20.2	13.42
				48	09 45 05.72 +39 00 35.6	3.51
RXSJ0945.4+3521	0.42±0.14	A	0.207			
				15	09 45 25.88 +35 21 03.5	140.45
				51	09 45 23.37 +35 21 59.8	1.18
RXSJ0945.6+3535	0.27±0.11	QSO	1.128			
				10	09 45 38.10 +35 34 55.0	216.81
				10	09 45 37.80 +35 35 01.7	26.22
RXSJ0948.9+4039	0.45±0.15	QSO	1.252			
				16	09 48 57.12 +40 40 13.5	1.93
				19	09 48 55.36 +40 39 44.7	1439.97
RXSJ0952.1+2352	0.44±0.17	QSO	0.96			
				15	09 52 06.38 +23 52 45.3	32.49
				40	09 52 04.99 +23 52 29.5	5.97
				50	09 52 08.85 +23 53 38.8	6.47
RXSJ0953.4+2248	0.59±0.22	Cl				
				26	09 53 27.25 +22 48 29.1	7.12
				30	09 53 26.51 +22 48 29.4	1.36
RXSJ0953.5+3917	0.45±0.16	QSO	0.919			
				5	09 53 31.66 +39 17 29.7	4.97
				45	09 53 28.05 +39 17 22.0	1.17
RXSJ0953.8+3853	0.26±0.11			
				23	09 53 52.44 +38 53 26.8	3.00
				24	09 53 50.15 +38 54 03.5	3.66
RXSJ0954.4+3019	0.71±0.20			
				5	09 54 27.83 +30 19 13.2	23.11

continued on next page

ROSAT Name (1)	F_x ($10^{-12} \text{ erg s}^{-1} \text{ cm}^{-2}$) (2)	Type (3)	z (4)	Δ_{XR} ($''$) (5)	FIRST Position (J2000) (6)	F_r (mJy) (7)
				40	09 54 27.51 +30 19 57.3	41.56
RXSJ0956.8+2515	0.90±0.23	QSO	0.712	8	09 56 49.87 +25 15 16.0	1041.77
				19	09 56 51.28 +25 15 09.9	2.30
				27	09 56 47.95 +25 15 14.3	1.53
RXSJ0957.1+2433	2.71±0.40	9	09 57 08.11 +24 33 28.0	5.40
				12	09 57 07.22 +24 33 16.1	1.01
RXSJ1000.3+2233	0.92±0.27	QSO	0.418	9	10 00 22.67 +22 33 34.4	157.05
				24	10 00 21.34 +22 33 07.7	300.05
RXSJ1004.7+2225	1.06±0.29	QSO	0.974	20	10 04 45.75 +22 25 19.4	33.93
				31	10 04 45.56 +22 24 51.1	144.65
				46	10 04 45.79 +22 25 55.7	191.99
RXSJ1006.1+3236	0.51±0.16	4	10 06 07.35 +32 36 31.1	158.39
				11	10 06 07.70 +32 36 26.2	132.64
				19	10 06 08.18 +32 36 20.0	97.53
RXSJ1006.7+2701	0.65±0.22	2	10 06 42.91 +27 01 49.1	7.29
				32	10 06 42.63 +27 01 15.3	13.83
RXSJ1010.0+3003	2.08±0.34	QSO	0.260	20	10 10 00.71 +30 03 21.5	1.54
				44	10 09 59.81 +30 04 08.2	1.68
				54	10 09 59.11 +30 04 13.5	1.59
RXSJ1010.4+4132	3.09±0.31	QSO	0.6123	5	10 10 27.52 +41 32 38.9	258.74
				8	10 10 27.75 +41 32 50.2	73.60
				24	10 10 27.31 +41 32 19.4	900.57
RXSJ1012.2+2312	0.61±0.21	38	10 12 16.41 +23 12 14.6	178.13
				38	10 12 14.20 +23 13 08.2	1.65
RXSJ1012.4+2613	0.84±0.23	6	10 12 26.40 +26 13 30.4	24.81
				34	10 12 28.47 +26 13 12.6	1.85
RXSJ1012.9+3932	0.81±0.19	G	...	9	10 12 58.37 +39 32 39.0	20.97
				57	10 13 02.59 +39 32 38.9	1.08
RXSJ1014.7+2301	0.92±0.24	QSO	0.565	14	10 14 47.09 +23 01 16.4	673.56
				16	10 14 47.12 +23 01 05.4	143.03

continued on next page

ROSAT Name (1)	F_x ($10^{-12}\text{erg s}^{-1}\text{cm}^{-2}$) (2)	Type (3)	z (4)	Δ_{XR} ($''$) (5)	FIRST Position (J2000) (6)	F_r (mJy) (7)
				36	10 14 45.54 +23 01 48.4	1.08
RXSJ1017.8+2732	1.70±0.30	QSO?	0.469	9	10 17 48.70 +27 31 58.8	147.33
				12	10 17 50.02 +27 32 08.9	844.36
RXSJ1018.1+3542	0.46±0.16	QSO	1.226	9	10 18 10.99 +35 42 39.7	571.31
				25	10 18 12.35 +35 42 44.0	7.10
				32	10 18 07.87 +35 42 38.5	1.60
RXSJ1018.4+3805	1.20±0.22	BA	0.380	11	10 18 27.27 +38 05 43.5	5.58
				14	10 18 25.44 +38 05 32.6	32.69
				32	10 18 24.56 +38 05 18.3	5.39
				39	10 18 24.31 +38 05 10.6	17.03
RXSJ1023.2+3605	0.36±0.13	32	10 23 16.07 +36 04 47.4	2.78
				44	10 23 15.76 +36 04 35.6	19.71
RXSJ1024.9+2800	0.25±0.12	G	0.0214	11	10 24 56.95 +28 00 31.0	16.62
				53	10 24 59.31 +28 01 26.1	13.37
RXSJ1029.2+2623	0.60±0.17	9	10 29 12.49 +26 23 31.7	4.20
				32	10 29 14.34 +26 23 39.1	1.01
RXSJ1030.9+3103	7.04±0.51	BA	0.1782	4	10 30 59.01 +31 03 02.0	57.04
				11	10 30 59.10 +31 02 55.7	58.74
				24	10 30 59.44 +31 02 42.5	9.52
RXSJ1031.7+3503	6.88±0.55	Cl	0.1259	8	10 31 43.69 +35 03 03.9	1.04
				48	10 31 41.79 +35 02 31.8	10.06
RXSJ1032.2+2756	0.49±0.15	18	10 32 14.04 +27 56 01.6	34.39
				33	10 32 13.88 +27 56 51.9	1.91
				40	10 32 15.80 +27 56 48.2	1.04
				42	10 32 13.95 +27 57 00.8	3.91
RXSJ1032.2+4016	0.75±0.17	Cl	0.0799	10	10 32 13.97 +40 16 16.4	5.09
				60	10 32 19.51 +40 15 58.0	1.16
RXSJ1032.5+3159	0.33±0.13	16	10 32 33.48 +31 59 14.8	3.42
				35	10 32 29.50 +31 59 24.9	1.14
RXSJ1033.0+3430	0.43±0.16	31	10 33 04.77 +34 31 29.9	57.75

continued on next page

ROSAT Name (1)	F_x ($10^{-12} \text{erg s}^{-1} \text{cm}^{-2}$) (2)	Type (3)	z (4)	Δ_{XR} ($''$) (5)	FIRST Position (J2000) (6)		F_r (mJy) (7)
				37	10 33 04.96	+34 31 35.4	56.93
				37	10 33 05.79	+34 31 32.5	1.14
RXSJ1034.9+3911	0.36±0.15	6	10 34 55.93	+39 11 06.4	5.45
				34	10 34 55.98	+39 10 28.0	7.25
RXSJ1035.1+3406	0.39±0.15	QSO	0.679	8	10 35 11.67	+34 06 25.1	34.87
				9	10 35 11.81	+34 06 10.5	5.34
				21	10 35 11.46	+34 06 39.5	36.58
				22	10 35 11.58	+34 05 56.5	6.64
				23	10 35 10.62	+34 05 57.3	2.09
RXSJ1035.9+2853	0.81±0.21	48	10 35 53.93	+28 53 17.9	1.91
				52	10 35 59.85	+28 54 16.4	1.18
RXSJ1036.0+4125	0.23±0.10	6	10 36 04.73	+41 25 17.2	1.44
				42	10 36 06.02	+41 26 02.1	5.58
RXSJ1040.7+3957	7.20±0.52	QSO/Cl	0.1386	5	10 40 43.33	+39 57 03.5	8.22
				11	10 40 44.48	+39 57 12.0	5.72
RXSJ1043.5+3432	0.62±0.18	16	10 43 34.82	+34 32 32.1	78.88
				56	10 43 32.20	+34 33 29.8	1.13
RXSJ1046.3+3427	0.51±0.17	18	10 46 20.19	+34 27 08.3	35.95
				55	10 46 25.19	+34 27 44.2	1.03
				57	10 46 16.93	+34 27 46.7	1.04
RXSJ1051.0+4019	0.80±0.18	2	10 51 05.35	+40 19 59.6	1.47
				12	10 51 04.75	+40 19 51.4	1.15
RXSJ1052.4+3729	0.50±0.17	9	10 52 23.38	+37 29 54.7	2.92
				12	10 52 24.10	+37 30 04.4	2.54
				16	10 52 23.07	+37 29 41.2	1.73
				49	10 52 21.24	+37 29 16.3	9.30
				56	10 52 20.61	+37 29 14.7	3.28
RXSJ1055.3+3727	0.77±0.21	9	10 55 21.22	+37 26 52.7	3.79
				20	10 55 21.65	+37 26 41.2	1.78
				24	10 55 22.30	+37 26 39.8	3.16
				34	10 55 20.15	+37 27 31.3	14.22
				36	10 55 22.35	+37 26 26.5	2.85
RXSJ1056.8+3704	0.77±0.25	QSO	0.39				

continued on next page

ROSAT Name (1)	F_x ($10^{-12}\text{erg s}^{-1}\text{cm}^{-2}$) (2)	Type (3)	z (4)	Δ_{XR} ($''$) (5)	FIRST Position (J2000) (6)	F_r (mJy) (7)
				12	10 56 50.58 +37 04 38.6	14.23
				43	10 56 48.17 +37 04 50.8	19.43
RXSJ1059.8+4051	0.35±0.14	QSO	1.74	30	10 59 51.93 +40 51 30.7	67.02
				31	10 59 51.91 +40 51 13.7	107.39
				35	10 59 52.03 +40 51 05.8	61.94
RXSJ1103.2+3014	0.99±0.26	BA	0.380	11	11 03 13.32 +30 14 42.3	107.68
				12	11 03 13.86 +30 14 56.4	1.23
				14	11 03 13.64 +30 14 41.0	3.63
				32	11 03 10.59 +30 14 49.0	4.28
				35	11 03 15.31 +30 14 34.6	4.29
				45	11 03 16.03 +30 14 30.6	2.46
RXSJ1104.4+3812	341±3.65	BA	0.0300	3	11 04 27.33 +38 12 31.6	557.26
				10	11 04 27.90 +38 12 30.8	2.99
				11	11 04 26.25 +38 12 34.8	1.20
RXSJ1107.4+3616	1.48±0.34	G	0.393	9	11 07 27.31 +36 16 18.2	168.85
				14	11 07 26.50 +36 16 04.8	96.53
RXSJ1108.1+2609	0.50±0.21	39	11 08 12.39 +26 10 34.5	21.03
				44	11 08 13.52 +26 10 33.4	4.43
				44	11 08 11.37 +26 10 39.8	6.10
				51	11 08 10.78 +26 10 45.4	5.17
RXSJ1110.2+3348	0.34±0.15	41	11 10 13.52 +33 47 45.5	4.36
				54	11 10 12.93 +33 47 31.9	1.02
RXSJ1111.6+4050	3.67±0.43	G	0.0734	22	11 11 39.03 +40 50 22.3	66.26
				29	11 11 38.81 +40 50 08.7	50.20
				31	11 11 39.62 +40 50 16.2	87.72
RXSJ1114.4+2257	0.45±0.16	8	11 14 27.27 +22 57 54.0	174.88
				16	11 14 25.59 +22 58 00.8	102.73
RXSJ1114.4+4133	1.53±0.28	G	...	3	11 14 28.42 +41 33 27.5	3.32
				24	11 14 26.04 +41 33 30.4	65.61
				25	11 14 26.08 +41 33 21.7	19.05
				41	11 14 25.35 +41 33 02.2	20.81
RXSJ1114.6+4037	1.25±0.29	QSO	0.734	18	11 14 38.81 +40 37 19.1	1740.12
				22	11 14 37.76 +40 37 23.0	934.50

continued on next page

ROSAT Name (1)	F_x ($10^{-12} \text{erg s}^{-1} \text{cm}^{-2}$) (2)	Type (3)	z (4)	Δ_{XR} ($''$) (5)	FIRST Position (J2000) (6)	F_r (mJy) (7)
RXSJ1115.9+2429	0.39±0.15	14	11 15 57.45 +24 29 46.7	20.49
				22	11 15 58.90 +24 29 38.6	1.00
				32	11 15 56.19 +24 30 01.5	5.84
RXSJ1116.0+2440	0.59±0.19	G	0.1021	24	11 16 03.86 +24 41 00.9	11.87
				33	11 16 04.76 +24 41 13.3	1.62
				34	11 16 02.73 +24 40 60.0	1.17
				35	11 16 04.03 +24 41 13.6	1.41
				38	11 16 03.40 +24 41 13.0	1.73
RXSJ1117.1+2700	0.67±0.21	21	11 17 05.09 +27 00 34.1	233.81
				31	11 17 04.42 +27 00 39.0	272.88
				46	11 17 07.27 +26 59 38.1	1.10
RXSJ1117.3+2519	1.12±0.26	43	11 17 22.27 +25 19 05.5	22.09
				52	11 17 23.19 +25 19 01.2	18.41
RXSJ1117.8+2918	0.88±0.25	BA	0.0229	11	11 17 52.52 +29 18 12.5	1.79
				11	11 17 51.12 +29 18 07.4	2.25
				46	11 17 55.19 +29 18 16.6	1.79
RXSJ1118.1+2712	0.51±0.20	9	11 18 11.50 +27 12 07.3	6.25
				31	11 18 13.24 +27 12 31.4	1.20
				35	11 18 13.81 +27 12 20.8	1.13
				50	11 18 14.86 +27 12 26.1	1.13
RXSJ1119.5+2226	2.85±0.41	QSO	0.42	8	11 19 30.32 +22 26 49.3	90.58
				40	11 19 28.00 +22 26 50.5	1.75
RXSJ1120.4+4043	0.63±0.24	49	11 20 22.02 +40 43 53.5	16.56
				49	11 20 22.30 +40 43 41.1	5.16
RXSJ1124.7+3846	0.83±0.28	G	0.00694	21	11 24 43.03 +38 45 51.9	12.47
				22	11 24 43.56 +38 45 46.7	9.11
				24	11 24 42.38 +38 45 58.0	1.81
				27	11 24 44.28 +38 45 40.0	12.33
RXSJ1125.3+4229	0.77±0.23	Cl	...	25	11 25 16.31 +42 29 11.0	6.84
				32	11 25 15.62 +42 29 14.9	4.75
RXSJ1125.6+3339	0.37±0.17	19	11 25 40.26 +33 39 24.1	8.38
				27	11 25 39.60 +33 39 21.3	4.45

continued on next page

ROSAT Name (1)	F_x ($10^{-12} \text{erg s}^{-1} \text{cm}^{-2}$) (2)	Type (3)	z (4)	Δ_{XR} ($''$) (5)	FIRST Position (J2000) (6)	F_r (mJy) (7)
RXSJ1128.2+2252	0.30±0.13	6	11 28 15.63 +22 52 10.4	32.69
				7	11 28 15.16 +22 51 58.5	3.93
				19	11 28 14.74 +22 51 49.0	96.49
				38	11 28 14.02 +22 51 32.8	1.64
RXSJ1130.0+3441	0.57±0.23	41	11 30 08.04 +34 41 41.7	1.13
				53	11 30 09.13 +34 41 44.9	5.03
RXSJ1130.8+3815	0.62±0.23	QSO	1.733	14	11 30 53.27 +38 15 18.4	667.02
				28	11 30 53.37 +38 15 03.4	2.76
RXSJ1133.2+2812	0.95±0.32	QSO	0.513	8	11 33 14.76 +28 11 59.7	9.73
				59	11 33 18.48 +28 11 43.5	8.44
RXSJ1134.1+2533	0.43±0.16	32	11 34 09.33 +25 34 08.4	1.20
				32	11 34 10.26 +25 33 44.8	1.69
RXSJ1140.8+2525	1.26±0.25	25	11 40 52.62 +25 25 32.4	3.72
				38	11 40 55.70 +25 26 12.4	2.62
				42	11 40 51.00 +25 25 26.2	5.69
				44	11 40 50.63 +25 25 27.8	26.71
				56	11 40 49.95 +25 25 20.2	9.03
RXSJ1143.6+2315	0.56±0.20	QSO	0.837	7	11 43 37.89 +23 15 02.5	100.26
				16	11 43 36.53 +23 14 51.7	17.09
RXSJ1147.3+3500	0.68±0.23	G	0.063	13	11 47 23.96 +35 00 54.9	4.56
				17	11 47 23.04 +35 01 02.0	4.11
				26	11 47 22.13 +35 01 07.3	608.81
				39	11 47 21.10 +35 01 14.5	2.59
RXSJ1147.9+2635	0.80±0.21	QSO	0.867	9	11 47 59.76 +26 35 42.5	294.50
				21	11 47 59.01 +26 35 27.0	1.18
				57	11 47 57.54 +26 34 55.2	1.32
RXSJ1148.3+3154	1.16±0.23	QSO	0.549	5	11 48 18.88 +31 54 09.8	48.24
				6	11 48 19.40 +31 54 16.3	3.51
				14	11 48 18.27 +31 54 03.5	15.76
RXSJ1148.5+2332	0.42±0.15	28	11 48 33.49 +23 32 29.9	4.63
				37	11 48 32.62 +23 32 29.4	4.31
RXSJ1149.5+2439	9.63±0.60	B	...			

continued on next page

ROSAT Name (1)	F_x ($10^{-12} \text{erg s}^{-1} \text{cm}^{-2}$) (2)	Type (3)	z (4)	Δ_{XR} ($''$) (5)	FIRST Position (J2000) (6)	F_r (mJy) (7)
				1	11 49 30.36 +24 39 27.7	12.99
				21	11 49 30.71 +24 39 07.2	6.62
RXSJ1151.6+3355	0.48±0.20	19	11 51 39.68 +33 55 41.7	6.65
				52	11 51 39.11 +33 56 16.2	1.10
				58	11 51 43.63 +33 54 42.6	1.00
				60	11 51 38.02 +33 56 18.1	14.93
RXSJ1154.8+2756	0.29±0.12	22	11 54 53.25 +27 55 54.8	1.21
				32	11 54 54.11 +27 55 51.3	5.01
				36	11 54 49.99 +27 55 57.7	42.96
RXSJ1156.0+3432	0.66±0.20	Cl	...	7	11 56 05.95 +34 32 30.3	13.76
				30	11 56 05.51 +34 33 05.3	32.59
				31	11 56 08.14 +34 32 29.9	4.16
RXSJ1157.3+3336	3.11±0.39	Cl	0.213	29	11 57 16.75 +33 36 39.6	3.59
				30	11 57 16.68 +33 36 53.4	4.12
				31	11 57 16.89 +33 36 30.0	6.90
RXSJ1158.4+2627	0.34±0.14	39	11 58 26.67 +26 27 20.8	2.06
				41	11 58 26.79 +26 27 37.6	2.34
RXSJ1200+2605	0.36±0.13	16	12 00 46.29 +26 04 53.6	1.69
				55	12 00 42.15 +26 05 18.6	2.41
RXSJ1200.8+2750	0.43±0.15	15	12 00 48.70 +27 50 58.7	4.89
				52	12 00 44.73 +27 50 20.7	2.14
RXSJ1200.9+2615	1.95±0.30	46	12 00 52.80 +26 15 16.4	1.28
				50	12 00 52.65 +26 15 03.0	2.20
				59	12 00 51.84 +26 15 13.9	4.13
RXSJ1202.5+2756	0.86±0.20	QSO	0.672	8	12 02 34.08 +27 56 25.9	105.55
				10	12 02 33.24 +27 56 22.0	13.38
RXSJ1226.7+2631	1.67±0.27	QSO	0.48	5	12 02 40.68 +26 31 38.6	61.67
				41	12 02 38.75 +26 32 15.8	5.35
				46	12 02 38.19 +26 32 15.8	6.67
RXSJ1202.7+2651	0.24±0.10	39	12 02 39.61 +26 50 59.2	20.71
				60	12 02 45.05 +26 50 22.0	5.38

continued on next page

ROSAT Name (1)	F_x ($10^{-12} \text{erg s}^{-1} \text{cm}^{-2}$) (2)	Type (3)	z (4)	Δ_{XR} (n) (5)	FIRST Position (J2000) (6)	F_r (mJy) (7)
RXSJ1202.7+3735	0.50±0.18	QSO	1.19	17	12 02 43.56 +37 35 51.7	16.29
				59	12 02 41.49 +37 36 31.4	39.42
RXSJ1203.0+2353	0.88±0.20	15	12 03 01.43 +23 53 19.7	7.49
				57	12 03 03.73 +23 53 59.6	4.16
RXSJ1203.0+2836	1.16±0.23	Cl	...	13	12 03 01.65 +28 35 50.7	17.75
				22	12 03 01.58 +28 35 41.5	12.49
RXSJ1203.9+3711	1.07±0.25	10	12 03 54.77 +37 11 37.4	4.59
				32	12 03 53.32 +37 12 04.0	4.35
				57	12 03 50.23 +37 10 57.5	1.13
RXSJ1204.9+2237	0.72±0.21	Cl	...	19	12 04 57.64 +22 37 08.7	11.68
				24	12 04 57.39 +22 37 02.7	12.11
RXSJ1207.4+2755	0.42±0.13	QSO	2.177	10	12 07 27.89 +27 54 58.7	596.14
				59	12 07 32.71 +27 54 58.2	1.10
RXSJ1207.8+2534	0.43±0.16	16	12 07 51.52 +25 34 40.7	35.48
				45	12 07 53.90 +25 35 29.3	39.81
RXSJ1207.8+2802	1.05±0.21	BA	0.354	20	12 07 54.80 +28 02 58.0	1.15
				51	12 07 50.29 +28 02 59.6	1.47
RXSJ1208.0+2514	0.49±0.16	G	0.0226	11	12 08 03.93 +25 14 26.7	1.19
				15	12 08 05.57 +25 14 14.1	49.93
				25	12 08 06.19 +25 14 09.9	6.79
				27	12 08 04.00 +25 13 53.6	1.04
				50	12 08 01.13 +25 14 40.3	8.12
RXSJ1208.3+2219	0.29±0.13	3	12 08 21.99 +22 19 58.4	7.20
				41	12 08 24.72 +22 20 04.9	9.09
				42	12 08 18.75 +22 20 01.7	6.41
				53	12 08 17.99 +22 20 00.0	12.46
				56	12 08 25.82 +22 20 06.9	9.27
RXSJ1209.4+2640	0.66±0.19	5	12 09 24.30 +26 40 25.1	1.81
				42	12 09 24.85 +26 39 47.1	3.29
RXSJ1209.7+2547	0.51±0.17	26	12 09 45.10 +25 47 03.6	389.85
				27	12 09 45.60 +25 46 53.3	6.28

continued on next page

ROSAT Name (1)	F_x ($10^{-12}\text{erg s}^{-1}\text{cm}^{-2}$) (2)	Type (3)	z (4)	Δ_{XR} (//) (5)	FIRST Position (J2000) (6)	F_r (mJy) (7)
RXSJ1209.7+2643	0.46±0.15	47	12 09 47.15 +26 43 57.4	1.07
				52	12 09 48.74 +26 43 58.3	3.35
RXSJ1210.6+3157	1.40±0.35	QSO	0.388	17	12 10 37.58 +31 57 06.0	19.15
				37	12 10 37.56 +31 57 37.1	66.09
				38	12 10 37.34 +31 56 31.6	4.29
				50	12 10 37.59 +31 56 17.2	16.73
RXSJ1212.2+3101	0.54±0.16	21	12 12 14.34 +31 01 22.0	7.69
				24	12 12 14.24 +31 01 30.9	2.01
				39	12 12 13.19 +31 01 08.4	1.01
				44	12 12 12.85 +31 01 04.8	4.91
RXSJ1212.9+2726	1.02±0.21	15	12 12 59.10 +27 27 04.6	6.42
				41	12 12 55.47 +27 26 38.1	1.16
RXSJ1213.7+2253	0.51±0.17	22	12 13 40.58 +22 53 46.1	5.26
				50	12 13 45.58 +22 53 53.7	1.01
RXSJ1214.2+2554	0.53±0.16	5	12 14 12.19 +25 53 56.0	89.72
				21	12 14 11.17 +25 54 18.6	52.77
RXSJ1215.1+3311	6.30±0.90	G	0.00362	30	12 15 05.05 +33 11 50.7	6.94
				60	12 15 09.10 +33 10 37.3	2.12
RXSJ1216.9+3230	0.48±0.19	24	12 16 58.95 +32 31 05.7	3.03
				25	12 16 59.00 +32 30 52.1	2.80
				43	12 17 00.43 +32 31 06.7	2.25
RXSJ1220.1+3431	0.48±0.16	B	...	8	12 20 08.32 +34 31 21.6	251.86
				10	12 20 07.36 +34 31 33.7	2.08
				57	12 20 06.87 +34 32 23.4	1.95
RXSJ1220.5+3343	0.72±0.19	QSO	1.519	23	12 20 33.68 +33 43 15.6	586.77
				30	12 20 33.89 +33 43 08.0	1929.96
RXSJ1221.5+2814	2.24±0.31	B	0.102	9	12 21 31.70 +28 13 58.5	908.33
				17	12 21 31.44 +28 13 45.9	1.59
RXSJ1221.8+3130	0.21±0.10	12	12 21 52.61 +31 30 57.3	31.36
				16	12 21 51.99 +31 30 53.5	250.80

continued on next page

ROSAT Name (1)	F_x ($10^{-12} \text{erg s}^{-1} \text{cm}^{-2}$) (2)	Type (3)	z (4)	Δ_{XR} (//) (5)	FIRST Position (J2000) (6)	F_r (mJy) (7)
				28	12 21 55.01 +31 31 01.7	116.17
				59	12 21 48.58 +31 30 56.2	1.14
RXSJ1223.2+3706	1.03±0.20	QSO	0.489			
				7	12 23 12.31 +37 07 02.0	126.32
				13	12 23 11.22 +37 07 01.9	24.36
				35	12 23 09.32 +37 07 03.3	88.51
RXSJ1223.9+2729	0.86±0.21			
				35	12 23 52.51 +27 29 55.8	1.54
				38	12 23 53.19 +27 30 05.4	1.75
				45	12 23 53.64 +27 30 13.6	2.03
RXSJ1225.6+2458	2.13±0.30	QSO	0.268			
				5	12 25 39.55 +24 58 36.4	6.87
				15	12 25 39.06 +24 58 43.4	1.01
				21	12 25 40.39 +24 58 53.1	14.66
				33	12 25 38.40 +24 58 08.2	55.31
				35	12 25 40.90 +24 59 05.7	97.54
RXSJ1225.8+4126	0.57±0.19			
				15	12 25 46.62 +41 26 05.3	4.18
				36	12 25 49.65 +41 26 33.6	1.84
RXSJ1226.0+2604	1.46±0.28			
				10	12 26 04.12 +26 04 28.0	9.64
				27	12 26 03.46 +26 04 08.6	1.18
RXSJ1226.4+3113	0.43±0.15	G	0.00239			
				17	12 26 27.57 +31 13 05.6	1.65
				22	12 26 26.71 +31 13 43.1	1.98
RXSJ1228.9+3556	0.41±0.13			
				13	12 28 55.33 +35 56 29.7	1.16
				14	12 28 56.69 +35 56 35.4	8.68
				35	12 28 58.60 +35 56 42.7	1.03
RXSJ1230.5+4139	0.49±0.15	G	0.00188			
				35	12 30 31.40 +41 39 08.6	1.29
				40	12 30 34.17 +41 39 00.1	1.09
				41	12 30 29.46 +41 39 27.4	3.34
				48	12 30 34.81 +41 38 54.5	2.26
RXSJ1231.6+4017	0.53±0.15	QSO?	0.649			
				5	12 31 40.66 +40 17 31.6	186.72
				9	12 31 39.85 +40 17 35.9	46.38
RXSJ1231.7+2847	2.13±0.36	QSO	1.03			
				2	12 31 44.72 +28 47 52.7	1.59
				10	12 31 44.04 +28 47 50.0	3.28
				15	12 31 43.59 +28 47 49.7	93.78
RXSJ1233.7+2241	0.24±0.10			
				51	12 33 43.33 +22 41 45.7	1.34

continued on next page

ROSAT Name (1)	F_x ($10^{-12}\text{erg s}^{-1}\text{cm}^{-2}$) (2)	Type (3)	z (4)	Δ_{XR} (μ) (5)	FIRST Position (J2000) (6)	F_r (mJy) (7)
				53	12 33 50.59 +22 42 09.1	1.36
RXSJ1234.0+2745	0.40±0.14	22	12 34 04.68 +27 44 57.5	4.16
				27	12 34 02.03 +27 44 47.5	4.30
RXSJ1234.6+2350	2.30±0.27	G?	...	5	12 34 38.64 +23 50 13.0	1.47
				26	12 34 37.12 +23 50 16.1	3.84
				29	12 34 38.27 +23 49 47.6	6.01
RXSJ1234.9+2300	0.77±0.22	15	12 34 52.99 +23 00 59.5	7.49
				15	12 34 52.97 +23 00 50.2	20.92
RXSJ1236.8+2507	1.50±0.23	QSO	0.546	6	12 36 51.57 +25 07 50.7	16.25
				23	12 36 49.89 +25 07 38.6	4.79
				38	12 36 53.83 +25 08 06.3	20.79
				41	12 36 48.82 +25 07 28.1	24.54
RXSJ1238.3+4124	0.87±0.19	4	12 38 19.62 +41 24 20.5	8.06
				35	12 38 18.51 +41 23 50.6	4.49
				49	12 38 21.26 +41 25 08.9	1.40
RXSJ1240.3+3503	0.55±0.15	QSO	1.199	15	12 40 21.53 +35 03 05.6	90.88
				15	12 40 21.02 +35 02 51.0	87.60
RXSJ1240.5+3037	0.28±0.11	A	0.224	15	12 40 35.82 +30 37 22.8	1.20
				17	12 40 34.15 +30 37 46.6	1.21
RXSJ1240.7+3336	0.56±0.15	21	12 40 44.58 +33 03 55.3	6.89
				24	12 40 44.45 +33 04 01.9	102.33
				32	12 40 45.06 +33 03 27.3	36.07
RXSJ1241.7+3503	2.90±0.30	G	0.023	8	12 41 44.53 +35 03 45.4	1.39
				14	12 41 43.76 +35 04 04.9	1.66
RXSJ1242.1+3317	11.1±0.55	8	12 42 10.63 +33 17 03.0	5.80
				33	12 42 12.03 +33 17 34.9	1.73
RXSJ1242.7+3002	0.24±0.09	26	12 42 45.60 +30 02 22.0	33.36
				30	12 42 44.97 +30 02 44.6	1.30
				42	12 42 46.26 +30 01 56.1	4.34
				49	12 42 46.43 +30 01 47.6	4.00
RXSJ1246.7+3452	0.25±0.10	15	12 46 41.89 +34 52 51.7	9.32

continued on next page

ROSAT Name (1)	F_x ($10^{-12} \text{erg s}^{-1} \text{cm}^{-2}$) (2)	Type (3)	z (4)	Δ_{XR} (//) (5)	FIRST Position (J2000) (6)	F_r (mJy) (7)
				28	12 46 41.86 +34 52 29.2	81.12
				32	12 46 41.80 +34 53 20.2	26.44
RXSJ1247.1+3246	0.78±0.17	G?	...	17	12 47 10.61 +32 46 47.4	1.10
				25	12 47 09.69 +32 47 05.1	46.39
RXSJ1247.2+3136	0.57±0.24	8	12 47 16.39 +31 36 30.9	2.56
				29	12 47 18.50 +31 36 18.1	1.55
RXSJ1247.3+3209	0.99±0.18	QSO	0.949	4	12 47 20.82 +32 09 00.9	77.07
				7	12 47 21.45 +32 09 06.0	122.97
				16	12 47 20.17 +32 08 51.1	90.55
RXSJ1248.2+3624	0.81±0.17	B	...	6	12 48 13.88 +36 24 24.0	2.36
				12	12 48 14.32 +36 24 32.0	1.41
				19	12 48 14.78 +36 24 37.7	2.20
RXSJ1249.2+2817	0.22±0.09	14	12 49 18.40 +28 17 43.9	70.33
				18	12 49 16.54 +28 18 04.7	1.93
				40	12 49 20.13 +28 17 32.4	3.15
RXSJ1250.2+3156	1.89±0.24	G?	...	9	12 50 15.55 +31 55 59.4	4.43
				38	12 50 17.11 +31 56 31.9	1.35
RXSJ1250.4+3016	0.33±0.12	QSO	1.058	13	12 50 24.61 +30 16 31.0	175.36
				16	12 50 26.33 +30 16 48.5	101.33
RXSJ1250.8+4107	3.39±0.32	BA	0.00103	6	12 50 53.06 +41 07 13.6	8.91
				47	12 50 56.64 +41 07 08.0	1.29
				51	12 50 55.24 +41 06 32.3	1.01
				55	12 50 56.83 +41 06 47.2	1.09
RXSJ1252.4+2913	0.39±0.12	QSO	0.82	13	12 52 24.97 +29 13 21.2	1.37
				35	12 52 23.03 +29 12 53.4	1.24
RXSJ1252.5+2233	0.90±0.24	7	12 52 30.84 +22 33 29.7	2.73
				30	12 52 31.70 +22 33 51.8	1.39
				34	12 52 32.65 +22 33 38.5	2.94
RXSJ1255.5+3521	0.94±0.19	G	0.16129	19	12 55 31.26 +35 21 10.4	9.23
				25	12 55 32.43 +35 21 29.3	6.61
RXSJ1255.7+3110	0.49±0.14			

continued on next page

ROSAT Name (1)	F_x ($10^{-12} \text{erg s}^{-1} \text{cm}^{-2}$) (2)	Type (3)	z (4)	Δ_{XR} ($''$) (5)	FIRST Position (J2000) (6)	F_r (mJy) (7)
				1	12 55 42.55 +31 10 48.4	5.19
				17	12 55 43.15 +31 11 03.4	1.25
				20	12 55 41.65 +31 10 32.3	1.94
RXSJ1259.1+4129	0.95±0.17	11	12 59 08.68 +41 29 37.6	10.35
				23	12 59 09.56 +41 29 30.0	5.64
				40	12 59 10.26 +41 29 14.8	1.66
RXSJ1259.2+2754	1.71±0.96	Cl?	0.0215	10	12 59 12.89 +27 54 38.4	1.34
				34	12 59 12.22 +27 55 21.8	2.29
RXSJ1300.7+2808	2.59±0.31	36	13 00 50.68 +28 07 59.7	23.39
				40	13 00 51.03 +28 08 07.9	11.83
RXSJ1302.0+3915	0.32±0.11	13	13 02 01.21 +39 15 25.6	12.50
				33	13 02 02.96 +39 15 24.6	1.22
RXSJ1304.8+2454	2.05±0.26	2	13 04 51.43 +24 54 46.0	22.21
				51	13 04 55.01 +24 54 45.2	1.04
RXSJ1306.3+3917	0.71±0.15	46	13 06 26.06 +39 17 36.5	1.04
				56	13 06 17.67 +39 17 36.1	1.01
RXSJ1308.3+3546	0.33±0.12	21	13 08 23.72 +35 46 37.2	215.90
				37	13 08 25.05 +35 46 28.8	2.18
RXSJ1308.9+2612	0.51±0.15	31	13 08 55.40 +26 11 58.0	1.02
				38	13 08 56.93 +26 11 56.6	1.06
RXSJ1309.1+4232	0.34±0.11	11	13 09 10.34 +42 32 25.2	1.90
				39	13 09 10.47 +42 33 03.5	1.08
				46	13 09 10.42 +42 33 10.6	1.33
				56	13 09 09.72 +42 31 33.1	1.80
RXSJ1310.0+3254	0.32±0.11	26	13 10 03.84 +32 54 02.5	4.07
				28	13 10 04.85 +32 53 44.7	7.86
				48	13 10 05.91 +32 53 21.8	2.82
RXSJ1310.4+3220	0.79±0.15	B	0.996	14	13 10 28.67 +32 20 44.0	1459.05
				25	13 10 28.61 +32 20 54.5	28.62
				58	13 10 24.36 +32 20 49.0	1.86
RXSJ1311.5+3943	0.27±0.10			

continued on next page

ROSAT Name (1)	F_x ($10^{-12} \text{erg s}^{-1} \text{cm}^{-2}$) (2)	Type (3)	z (4)	Δ_{XR} ($''$) (5)	FIRST Position (J2000) (6)	F_r (mJy) (7)
RXSJ1341.0+3959	7.51±0.38	Cl	0.1691			
				5	13 41 05.13 +39 59 45.6	38.06
				10	13 41 05.67 +39 59 44.3	4.82
				16	13 41 05.67 +39 59 54.3	1.21
RXSJ1341.5+3532	0.21±0.08	QSO	0.782			
				10	13 41 33.12 +35 32 51.9	52.49
				31	13 41 32.31 +35 33 10.9	2.41
RXSJ1341.8+2622	7.47±0.49	G/Cl	0.0757,0.0696			
				23	13 41 50.91 +26 22 28.3	34.03
				25	13 41 52.85 +26 22 55.0	1.19
				30	13 41 50.58 +26 22 17.7	70.46
				45	13 41 49.26 +26 22 26.9	9.48
				52	13 41 53.84 +26 23 19.3	1.18
RXSJ1342.0+3707	0.92±0.15	QSO	1.11			
				14	13 41 59.91 +37 07 10.2	24.50
				57	13 42 04.53 +37 07 53.3	4.04
				57	13 42 02.10 +37 08 11.0	2.58
RXSJ1342.1+2709	0.51±0.15	G	...			
				11	13 42 08.38 +27 09 30.7	238.13
				15	13 42 08.20 +27 09 27.0	4.67
RXSJ1342.5+3507	0.21±0.08			
				4	13 42 32.45 +35 07 07.5	92.97
				7	13 42 31.64 +35 07 11.5	72.14
				14	13 42 31.00 +35 07 10.6	379.99
				58	13 42 36.82 +35 07 10.2	1.01
RXSJ1342.9+2828	0.50±0.17	QSO	1.037			
				18	13 42 55.07 +28 28 20.5	59.78
				19	13 42 54.39 +28 28 05.9	65.57
				31	13 42 53.64 +28 27 54.1	27.23
RXSJ1342.9+2844	1.06±0.23	QSO	0.905			
				7	13 43 00.12 +28 44 07.0	217.37
				23	13 43 01.14 +28 44 18.7	1.32
RXSJ1345.3+4142	1.02±0.16	G	0.00861			
				7	13 45 19.09 +41 42 44.7	5.34
				33	13 45 15.52 +41 42 43.5	1.07
RXSJ1345.4+4125	0.30±0.11			
				5	13 45 23.81 +41 25 41.8	18.13
				19	13 45 24.48 +41 25 20.1	9.15
				34	13 45 22.81 +41 26 08.7	5.58
RXSJ1345.9+3650	0.76±0.14			
				18	13 45 55.90 +36 50 18.0	30.71
				19	13 45 54.96 +36 50 10.7	22.63
				24	13 45 54.36 +36 50 05.3	13.07

continued on next page

ROSAT Name (1)	F_x ($10^{-12}\text{erg s}^{-1}\text{cm}^{-2}$) (2)	Type (3)	z (4)	Δ_{XR} ($''$) (5)	FIRST Position (J2000) (6)	F_r (mJy) (7)
RXSJ1347.8+2836	1.11±0.22	10	13 47 51.59 +28 36 30.0	34.97
				15	13 47 52.17 +28 36 29.2	19.00
				28	13 47 49.84 +28 36 19.1	80.74
				59	13 47 54.16 +28 37 24.7	1.15
RXSJ1350.7+2331	1.56±0.28	1	13 50 45.65 +23 31 45.3	67.57
				15	13 50 46.72 +23 31 52.4	2.31
				24	13 50 47.41 +23 31 39.3	29.76
				47	13 50 48.62 +23 31 21.8	1.24
				52	13 50 49.12 +23 31 24.0	1.00
				53	13 50 41.90 +23 31 38.3	14.38
RXSJ1351.0+3042	0.28±0.12	12	13 51 01.82 +30 42 26.0	2.76
				17	13 51 01.13 +30 42 27.2	3.50
RXSJ1351.0+3053	0.17±0.08	11	13 51 03.87 +30 53 43.6	6.77
				23	13 51 02.36 +30 53 18.9	4.39
				24	13 51 03.27 +30 53 55.4	12.72
				38	13 51 03.28 +30 54 10.1	21.40
RXSJ1351.9+4106	0.32±0.10	10	13 51 55.65 +41 06 32.8	1.25
				23	13 51 54.17 +41 06 43.9	19.57
				27	13 51 57.52 +41 06 16.3	6.48
RXSJ1353.1+2809	0.86±0.18	19	13 53 08.36 +28 09 09.0	16.14
				22	13 53 06.89 +28 09 00.5	3.03
				35	13 53 06.48 +28 08 48.5	19.62
				36	13 53 07.25 +28 08 45.6	4.67
				36	13 53 09.64 +28 09 41.0	3.42
				39	13 53 10.23 +28 09 27.2	3.71
				48	13 53 10.64 +28 09 39.8	2.60
				49	13 53 11.01 +28 09 21.4	18.77
RXSJ1355.7+3024	0.30±0.11	QSO	1.018	17	13 55 41.90 +30 24 18.4	2.25
				26	13 55 41.11 +30 24 12.0	123.06
RXSJ1358.8+4140	0.24±0.09	17	13 58 48.81 +41 40 13.8	1.99
				45	13 58 46.03 +41 39 55.2	1.06
RXSJ1358.8+3904	0.39±0.11	QSO	0.80	14	13 58 48.50 +39 04 15.6	1.72
				24	13 58 47.65 +39 04 14.9	2.27
				24	13 58 47.90 +39 04 03.3	282.87
				30	13 58 48.10 +39 03 52.0	2.59
				32	13 58 50.35 +39 04 47.0	1.31
				32	13 58 48.86 +39 03 44.6	2.39

continued on next page

ROSAT Name (1)	F_x ($10^{-12}\text{erg s}^{-1}\text{cm}^{-2}$) (2)	Type (3)	z (4)	Δ_{XR} ($''$) (5)	FIRST Position (J2000) (6)	F_r (mJy) (7)
				34	13 58 46.87 +39 04 22.0	2.62
				37	13 58 47.39 +39 03 51.3	1.49
RXSJ1358.8+2511	2.75±0.33	9	13 58 52.02 +25 11 40.6	2.93
				48	13 58 48.89 +25 11 19.8	6.12
RXSJ1400.0+3910	0.22±0.09	7	14 00 02.68 +39 10 44.4	44.76
				22	14 00 03.59 +39 11 04.5	39.78
RXSJ1400.2+2821	0.43±0.15	19	14 00 18.17 +28 21 00.2	4.65
				19	14 00 15.89 +28 21 22.6	1.03
				35	14 00 14.80 +28 21 29.7	3.14
				40	14 00 18.34 +28 20 36.6	1.03
				52	14 00 19.12 +28 20 28.7	1.15
RXSJ1401.1+2840	0.30±0.12	G?	0.1104	51	14 01 06.37 +28 40 22.6	61.79
				55	14 01 05.70 +28 40 44.6	102.85
RXSJ1401.7+2324	0.62±0.18	BA	0.22	8	14 01 46.99 +23 24 13.8	1.04
				10	14 01 48.10 +23 24 16.0	7.03
				22	14 01 49.03 +23 24 18.8	26.52
RXSJ1401.9+2341	0.40±0.15	24	14 02 00.22 +23 40 46.9	8.62
				42	14 01 59.60 +23 40 23.9	1.62
RXSJ1405.0+2925	0.36±0.13	10	14 05 00.81 +29 25 14.0	7.15
				15	14 05 02.31 +29 25 16.0	2.91
				22	14 05 02.99 +29 25 13.7	67.34
				45	14 04 58.00 +29 25 16.2	82.52
RXSJ1406.4+2509	0.46±0.15	QSO	0.87	5	14 06 26.60 +25 09 21.3	67.51
				10	14 06 26.21 +25 09 25.7	28.42
				19	14 06 26.03 +25 09 33.5	13.60
				21	14 06 25.35 +25 09 29.7	5.19
				51	14 06 30.13 +25 08 58.3	2.78
RXSJ1406.8+2245	0.24±0.10	23	14 06 52.58 +22 45 05.7	6.84
				50	14 06 54.33 +22 44 41.6	14.74
RXSJ1409.4+2618	2.30±0.29	QSO	0.940	7	14 09 23.90 +26 18 21.0	8.85
				51	14 09 27.86 +26 18 18.1	6.41
				56	14 09 27.92 +26 18 05.7	1.28
RXSJ1411.9+4239	0.83±0.16	QSO	0.88			

continued on next page

ROSAT Name (1)	F_x ($10^{-12}\text{erg s}^{-1}\text{cm}^{-2}$) (2)	Type (3)	z (4)	Δ_{XR} (//) (5)	FIRST Position (J2000) (6)	F_r (mJy) (7)
				20	14 11 59.73 +42 39 50.4	71.15
				32	14 12 02.27 +42 39 23.0	6.04
RXSJ1412.8+2532	0.35±0.14	37	14 12 45.89 +25 31 57.2	7.47
				47	14 12 45.18 +25 31 54.1	10.68
				59	14 12 50.77 +25 33 06.2	2.18
RXSJ1414.7+3928	0.54±0.13	5	14 14 46.65 +39 28 18.9	11.32
				21	14 14 45.74 +39 28 36.9	1.46
RXSJ1416.4+3721	0.63±0.14	12	14 16 30.67 +37 21 37.1	29.39
				35	14 16 31.04 +37 22 03.0	12.72
				37	14 16 28.59 +37 20 57.5	1.13
				42	14 16 28.21 +37 20 53.4	7.99
				47	14 16 28.67 +37 20 46.3	7.07
				49	14 16 26.01 +37 21 49.9	2.43
RXSJ1417.9+2543	23.9±0.84	B	0.237	4	14 17 56.68 +25 43 26.2	39.50
				7	14 17 56.66 +25 43 22.3	2.47
				24	14 17 55.13 +25 43 21.3	1.65
RXSJ1417.9+4051	0.19±0.09	6	14 17 58.61 +40 52 01.8	45.91
				7	14 17 58.11 +40 51 50.0	18.02
RXSJ1417.9+2508	69.4±1.47	BA	0.0172	4	14 17 59.48 +25 08 14.2	11.03
				54	14 17 55.67 +25 08 08.4	3.11
RXSJ1418.9+3946	0.31±0.10	6	14 18 58.89 +39 46 26.8	59.91
				11	14 18 58.83 +39 46 41.0	16.79
				22	14 18 58.83 +39 46 52.3	64.06
RXSJ1419.9+2706	0.80±0.18	4	14 19 59.30 +27 06 25.5	201.08
				15	14 19 59.16 +27 06 44.8	6.46
				17	14 19 58.51 +27 06 43.6	2.04
				38	14 19 56.72 +27 06 44.5	1.08
RXSJ1420.6+3955	0.37±0.10	7	14 20 40.11 +39 55 06.9	7.58
				24	14 20 38.52 +39 55 02.5	14.39
				60	14 20 35.76 +39 55 25.9	1.37
RXSJ1421.4+3943	0.29±0.10	QSO	0.622	11	14 21 25.68 +39 43 28.9	41.39
				27	14 21 28.65 +39 43 44.9	1.98
				34	14 21 29.47 +39 43 36.1	1.33
				40	14 21 29.91 +39 43 38.8	4.91

continued on next page

ROSAT Name	F_x ($10^{-12}\text{erg s}^{-1}\text{cm}^{-2}$)	Type	z	Δ_{XR} ($''$)	FIRST Position (J2000)	F_r (mJy)
(1)	(2)	(3)	(4)	(5)	(6)	(7)
RXSJ1421.4+3119	0.27±0.10	QSO	1.547			
				7	14 21 29.64 +31 19 03.6	81.43
				13	14 21 29.13 +31 18 59.5	78.08
				14	14 21 30.06 +31 18 58.0	104.24
RXSJ1422.0+3118	0.42±0.13			
				6	14 22 00.02 +31 18 20.3	8.87
				28	14 21 58.37 +31 18 13.0	19.72
RXSJ1425.8+2404	1.33±0.29	QSO	0.649			
				5	14 25 50.65 +24 04 03.5	121.14
				8	14 25 50.85 +24 04 14.5	611.44
				14	14 25 50.32 +24 03 55.7	394.80
				56	14 25 52.72 +24 04 57.3	1.53
RXSJ1426.1+4024	0.71±0.14	QSO	0.664			
				18	14 26 06.19 +40 24 32.0	26.26
				22	14 26 09.30 +40 24 41.7	2.37
				29	14 26 09.90 +40 24 43.3	6.32
				29	14 26 09.81 +40 24 50.4	5.24
				54	14 26 02.90 +40 24 27.5	10.98
RXSJ1426.2+2729	1.03±0.23			
				30	14 26 17.10 +27 29 31.1	4.40
				35	14 26 18.00 +27 29 48.0	6.96
RXSJ1426.5+2702	0.29±0.13			
				19	14 26 36.26 +27 02 26.6	90.71
				20	14 26 36.81 +27 02 39.8	72.44
				23	14 26 37.06 +27 02 42.8	119.56
RXSJ1427.0+3412	0.11±0.06			
				15	14 26 59.72 +34 12 00.2	10.80
				15	14 27 01.70 +34 12 17.4	11.12
				44	14 26 57.88 +34 11 42.1	20.08
				49	14 26 58.19 +34 11 31.9	4.33
RXSJ1427.5+2631	0.60±0.18	QSO	0.366			
				19	14 27 35.26 +26 32 07.8	1.55
				27	14 27 35.61 +26 32 14.6	42.72
				39	14 27 32.08 +26 31 46.7	1.63
				53	14 27 31.26 +26 31 31.3	4.80
				60	14 27 30.90 +26 31 24.5	4.34
RXSJ1427.9+3247	0.82±0.17			
				10	14 27 58.72 +32 47 41.6	17.70
				34	14 28 01.57 +32 47 29.9	7.45
				42	14 27 55.68 +32 47 44.6	1.97
				43	14 28 02.19 +32 47 42.1	22.40
				48	14 27 55.16 +32 47 38.7	4.98
RXSJ1428.2+3913	0.48±0.12			
				58	14 28 13.27 +39 12 27.9	1.03

continued on next page

ROSAT Name (1)	F_x ($10^{-12} \text{erg s}^{-1} \text{cm}^{-2}$) (2)	Type (3)	z (4)	Δ_{XR} (//) (5)	FIRST Position (J2000) (6)	F_r (mJy) (7)
				59	14 28 13.90 +39 12 18.8	162.92
RXSJ1428.5+4240	53.9±1.17	B	0.129	7	14 28 32.62 +42 40 21.2	38.19
				9	14 28 33.39 +42 40 29.8	1.09
RXSJ1431.1+2538	4.18±0.42	Cl	0.0908	16	14 31 06.83 +25 38 01.4	7.38
				51	14 31 05.61 +25 37 24.6	1.01
RXSJ1433.5+3208	0.24±0.10	9	14 33 33.74 +32 09 08.3	7.75
				13	14 33 32.96 +32 09 03.9	47.97
				27	14 33 35.83 +32 09 11.0	54.81
RXSJ1433.9+2925	0.21±0.09	Cl?	...	31	14 33 56.07 +29 25 27.7	1.00
				46	14 33 55.46 +29 25 07.8	1.06
				46	14 33 51.06 +29 25 54.8	3.20
RXSJ1433.9+4240	0.44±0.12	27	14 33 56.69 +42 40 16.8	10.90
				35	14 33 57.09 +42 40 03.7	9.60
RXSJ1434.7+3328	0.98±0.16	9	14 34 45.32 +33 28 20.6	26.48
				11	14 34 46.56 +33 28 20.0	1.63
RXSJ1435.6+4154	0.23±0.09	23	14 35 36.87 +41 54 09.7	1.05
				29	14 35 37.28 +41 54 00.1	16.34
RXSJ1435.8+3957	0.24±0.09	21	14 35 54.94 +39 57 29.5	16.31
				43	14 35 57.10 +39 57 29.4	1.04
RXSJ1437.6+3906	0.22±0.08	18	14 37 35.00 +39 06 51.7	5.13
				25	14 37 37.70 +39 07 17.0	1.02
RXSJ1437.9+3519	0.27±0.09	QSO	0.540	6	14 37 56.46 +35 19 36.5	16.53
				9	14 37 56.45 +35 19 50.3	14.97
				51	14 37 52.05 +35 19 40.1	11.06
RXSJ1438.8+3710	0.18±0.07	8	14 38 53.90 +37 10 50.0	4.26
				16	14 38 53.62 +37 10 35.5	358.21
				50	14 38 50.99 +37 11 32.7	1.21
RXSJ1440.4+2607	0.40±0.15	4	14 40 30.06 +26 07 46.5	2.14
				52	14 40 25.91 +26 07 48.8	1.34

continued on next page

ROSAT Name (1)	F_x ($10^{-12}\text{erg s}^{-1}\text{cm}^{-2}$) (2)	Type (3)	z (4)	Δ_{XR} ($''$) (5)	FIRST Position (J2000) (6)	F_r (mJy) (7)
RXSJ1442.0+2812	0.40±0.13	9 29	14 42 04.35 +28 12 10.3 14 42 03.18 +28 12 29.4	2.03 9.30
RXSJ1442.3+2218	5.69±0.53	G?	...	10 60 60	14 42 19.37 +22 18 11.9 14 42 23.19 +22 18 26.7 14 42 22.94 +22 18 42.9	17.98 1.14 7.12
RXSJ1442.5+3234	0.37±0.12	12 48	14 42 32.21 +32 34 50.0 14 42 28.29 +32 34 43.4	1.95 17.28
RXSJ1443.3+3740	0.25±0.09	3 16 26	14 43 22.85 +37 40 15.3 14 43 23.40 +37 40 30.6 14 43 23.62 +37 40 41.6	1.29 1.34 1.13
RXSJ1444.4+3113	1.50±0.22	Cl	0.232	11 54 60	14 44 27.97 +31 13 13.9 14 44 31.79 +31 13 36.5 14 44 27.97 +31 14 03.5	59.31 2.65 1.27
RXSJ1445.0+3227	0.29±0.10	50 52	14 45 04.61 +32 27 05.9 14 45 04.67 +32 26 57.5	3.34 2.20
RXSJ1446.8+3152	0.33±0.12	43 53	14 46 55.50 +31 51 32.1 14 46 55.67 +31 51 22.0	27.42 16.51
RXSJ1448.1+3527	0.88±0.18	7 45 59	14 48 11.97 +35 27 06.5 14 48 09.17 +35 26 32.1 14 48 08.33 +35 26 21.8	7.06 1.03 1.24
RXSJ1448.4+3559	4.08±0.35	H	0.11	10 56	14 48 25.10 +35 59 47.2 14 48 28.30 +36 00 40.7	1.44 3.17
RXSJ1449.7+4133	0.25±0.09	12 18 20 48	14 49 42.48 +41 34 01.8 14 49 42.28 +41 34 11.4 14 49 43.01 +41 33 39.5 14 49 41.14 +41 34 41.8	10.54 1.41 2.70 1.32
RXSJ1451.4+2515	0.67±0.21	8 43	14 51 23.12 +25 15 46.6 14 51 25.60 +25 16 20.1	25.53 2.48
RXSJ1453.5+3113	0.28±0.11	12 26	14 53 32.33 +31 13 32.7 14 53 33.86 +31 13 20.1	13.55 7.12

continued on next page

ROSAT Name (1)	F_x ($10^{-12}\text{erg s}^{-1}\text{cm}^{-2}$) (2)	Type (3)	z (4)	Δ_{XR} (//) (5)	FIRST Position (J2000) (6)	F_r (mJy) (7)
RXSJ1454.0+3418	0.52±0.12	11	14 54 03.40 +34 18 10.2	1.38
				30	14 54 00.62 +34 18 00.4	14.84
				38	14 54 05.49 +34 18 30.0	1.41
				44	14 54 06.07 +34 18 27.7	2.48
RXSJ1454.0+2904	0.16±0.07	12	14 54 06.33 +29 04 24.7	4.86
				16	14 54 04.88 +29 04 43.7	3.14
				25	14 54 03.75 +29 04 39.6	1.14
				25	14 54 04.54 +29 04 51.9	1.59
				29	14 54 04.00 +29 04 51.2	1.25
				37	14 54 07.27 +29 04 59.1	1.10
				40	14 54 07.94 +29 04 06.1	22.63
RXSJ1455.7+3614	0.35±0.10	3	14 55 46.62 +36 14 13.0	2.12
				20	14 55 47.93 +36 14 05.1	4.16
				22	14 55 45.29 +36 14 28.2	2.48
				31	14 55 44.56 +36 14 32.8	38.35
				31	14 55 48.73 +36 13 58.7	20.76
RXSJ1458.3+4121	0.36±0.12	25	14 58 20.77 +41 21 02.1	9.04
				43	14 58 19.76 +41 20 38.6	3.09
RXSJ1458.5+3800	0.24±0.09	Cl	...	21	14 58 34.59 +37 59 45.4	1.37
				23	14 58 34.26 +37 59 41.9	1.30
				29	14 58 34.35 +37 59 36.0	1.35
RXSJ1459.0+3319	0.31±0.11	17	14 59 00.93 +33 19 20.0	4.90
				42	14 58 59.76 +33 19 39.7	13.97
RXSJ1459.6+4118	0.21±0.09	8	14 59 40.78 +41 17 59.8	21.28
				18	14 59 39.18 +41 17 57.5	29.71
RXSJ1501.3+3443	0.40±0.12	9	15 01 24.06 +34 43 46.6	13.43
				25	15 01 25.20 +34 43 53.3	2.19
RXSJ1501.6+3311	0.33±0.11	24	15 01 39.53 +33 12 18.6	2.09
				42	15 01 43.82 +33 12 00.5	12.34
RXSJ1502.7+2540	2.10±0.38	BA?	0.191	32	15 02 44.94 +25 40 29.7	2.16
				59	15 02 50.09 +25 41 12.1	3.34
RXSJ1503.5+2834	0.31±0.13	6	15 03 35.28 +28 34 24.9	1.69
				15	15 03 33.64 +28 34 27.4	1.70

continued on next page

ROSAT Name (1)	F_x ($10^{-12} \text{erg s}^{-1} \text{cm}^{-2}$) (2)	Type (3)	z (4)	Δ_{XR} ($''$) (5)	FIRST Position (J2000) (6)	F_r (mJy) (7)
				58	15 03 37.24 +28 35 13.8	11.07
RXSJ1508.7+2709	6.07±0.56	6	15 08 42.09 +27 09 04.8	1.13
				6	15 08 42.61 +27 09 07.7	30.54
RXSJ1508.8+3014	0.86±0.21	21	15 08 51.95 +30 14 34.0	6.37
				28	15 08 52.62 +30 14 31.8	2.72
				41	15 08 53.64 +30 14 34.2	1.26
RXSJ1508.9+3154	0.43±0.14	19	15 08 58.30 +31 54 39.4	5.07
				44	15 08 54.00 +31 54 27.7	1.17
RXSJ1511.5+3228	0.38±0.13	8	15 11 30.79 +32 28 21.3	13.42
				16	15 11 31.29 +32 28 39.9	8.38
				22	15 11 31.21 +32 28 46.1	3.27
				25	15 11 31.93 +32 28 48.4	15.86
				36	15 11 30.98 +32 27 48.5	13.85
RXSJ1512.3+3900	0.69±0.14	10	15 12 23.84 +39 00 42.4	1.81
				33	15 12 26.18 +39 00 43.1	1.43
				41	15 12 26.96 +39 00 39.8	4.59
RXSJ1514.1+2943	0.34±0.16	37	15 14 07.13 +29 42 55.4	15.17
				49	15 14 06.17 +29 42 51.5	9.43
RXSJ1514.3+4244	2.00±0.29	G?	...	3	15 14 20.52 +42 44 45.4	1.04
				50	15 14 17.29 +42 45 17.2	1.17
RXSJ1514.7+3650	3.34±0.28	QSO	0.3707	9	15 14 43.04 +36 50 50.4	48.97
				26	15 14 40.96 +36 50 59.5	86.72
				27	15 14 44.88 +36 50 42.4	148.51
RXSJ1514.8+3022	0.46±0.18	3	15 14 53.11 +30 22 22.8	1.61
				21	15 14 53.28 +30 22 40.1	23.67
RXSJ1516.7+2918	2.14±0.37	G?	...	9	15 16 41.59 +29 18 09.5	67.90
				19	15 16 42.94 +29 17 48.1	1.31
				28	15 16 43.63 +29 17 43.4	1.92
RXSJ1519.2+3623	0.99±0.18	6	15 19 13.33 +36 23 43.4	28.61
				18	15 19 12.77 +36 23 32.5	1.06
				22	15 19 14.54 +36 24 06.8	4.97
				29	15 19 13.81 +36 24 15.7	3.68

continued on next page

ROSAT Name (1)	F_x ($10^{-12}\text{erg s}^{-1}\text{cm}^{-2}$) (2)	Type (3)	z (4)	Δ_{XR} ($''$) (5)	FIRST Position (J2000) (6)	F_r (mJy) (7)
				31	15 19 14.74 +36 24 15.8	3.32
				32	15 19 12.22 +36 23 21.2	1.41
				40	15 19 11.79 +36 23 14.4	2.32
				60	15 19 10.57 +36 23 00.8	5.72
RXSJ1524.1+3509	0.49±0.17	41	15 24 06.50 +35 09 11.8	1.36
				58	15 24 13.94 +35 09 48.7	1.23
RXSJ1525.1+3533	0.26±0.12	26	15 25 10.08 +35 33 28.9	1.12
				41	15 25 11.99 +35 33 15.0	1.90
				44	15 25 12.29 +35 33 00.8	1.29
RXSJ1527.7+2904	0.75±0.24	G/Cl?	0.0631	29	15 27 43.01 +29 04 02.4	1.13
				40	15 27 43.38 +29 03 41.0	4.18
RXSJ1528.7+3637	0.38±0.14	6	15 28 46.69 +36 37 51.9	1.20
				40	15 28 46.01 +36 38 33.4	13.19
RXSJ1529.7+3508	0.39±0.14	9	15 29 42.21 +35 08 51.5	66.96
				15	15 29 43.14 +35 08 55.8	14.87
RXSJ1531.4+3533	0.47±0.15	G	0.342	8	15 31 25.93 +35 33 41.5	663.27
				14	15 31 25.25 +35 33 39.7	90.96
				20	15 31 24.81 +35 33 38.8	623.94
				22	15 31 25.19 +35 33 52.0	1.15
				41	15 31 27.72 +35 32 58.4	1.14
				60	15 31 28.51 +35 32 41.9	1.16
RXSJ1531.7+4319	0.27±0.11	2	15 31 45.16 +43 19 33.7	8.91
				19	15 31 46.62 +43 19 25.2	5.37
RXSJ1533.6+3544	1.56±0.27	14	15 33 39.78 +35 44 45.5	189.51
				17	15 33 40.55 +35 44 40.2	376.58
				36	15 33 38.76 +35 45 08.3	1.23
RXSJ1535.3+3422	1.07±0.25	17	15 35 22.06 +34 22 58.4	14.74
				20	15 35 22.32 +34 22 45.7	8.31
				30	15 35 23.22 +34 22 54.0	10.62
				30	15 35 22.76 +34 23 10.0	3.89
RXSJ1536.9+2424	1.58±0.42	36	15 36 58.62 +24 23 45.9	1.30
				49	15 36 57.82 +24 25 05.3	9.17
				56	15 36 56.11 +24 25 10.5	12.30

continued on next page

ROSAT Name (1)	F_x ($10^{-12}\text{erg s}^{-1}\text{cm}^{-2}$) (2)	Type (3)	z (4)	Δ_{XR} ($''$) (5)	FIRST Position (J2000) (6)	F_r (mJy) (7)
RXSJ1544.7+3713	0.38±0.15	QSO	0.974	26	15 44 45.03 +37 13 09.0	602.99
				29	15 44 44.60 +37 13 20.8	1.30
RXSJ1545.1+3452	1.33±0.36	13	15 45 11.00 +34 52 46.9	14.71
				28	15 45 09.21 +34 52 49.3	1.08
RXSJ1550.1+2717	0.42±0.20	13	15 50 10.76 +27 18 00.4	27.21
				19	15 50 11.81 +27 17 59.5	103.31
				23	15 50 12.31 +27 17 56.3	83.17
RXSJ1557.1+2748	0.90±0.29	18	15 57 09.10 +27 48 38.5	28.54
				37	15 57 10.79 +27 48 40.3	14.43
				60	15 57 12.47 +27 48 37.2	1.70
RXSJ1557.4+3304	0.47±0.19	QSO	0.942	23	15 57 28.34 +33 04 45.9	22.56
				34	15 57 29.94 +33 04 47.0	77.06
				42	15 57 30.93 +33 04 43.1	21.96
RXSJ1557.7+3530	2.88±0.41	G	0.1579	35	15 57 42.38 +35 30 34.6	55.00
				36	15 57 42.08 +35 30 27.4	60.39
				41	15 57 42.42 +35 30 47.2	24.01
				50	15 57 41.61 +35 29 52.1	84.17
RXSJ1602.1+2619	2.40±0.33	G?	0.0719	10	16 02 08.81 +26 19 31.0	36.34
				12	16 02 08.91 +26 19 45.7	2.20
				17	16 02 09.46 +26 19 53.5	1.18
RXSJ1602.4+2741	0.51±0.17	13	16 02 26.88 +27 41 41.6	15.87
				25	16 02 26.95 +27 41 28.3	87.81
				30	16 02 27.41 +27 41 25.4	108.66
				38	16 02 27.63 +27 42 26.3	1.23
RXSJ1603.0+3851	0.46±0.17	5	16 03 03.55 +38 52 00.2	19.05
				12	16 03 03.61 +38 51 45.0	8.50
				27	16 03 03.70 +38 51 29.1	4.49
				36	16 03 03.84 +38 51 20.0	6.32
RXSJ1604.1+2608	0.48±0.18	30	16 04 10.94 +26 08 00.9	1.28
				32	16 04 11.03 +26 08 06.8	1.48
RXSJ1604.1+3006	0.64±0.18	7	16 04 10.51 +30 06 26.8	28.78
				17	16 04 11.28 +30 06 25.8	32.32

continued on next page

ROSAT Name (1)	F_x ($10^{-12} \text{erg s}^{-1} \text{cm}^{-2}$) (2)	Type (3)	z (4)	Δ_{XR} (//) (5)	FIRST Position (J2000) (6)	F_r (mJy) (7)
RXSJ1604.9+2356	8.39±0.62	G/Cl	0.0320	8	16 04 56.33 +23 55 59.7	80.48
				12	16 04 57.04 +23 55 53.2	66.81
				23	16 04 57.99 +23 55 48.7	21.10
				30	16 04 54.62 +23 56 09.8	5.44
				47	16 04 59.97 +23 55 47.1	1.03
				54	16 05 00.65 +23 55 51.3	1.09
RXSJ1605.2+2501	0.45±0.17	12	16 05 15.69 +25 01 39.0	88.95
				14	16 05 15.85 +25 01 54.1	43.37
RXSJ1605.7+2455	0.42±0.16	6	16 05 42.55 +24 55 47.0	1.02
				50	16 05 38.50 +24 55 51.9	7.45
				52	16 05 38.45 +24 56 00.2	15.21
RXSJ1606.8+2716	2.24±0.31	46	16 06 53.40 +27 17 04.4	15.22
				54	16 06 48.66 +27 17 15.3	1.94
RXSJ1608.1+2921	0.37±0.13	34	16 08 13.45 +29 21 33.6	5.09
				42	16 08 13.78 +29 21 26.4	16.96
				51	16 08 13.95 +29 21 16.1	6.56
RXSJ1608.3+4012	0.41±0.15	23	16 08 22.14 +40 12 17.9	68.39
				29	16 08 22.11 +40 12 10.2	39.09
RXSJ1610.4+3238	0.46±0.14	14	16 10 22.70 +32 38 19.6	137.27
				21	16 10 22.05 +32 38 28.8	132.09
RXSJ1611.9+2717	0.64±0.18	7	16 11 58.60 +27 17 54.2	19.28
				13	16 11 57.59 +27 17 57.1	1.24
				17	16 11 59.60 +27 17 49.5	2.96
RXSJ1612.5+2929	0.87±0.20	G	0.03133	41	16 12 37.70 +29 29 21.2	1.03
				42	16 12 38.08 +29 29 36.3	1.15
RXSJ1612.7+4152	0.58±0.17	32	16 12 39.95 +41 52 04.7	12.54
				38	16 12 39.07 +41 52 08.3	11.77
RXSJ1613.8+3742	0.34±0.11	13	16 13 51.68 +37 42 53.7	46.53
				18	16 13 50.77 +37 43 03.0	93.29
				43	16 13 48.90 +37 42 09.1	1.05
RXSJ1617.1+4106	2.10±0.22	8	16 17 07.22 +41 06 40.3	10.92

continued on next page

ROSAT Name (1)	F_x ($10^{-12}\text{erg s}^{-1}\text{cm}^{-2}$) (2)	Type (3)	z (4)	Δ_{XR} ($''$) (5)	FIRST Position (J2000) (6)	F_r (mJy) (7)
				13	16 17 06.36 +41 06 47.0	55.61
RXSJ1617.6+3459	0.60±0.15	G	0.0295	48	16 17 40.50 +35 00 15.6	47.40
				51	16 17 41.06 +35 00 11.4	17.67
				54	16 17 39.58 +35 00 30.6	15.15
RXSJ1621.0+2545	2.34±0.33	Cl	0.161	37	16 20 58.46 +25 46 13.1	1.45
				44	16 21 02.76 +25 46 17.4	1.62
RXSJ1621.4+3810	1.10±0.15	10	16 21 24.70 +38 10 08.9	5.73
				18	16 21 22.92 +38 10 15.4	1.51
				43	16 21 21.50 +38 10 34.4	1.45
RXSJ1621.4+4245	1.29±0.17	G?/Cl	0.1365	31	16 21 31.08 +42 45 23.4	12.68
				37	16 21 31.55 +42 45 18.3	16.30
				46	16 21 32.13 +42 45 010.0	7.61
				54	16 21 32.16 +42 44 54.5	3.61
RXSJ1623.0+3755	1.01±0.16	G	0.0310	19	16 23 03.11 +37 55 20.7	41.41
				28	16 23 04.06 +37 55 21.0	18.63
				37	16 23 04.36 +37 55 30.1	13.48
				51	16 23 06.13 +37 55 21.3	8.28
RXSJ1623.5+2633	0.60±0.21	G?	...	29	16 23 35.10 +26 34 26.1	6.87
				41	16 23 31.78 +26 33 43.9	2.44
				49	16 23 30.99 +26 34 06.8	2.98
RXSJ1624.3+3924	0.18±0.07	QSO	1.12	13	16 24 21.84 +39 24 49.0	76.71
				20	16 24 22.00 +39 24 41.0	132.32
				33	16 24 22.19 +39 24 28.1	13.61
RXSJ1624.6+2345	0.50±0.17	QSO?	0.927	10	16 24 38.87 +23 45 05.6	635.34
				10	16 24 39.29 +23 45 16.0	101.74
				18	16 24 39.69 +23 45 24.2	1249.00
RXSJ1624.7+3726	0.40±0.09	B	0.200	12	16 24 43.38 +37 26 42.5	23.23
				22	16 24 42.36 +37 26 28.2	1.97
RXSJ1625.2+2359	0.43±0.18	35	16 25 17.11 +23 59 55.4	1.51
				53	16 25 14.70 +24 00 22.0	1.55
RXSJ1625.9+4134	0.14±0.05	QSO	2.55	5	16 25 57.67 +41 34 40.6	1694.61
				16	16 25 55.95 +41 34 41.2	6.91

continued on next page

ROSAT Name (1)	F_x ($10^{-12} \text{erg s}^{-1} \text{cm}^{-2}$) (2)	Type (3)	z (4)	Δ_{XR} (μ) (5)	FIRST Position (J2000) (6)	F_r (mJy) (7)
				23	16 25 59.32 +41 34 39.4	7.28
				38	16 25 59.43 +41 34 08.1	4.64
				39	16 25 55.85 +41 35 12.9	3.14
RXSJ1627.1+3143	0.70±0.16	9	16 27 10.68 +31 43 47.6	1.11
				11	16 27 11.11 +31 43 56.5	2.78
				14	16 27 11.90 +31 43 59.4	28.96
				30	16 27 13.06 +31 44 08.2	53.91
RXSJ1627.5+3827	0.22±0.08	6	16 27 33.44 +38 27 19.6	3.48
				8	16 27 34.03 +38 27 27.7	1.06
RXSJ1628.6+3932	47.6±0.81	G/Cl	0.0311	15	16 28 36.51 +39 32 55.3	125.54
				17	16 28 38.25 +39 33 04.2	176.62
				23	16 28 39.62 +39 32 54.3	126.67
				38	16 28 40.62 +39 33 05.9	60.63
RXSJ1628.6+2527	2.57±0.35	12	16 28 39.35 +25 27 54.7	2.57
				12	16 28 39.02 +25 27 55.8	46.10
RXSJ1629.8+2426	0.95±0.26	A	0.0375	7	16 29 52.89 +24 26 38.4	18.94
				60	16 29 49.25 +24 26 02.6	1.11
RXSJ1629.9+4230	0.19±0.07	44	16 29 57.84 +42 30 51.5	16.24
				45	16 29 56.45 +42 30 43.0	6.65
				46	16 29 59.41 +42 30 56.9	6.39
RXSJ1631.4+2418	0.33±0.15	42	16 31 25.28 +24 18 31.7	1.13
				43	16 31 24.75 +24 18 42.2	1.42
RXSJ1633.0+3924	0.35±0.09	QSO	1.023	3	16 33 02.55 +39 24 20.5	15.24
				8	16 33 02.10 +39 24 27.6	41.29
				53	16 33 04.51 +39 23 34.3	1.23
RXSJ1633.1+4157	0.41±0.09	4	16 33 06.85 +41 57 40.2	1.49
				51	16 33 07.13 +41 56 45.3	1.53
RXSJ1635.2+3606	0.44±0.13	39	16 35 17.85 +36 06 11.0	1.06
				50	16 35 19.34 +36 06 46.8	1.18
RXSJ1636.2+2835	0.80±0.20	5	16 36 12.24 +28 35 12.4	16.52
				55	16 36 08.52 +28 34 52.3	2.61

continued on next page

ROSAT Name (1)	F_x ($10^{-12} \text{erg s}^{-1} \text{cm}^{-2}$) (2)	Type (3)	z (4)	Δ_{XR} ($''$) (5)	FIRST Position (J2000) (6)	F_r (mJy) (7)
RXSJ1636.6+2648	1.01±0.26	12	16 36 35.94 +26 48 12.0	17.29
				15	16 36 36.91 +26 47 48.3	1.58
				16	16 36 37.68 +26 48 05.3	980.50
				26	16 36 34.84 +26 48 15.5	140.13
				35	16 36 38.28 +26 48 27.9	1.33
				37	16 36 33.75 +26 48 06.8	1.22
RXSJ1637.2+2343	0.64±0.23	47	16 37 17.97 +23 43 09.2	47.04
				49	16 37 17.43 +23 42 50.5	221.32
RXSJ1640.9+3143	0.55±0.18	9	16 40 54.28 +31 43 46.8	2.47
				14	16 40 54.16 +31 43 29.8	24.17
				18	16 40 54.99 +31 43 49.8	1.19
				46	16 40 53.41 +31 42 56.7	7.74
RXSJ1642.9+3948	3.60±0.28	QSO	0.588	4	16 42 58.76 +39 48 26.8	22.30
				14	16 42 58.80 +39 48 37.2	6050.06
RXSJ1643.6+3316	0.37±0.14	6	16 43 39.51 +33 16 47.8	12.19
				12	16 43 39.15 +33 16 55.8	8.68
				46	16 43 41.49 +33 16 09.0	8.19
RXSJ1644.7+2619	2.59±0.37	BA	0.145	10	16 44 42.54 +26 19 13.2	87.53
				22	16 44 41.71 +26 19 17.0	16.54
RXSJ1644.8+3729	0.44±0.14	35	16 44 52.56 +37 30 09.3	3.56
				45	16 44 55.39 +37 29 43.7	14.67
				55	16 44 50.92 +37 30 30.4	23.37
RXSJ1645.9+3534	0.59±0.17	45	16 45 55.14 +35 35 25.8	2.68
				48	16 45 55.21 +35 35 30.1	2.00
				59	16 45 55.93 +35 35 45.6	2.26
RXSJ1646.9+2328	0.53±0.17	5	16 46 53.49 +23 28 25.6	3.65
				18	16 46 52.56 +23 28 23.8	2.54
RXSJ1647.4+2909	0.78±0.22	G	0.132	10	16 47 26.88 +29 09 49.8	115.47
				23	16 47 26.42 +29 10 03.4	8.60
				49	16 47 24.47 +29 10 13.2	3.21
				52	16 47 23.76 +29 09 57.8	5.29
RXSJ1650.1+4140	1.04±0.19	QSO	0.586	10	16 50 05.49 +41 40 32.6	170.28
				16	16 50 04.95 +41 40 32.3	2.44

continued on next page

ROSAT Name (1)	F_x ($10^{-12} \text{erg s}^{-1} \text{cm}^{-2}$) (2)	Type (3)	z (4)	Δ_{XR} (μ) (5)	FIRST Position (J2000) (6)	F_r (mJy) (7)
RXSJ1652.2+2238	0.26±0.11	5 16 52 16.04	+22 38 58.3	47.82
				5 16 52 16.21	+22 38 51.6	12.82
				23 16 52 15.43	+22 38 31.8	35.24
RXSJ1654.4+2333	1.22±0.23	25 16 54 23.55	+23 32 57.1	1.30
				34 16 54 23.48	+23 32 48.5	1.57
				36 16 54 23.86	+23 33 57.6	2.72
				56 16 54 27.52	+23 32 58.4	1.37
RXSJ1656.6+3714	0.55±0.14	19 16 56 38.32	+37 14 38.8	1.12
				24 16 56 38.31	+37 14 48.6	1.25
				32 16 56 38.26	+37 14 58.5	4.36
RXSJ1657.9+2916	0.81±0.17	55 16 58 01.07	+29 17 12.1	23.38
				60 16 58 02.42	+29 17 03.0	28.77
RXSJ1658.0+2751	2.09±0.30	G/Cl	0.0345	38 16 57 58.04	+27 50 58.5	1.36
				39 16 57 58.18	+27 51 15.8	14.11
				45 16 57 58.23	+27 51 31.2	2.19
				52 16 57 57.64	+27 51 31.8	1.21
RXSJ1658.0+3604	0.26±0.10	24 16 58 00.54	+36 04 42.7	11.68
				26 16 58 02.63	+36 05 04.3	46.80
RXSJ1658.3+3334	0.92±0.16	43 16 58 22.52	+33 34 00.8	1.02
				53 16 58 20.02	+33 33 19.4	4.96
RXSJ1659.4+2629	0.71±0.20	QSO	0.795	16 16 59 24.19	+26 29 37.3	391.07
				49 16 59 22.88	+26 30 39.2	17.12
RXSJ1659.7+3236	3.57±0.29	G	0.0984	18 16 59 43.94	+32 36 54.9	14.83
				41 16 59 42.10	+32 36 43.5	11.05
RXSJ1700.7+3008	0.22±0.10	G	0.035	11 17 00 45.21	+30 08 12.7	60.55
				45 17 00 42.87	+30 07 49.3	5.31
RXSJ1701.2+3534	0.85±0.14	14 17 01 12.37	+35 33 53.3	52.13
				26 17 01 12.06	+35 33 42.1	1.01
				33 17 01 11.28	+35 33 38.8	1.70
				39 17 01 11.18	+35 33 32.3	1.33
RXSJ1701.4+3851	0.50±0.14			

continued on next page

ROSAT Name (1)	F_x ($10^{-12} \text{erg s}^{-1} \text{cm}^{-2}$) (2)	Type (3)	z (4)	Δ_{XR} ($''$) (5)	FIRST Position (J2000) (6)	F_r (mJy) (7)
				41	17 10 56.98 +39 41 34.3	40.22
				48	17 10 56.34 +39 41 31.8	39.12
				49	17 11 04.56 +39 41 42.9	1.40
				52	17 11 05.01 +39 41 30.9	1.67
				54	17 11 05.09 +39 41 40.0	1.20
RXSJ1711.2+2415	0.46±0.17	42	17 11 13.46 +24 14 49.4	61.37
				49	17 11 12.91 +24 14 49.1	8.00
RXSJ1711.3+4349	0.22±0.08	20	17 11 23.29 +43 48 44.8	67.56
				45	17 11 25.58 +43 48 22.3	8.68
RXSJ1712.5+2450	2.22±0.33	Cl	...	12	17 12 35.90 +24 50 26.8	8.65
				35	17 12 36.53 +24 50 04.5	5.17
RXSJ1714.1+2904	0.78±0.20	20	17 14 09.63 +29 04 30.3	1.97
				24	17 14 10.28 +29 04 25.1	1.36
RXSJ1715.1+3619	0.40±0.13	22	17 15 07.55 +36 19 46.9	1.68
				33	17 15 08.38 +36 19 50.3	48.74
RXSJ1715.9+4340	0.58±0.14	6	17 15 55.77 +43 40 21.8	37.02
				9	17 15 55.56 +43 40 32.9	262.45
				12	17 15 56.11 +43 40 16.3	39.60
				19	17 15 56.59 +43 40 10.8	48.60
				24	17 15 56.57 +43 40 03.6	129.93
				58	17 15 52.96 +43 41 15.6	1.00
RXSJ1716.4+3411	0.76±0.18	21	17 16 29.42 +34 11 19.2	1.17
				37	17 16 27.47 +34 11 08.4	1.32
RXSJ1716.7+2915	0.49±0.16	14	17 16 42.39 +29 15 22.5	1.78
				25	17 16 42.75 +29 15 12.4	2.24
				55	17 16 42.14 +29 14 41.7	3.89
RXSJ1716.8+2616	0.46±0.16	6	17 16 51.09 +26 15 59.7	76.33
				11	17 16 51.83 +26 16 10.9	128.15
RXSJ1717.1+2404	0.51±0.18	17	17 17 05.56 +24 04 23.8	5.21
				20	17 17 05.24 +24 04 12.2	1.80
RXSJ1717.3+4226	3.39±0.29	Cl?	0.1829	8	17 17 19.21 +42 26 59.7	128.29
				8	17 17 18.33 +42 26 47.6	1.06

continued on next page

ROSAT Name (1)	F_x ($10^{-12} \text{erg s}^{-1} \text{cm}^{-2}$) (2)	Type (3)	z (4)	Δ_{XR} ($''$) (5)	FIRST Position (J2000) (6)	F_r (mJy) (7)
RXSJ1717.5+2549	0.87±0.21	32	17 17 34.73 +25 49 39.9	3.17
				38	17 17 34.19 +25 49 43.6	4.48
				49	17 17 33.93 +25 49 54.9	2.24
RXSJ1720.2+3825	0.54±0.15	25	17 20 10.36 +38 25 57.2	131.21
				26	17 20 09.61 +38 25 40.6	10.79
				28	17 20 09.46 +38 25 34.9	1.21
RXSJ1720.2+3536	2.76±0.30	16	17 20 16.77 +35 36 25.9	15.84
				53	17 20 15.53 +35 35 29.5	1.97
RXSJ1720.4+2851	0.51±0.17	14	17 20 28.21 +28 52 01.4	1.61
				60	17 20 23.00 +28 51 59.2	1.84
RXSJ1721.0+3306	0.64±0.16	12	17 21 02.56 +33 06 45.7	2.36
				21	17 21 02.72 +33 06 56.0	16.71
				39	17 21 02.98 +33 07 13.5	23.70
RXSJ1721.1+3542	1.30±0.22	BA	0.263	6	17 21 09.52 +35 42 15.7	386.51
				34	17 21 09.64 +35 41 39.1	27.66
				54	17 21 10.32 +35 41 18.6	1.68
				56	17 21 09.75 +35 41 16.9	10.67
				57	17 21 08.36 +35 43 06.2	5.05
RXSJ1721.2+2910	0.32±0.12	9	17 21 12.90 +29 10 26.8	1.13
				29	17 21 12.33 +29 10 50.5	1.20
RXSJ1722.2+3103	0.39±0.13	10	17 22 17.59 +31 03 30.9	24.31
				25	17 22 18.92 +31 03 22.7	1.92
				40	17 22 19.99 +31 03 13.0	3.11
				55	17 22 21.14 +31 03 12.1	15.08
RXSJ1722.4+3722	0.29±0.12	40	17 22 24.80 +37 23 13.6	3.26
				43	17 22 26.91 +37 21 54.8	430.94
RXSJ1722.6+3052	32.0±0.98	BA/G	0.04330,0.04637	2	17 22 39.97 +30 52 52.9	6.82
				42	17 22 39.28 +30 52 11.2	2.49
				46	17 22 38.21 +30 52 12.1	2.31
RXSJ1724.7+3202	0.59±0.16	CI?	...	11	17 24 46.77 +32 02 34.5	1.30
				19	17 24 47.24 +32 02 08.4	13.10

continued on next page

ROSAT Name (1)	F_x ($10^{-12} \text{erg s}^{-1} \text{cm}^{-2}$) (2)	Type (3)	z (4)	Δ_{XR} ($''$) (5)	FIRST Position (J2000) (6)	F_r (mJy) (7)
RXSJ1725.4+3804	1.17±0.21	18	17 25 29.41 +38 05 03.1	1.05
				31	17 25 31.39 +38 04 21.1	3.63
RXSJ1725.9+4217	0.36±0.11	18	17 25 57.17 +42 17 31.1	17.48
				31	17 25 57.81 +42 17 43.0	1.38
RXSJ1736.4+4213	0.31±0.10	18	17 36 25.85 +42 13 42.4	5.96
				26	17 36 27.89 +42 13 46.3	1.30
				43	17 36 29.91 +42 13 05.6	13.07
RXSJ2112.8-0633	0.60±0.24	41	21 12 53.20 -06 32 32.4	6.92
				51	21 12 51.26 -06 32 19.9	3.14
RXSJ2136.6+0042	1.82±0.38	QSO	1.932	12	21 36 38.60 +00 41 54.5	3545.21
				29	21 36 39.43 +00 42 21.2	6.66
				35	21 36 39.46 +00 42 29.6	6.17
				37	21 36 39.54 +00 41 32.9	4.93
				42	21 36 37.76 +00 41 20.4	5.75
				47	21 36 39.78 +00 41 23.7	4.73
RXSJ2139.6-0202	0.92±0.29	3	21 39 39.51 -02 02 26.1	1.39
				13	21 39 38.48 -02 02 27.7	1.56
				13	21 39 38.66 -02 02 15.7	1.04
				24	21 39 37.70 -02 02 23.1	3.17
				41	21 39 41.86 -02 02 08.9	1.07
RXSJ2149.6-0653	0.74±0.29	2	21 49 37.44 -06 53 12.2	13.05
				11	21 49 37.34 -06 53 23.0	1.49
				11	21 49 37.52 -06 52 60.0	1.45
				13	21 49 37.74 -06 53 23.5	1.09
				43	21 49 36.48 -06 53 53.6	1.21
RXSJ2209.1-0056	1.19±0.38	9	22 09 08.91 -00 55 59.6	3.36
				11	22 09 08.25 -00 55 59.0	20.69
				23	22 09 10.15 -00 56 01.1	1.09
RXSJ2256.5-0032	0.80±0.30	Cl	...	22	22 56 30.07 -00 32 09.6	1.44
				32	22 56 28.29 -00 32 54.0	2.68
RXSJ2317.5+0011	0.71±0.30	30	23 17 32.63 +00 10 44.6	3.90
				47	23 17 31.95 +00 10 31.2	17.52
				52	23 17 33.55 +00 10 19.6	2.11
RXSJ2319.8-0116	1.24±0.36			

continued on next page

ROSAT Name (1)	F_x ($10^{-12} \text{erg s}^{-1} \text{cm}^{-2}$) (2)	Type (3)	z (4)	Δ_{XR} ($''$) (5)	FIRST Position (J2000) (6)	F_r (mJy) (7)
				6	23 19 53.03 -01 16 25.4	24.05
				19	23 19 53.86 -01 16 20.5	7.88
				55	23 19 49.36 -01 16 49.9	1.04
RXSJ2333.4-0109	1.50±0.38	45	23 33 22.72 -01 08 54.8	1.35
				53	23 33 23.86 -01 08 28.3	1.06
RXSJ2341.1+0018	2.49±0.44	G?	...	13	23 41 06.92 +00 18 33.5	425.39
				16	23 41 06.00 +00 18 52.0	1.20
RXSJ2343.6+0019	0.57±0.24	54	23 43 39.55 +00 18 45.7	2.68
				59	23 43 39.38 +00 18 39.3	2.39
RXSJ2351.9-0109	11.7±0.86	BA	0.174	3	23 51 56.14 -01 09 14.0	165.86
				5	23 51 56.12 -01 09 06.9	347.07
				14	23 51 56.40 -01 09 25.1	447.23